



HAL
open science

Réduction d'interférence dans les systèmes de transmission sans fil

Yasser Fadlallah

► **To cite this version:**

Yasser Fadlallah. Réduction d'interférence dans les systèmes de transmission sans fil. Signal and Image processing. Université Européenne de Bretagne, 2013. English. NNT : . tel-01064897

HAL Id: tel-01064897

<https://theses.hal.science/tel-01064897>

Submitted on 17 Sep 2014

HAL is a multi-disciplinary open access archive for the deposit and dissemination of scientific research documents, whether they are published or not. The documents may come from teaching and research institutions in France or abroad, or from public or private research centers.

L'archive ouverte pluridisciplinaire **HAL**, est destinée au dépôt et à la diffusion de documents scientifiques de niveau recherche, publiés ou non, émanant des établissements d'enseignement et de recherche français ou étrangers, des laboratoires publics ou privés.

Sous le sceau de l'Université européenne de Bretagne

Télécom Bretagne

En accréditation conjointe avec l'Ecole Doctorale Sicma

Réduction d'interférence dans les systèmes de transmission sans fil

Thèse de Doctorat

Mention : Sciences et Technologies de l'information et de la Communication (STIC)

Présentée par **Yasser Fadlallah**

Département : Signal et Communications

Laboratoire : LabSTICC Pôle CACS/COM

Directeur de thèse : Ramesh Pyndiah

Soutenue le 04 Décembre 2013

Jury :

Pr. David Gesbert, professeur, Eurecom (Rapporteur)
Pr. Jean-Marc Brossier, professeur, Grenoble INP (Rapporteur)
Pr. Gilles Burel, professeur, Université de Bretagne Occidentale (Examineur)
Pr. Karim Abed-Meraim, professeur, Université d'Orléans (Examineur)
Dr. Ahmed Saadani, ingénieur de recherche, Orange Labs (Examineur)
Pr. Ramesh Pyndiah, professeur, Télécom Bretagne (Directeur de thèse)
Dr. Karine Amis, maître de conférences, Télécom Bretagne (Encadrant)
Dr. Abdeldjalil Aïssa-El-Bey, maître de conférences, Télécom Bretagne (Encadrant)

Abstract

Wireless communications have known an exponential growth and a fast progress over the past few decades. Nowadays, wireless mobile communications have evolved over time starting with the first generation primarily developed for voice communications, and reaching the fourth generation referred to as long term evolution that offers an increasing capacity with much more users via different radio interface together with core network improvements. Overall throughput and transmission reliability are among the essential measures of service quality in a mobile communication system. Such measures are mainly subjected to interference management constraint in a multi-user network.

Interference management is at the heart of wireless regulation and is essential for maintaining a desirable throughput while avoiding the detrimental impact of interference at the undesired receivers. Our work is incorporated within the framework of interference network where each user is equipped with single or multiple antennas. The goal is to resolve the challenges that wireless communications face taking into account the achievable rate and the complexity cost.

We address both transmission cases, downlink and uplink in mobile communication. First of all, we describe the interference alignment scheme proposed to deal with the interference caused by users sharing the same medium and using the same resources. Then, we consider the single input single output interference channel, and we show that although interference alignment is sub-optimal in the finite power region, it is able to achieve a significant overall throughput. We propose to optimize the design in order to achieve enhanced sum-rate performance in the practical SNR region. Firstly, we introduce a way to optimize the precoding subspaces at all transmitters, exploiting the fact that channel matrices in the interference channel model of a single input single output channel are diagonal. Secondly, we propose to optimize jointly the set of precoder bases within their associated precoding subspaces. To this end, we combine each precoder with a new combination precoder, and this latter seeks the optimal bases that maximizes

the network sum-rate.

The second part addresses the detection side in the downlink transmission in presence of the interference alignment scheme. The interference are assumed to be aligned at each receiver and of the same space dimensions as the desired signal, which transforms the decoding model into a determined linear model. Our approach of resolving the decoding problem is different from the classical approaches based on the interference estimation. The main idea is to separate the desired streams from the interference using higher-order cumulants blindly. We show the equivalence between the problem to resolve and the determined blind source separation problem. Then, we propose to separate the desired signal from the interference through a joint diagonalization of the fourth-order cumulants matrices.

The third part addresses the uplink transmission in the absence of any precoding scheme. We shows that jointly decoding both desired signal and interference can achieve a full receive diversity. In this respect, we describe the joint optimal detector, which is characterized by a very high computational cost depending on the dimension of the decoding problem. Then, we try to find out alternative detectors that significantly reduce the computational cost at the detriment of error rate performance. The proposed detectors are robust even if the decoding problems are underdetermined. We also propose a channel coding scheme that uses a convolutional code at the transmitter side and a turbo-detector at the receiver side in order to increase the reliability of transmission.

Acknowledgment

I would like to express my sincere thanks and deepest gratitude to those who have surrounded me with their kindness and wisdom, have enlightened my way with their experiences, and have supported me to accomplish my PhD studies.

I am deeply grateful to my supervisor Ramesh Pyndiah for providing me with his invaluable advice, guidance, and encouragement throughout the years of my PhD studies.

I would love to extend my thanks and gratitude to my advisors, Karine Amis and Abdeldjalil Assa-El-Bey, who have pursued every step of my work. Their profound scientific knowledge and curiosity were an important source of inspiration for me. Their comments and criticisms on both sides technical and non-technical have strongly improved the quality of my work. I am also indebted to them for the kindness and the encouragements they have showed.

A special thanks to Prof. Amir Khandani at University of Waterloo who accepted me to accomplish a part of my PhD under his supervision in Canada. It was a great opportunity to work with such a brilliant, insightful and kind supervisor.

I am also grateful to the committee members, Prof David Gesbert, Prof Jean-Marc Brossier, Prof Karim Abed-Meraim, Dr Ahmed Saadani and Prof Gilles Burel for reading and reviewing my thesis and enhancing me with their comments.

I do not forget to thank my friends who accompany me throughout these years, my housemates, my officemates, and my friends at the SC department and at Telecom Bretagne. Big thanks to my friends in my lovely city Brest with whom I enjoyed every single moment.

The whole acknowledgment goes out to my parents and my family for their unlimited support. There is no doubt in my mind that without them and their guidance, I have not been come thus far and achieved this degree.

Last but not least, my heartfelt recognition to my lovely wife for standing by my side in all difficult moments and supporting me with her intimacy.

All thanks and praises to you ALLAH, the most gracious.

Résumé des Travaux de Thèse

Introduction

Les communications mobiles sans fil ont connu un progrès très rapide pendant les dernières décennies. Ça a commencé avec les services vocaux offerts par les systèmes de la première génération en 1980, arrivant jusqu'aux systèmes de la quatrième génération avec des services internet haut débit et un nombre important d'utilisateurs, et dans quelques années les systèmes de la cinquième génération avec encore plus de débit et d'utilisateurs. En effet, les caractéristiques essentielles qui définissent les services et les qualités des services dans les systèmes de communication sans fil sont: le débit, la fiabilité de transmission et le nombre d'utilisateurs. Ces caractéristiques sont fortement dépendantes et liées entre elles, et sont soumises à la gestion des interférences entre les différents utilisateurs.

Les interférences entre-utilisateurs arrivent quand plusieurs émetteurs, dans une même zone, envoient simultanément à leurs propres destinataires en partageant la même bande de fréquence. Dans cette thèse, nous nous intéressons à la gestion d'interférence entre utilisateurs, méthodes classiques et avancées, de deux côtés émission et réception. Ensuite, nous proposons des nouvelles contributions dans des différents contextes afin d'améliorer les performances.

Cette thèse est divisée en plusieurs parties. Dans la première partie, une présentation concise de l'état de l'art sur des techniques de gestion et de réduction d'interférences entre utilisateurs. Ensuite, nous introduisons le concept d'une méthode dite d'Alignement d'Interférence, où nous proposons des améliorations algorithmiques dans les canaux mono-antenne afin d'augmenter le débit. Enfin, nous supposons les deux cas suivants: l'application et l'absence du schéma d'IA à l'émission, et nous proposons d'utiliser des méthodes existantes ou bien nouvelles pour la détection du côté récepteur.

Les éléments de l'état de l'art par lesquels nous nous sommes intéressés sont les types des canaux multi-utilisateurs et la gestion d'interférence dans ce genre

des canaux. Quand on parle des canaux multi-utilisateurs, on signifie souvent un des trois types de canaux suivants: le canal Broadcast (l'émetteur envoie simultanément à plusieurs récepteurs), le canal à accès multiple (plusieurs émetteurs envoient simultanément à un récepteur), et le canal à interférence (plusieurs paires émetteur-récepteur envoient simultanément, et chaque émetteur souhaite avoir son message décodé par son propre destinataire). Dans ces types de canaux, les interférences peuvent être gérées avec des techniques d'accès multiple comme par exemple la technique FDMA qui divise la bande de fréquence entre les utilisateurs, la technique TDMA qui divise le temps entre les utilisateurs, ou bien la technique CDMA qui attribue aux différents utilisateurs des codes pseudo-orthogonaux. Ces méthodes réussissent à éviter les interférences entre utilisateurs, par contre leur principale limitation est que le débit atteint par utilisateur est inversement proportionnel au nombre total d'utilisateurs.

D'autres méthodes avancées existent basées sur l'hypothèse d'une connaissance de l'état du canal à l'émission et l'hypothèse d'une application du principe de précodage au signal émis. Parmi les techniques les plus connues, nous citons la technique d'IA (Alignement d'interférence) proposée dans le contexte d'un canal à interférence et la technique DPC (Dirty Paper Coding) proposées dans le contexte d'un canal Broadcast. Le principe de la première technique IA est de concevoir les précodeurs de façon qu'à la réception les interférences et le signal désiré sont dans deux sous-espaces séparés et de dimension asymptotiquement égal. Cette technique aboutit à un débit asymptotique proportionnel au nombre d'utilisateurs. Le principe de la deuxième technique DPC est de concevoir le précodeur de telle sorte que chaque récepteur reçoit son message sans interférence. Cette technique offre un débit optimal qui tend vers la capacité du canal.

Alignement d'interférence dans les systèmes mono-antenne

Dans la première partie, nous nous mettons dans un contexte de canal à interférence et nous nous intéresserons d'abord à la technique d'IA. Pour expliquer le concept de l'IA, nous introduisons l'exemple de trois utilisateurs dans un canal *flat fading* à interférence, comme montre la figure 1. Nous supposons que chaque émetteur a un symbole à envoyer dans la direction d'un vecteur de deux dimensions, \mathbf{v}_1 pour le premier émetteur, \mathbf{v}_2 pour le deuxième et \mathbf{v}_3 pour le troisième. Toutes les matrices du canal entre tous les émetteurs et tous les récepteurs sont

considérés connues à tous les émetteurs. Le principe de l'IA est de choisir tous les vecteurs \mathbf{v}_1 , \mathbf{v}_2 et \mathbf{v}_3 de telle sorte qu'au premier récepteur, les vecteurs portant les interférences sont alignés et linéairement indépendants du vecteur portant le signal désiré, et la même chose pour les autres récepteurs. Dans cet exemple, il est possible d'envoyer trois symboles dans un espace de deux dimensions, et donc le débit atteignable asymptotique augmente linéairement avec le nombre d'utilisateur.

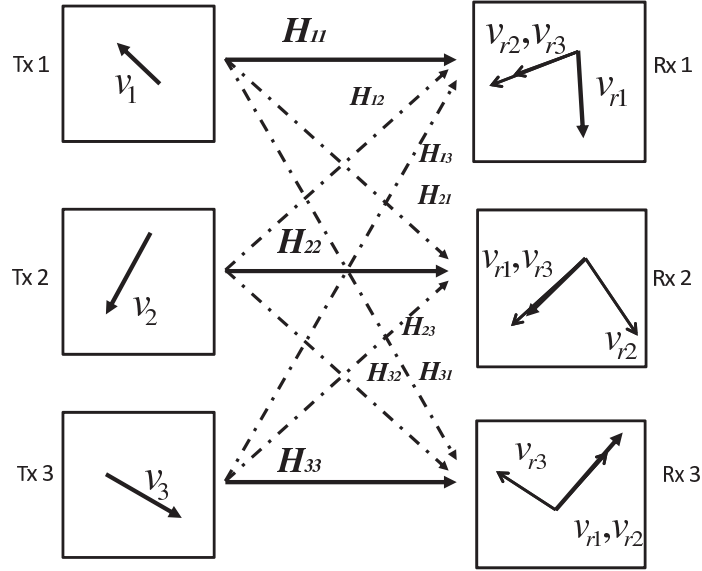


FIGURE 1: Canal à interférence mono-antenne entre trois utilisateurs en présence du schéma d'IA.

Parlant du modèle mathématique, le signal reçu au récepteur k est la superposition des signaux émis déphasés et atténués à laquelle s'ajoute le bruit. Le vecteur symbole \mathbf{s}_k au k ème émetteur est de dimensions d_k . Ce vecteur symbole est ensuite précodé par une matrice de précodage \mathbf{V}_k pour fournir un vecteur signal \mathbf{x}_k de dimension N . En pratique, l'envoi des N symboles de \mathbf{x}_k se fait comme suivant: dans le cas d'un système multi-antennes les symboles se portent sur les différentes antennes, et dans le cas d'un système mono-antenne un schéma OFDM est considéré, et les différents symboles seront émis sur des différentes sous-porteuses.

Les conditions pour lesquelles un schéma d'alignement se lève, c.à.d. les interférences s'alignent aux récepteurs, sont les suivantes

$$\begin{aligned} \text{rang}(\mathbf{U}_k \mathbf{H}_{kk} \mathbf{V}_k) &= d_k, \\ \mathbf{U}_k \mathbf{H}_{kj} \mathbf{V}_j &= 0, \forall j \neq k. \end{aligned} \quad (1)$$

où \mathbf{H}_{kj} est la matrice canal entre le j ème émetteur et le k ème récepteur. Autrement dit, nous cherchons les matrices \mathbf{U}_k et \mathbf{V}_k de telle sorte que, après décodage la matrice désignant l'espace désiré soit de rang plein et la matrice désignant l'espace non désiré soit nulle.

Considérons un schéma d'IA général pour une transmission mono-antenne, nous proposons deux étapes de calcul pour l'optimisation du schéma. Autrement dit, nous supposons une matrice de précodage quelconque suivant la technique IA, et nous proposons deux étapes de calcul pour modifier cette matrice afin de maximiser le débit du canal tout en gardant les interférences alignées. Les deux étapes d'optimisations sont les suivantes: l'optimisation des sous-espaces de précodage par la projection de tous les matrices de précodage sur une matrice diagonale variable \mathbf{W} commun entre tous les émetteurs, et l'optimisation des vecteurs de bases des précodeurs par l'introduction d'une matrice variable \mathbf{C}_k , $\forall k$.

L'optimisation des espaces de précodage peut se faire via la matrice \mathbf{W} afin de maximiser le débit total. Le problème de maximisation proposé est sous la contrainte d'une puissance totale constante. Les critères très connus sont utilisés à la réception comme le MMSE et le ZF. Avec un MMSE, la solution exige l'utilisation des algorithmes itératives comme par exemple l'algorithme de gradient projeté. Avec un ZF, une solution analytique très simple à implémenter est obtenue.

Concernant la deuxième étape d'optimisation, nous prenons le même critère comme précédemment (maximisation de débit), et nous cherchons les matrices \mathbf{C}_k qui résolvent le problème. Supposant un MMSE à la réception, le problème sera à plusieurs variables. Ce qui se résout en appliquant des algorithmes d'optimisations itératifs pour des fonctions coût à multi-variable. Supposons un ZF à la réception, le modèle revient à un modèle MIMO mono-utilisateur suite à la suppression des interférences, alors les techniques proposées en MIMO mono-utilisateur peut être utilisées.

Les performances en terme de débit sont illustrés dans les figures 2 et 3. Nous traçons le débit moyen par dimension dans un système mono-antenne de trois utilisateurs. Nous observons un gain important quand les optimisations proposés sont appliquées par rapport au schéma original d'IA non optimisé. Par contre, parmi les schémas comparés, celui qui maximise le SINR (rapport signal sur interférence plus bruit) est le plus performant au détriment des interférences résiduelles et d'une complexité très élevés par rapport au schéma OW-ZF qui optimise le schéma d'IA supposant un critère ZF.

Nous arrivons maintenant à la question d'optimalité du principe d'IA en terme

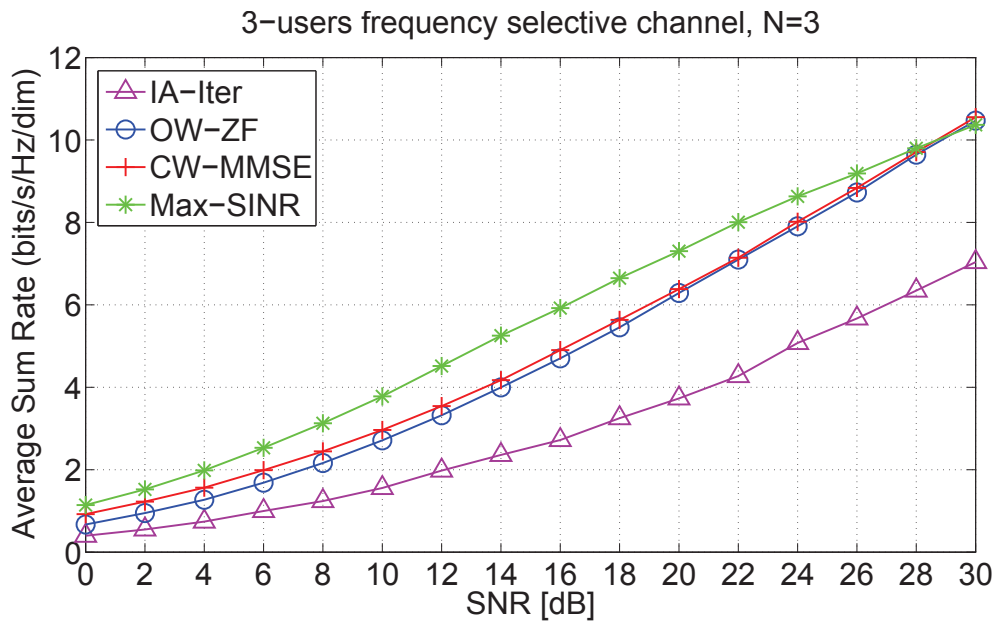


FIGURE 2: Comparaison du débit moyen par dimension pour plusieurs schéma de précodage quand $N = 3$.

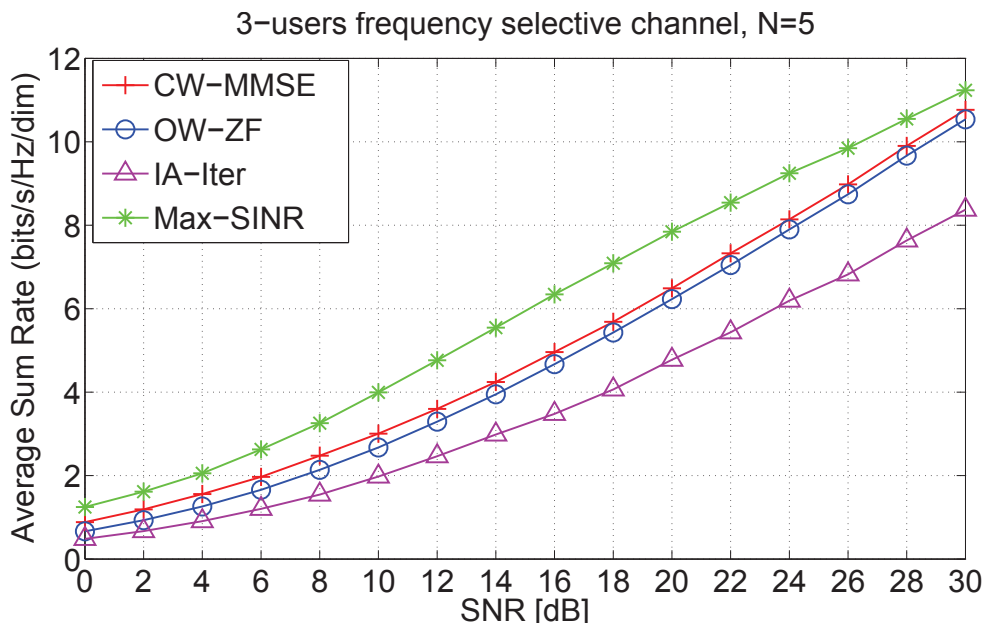


FIGURE 3: Comparaison du débit moyen par dimension pour plusieurs schéma de précodage quand $N = 5$.

de débit. Théoriquement, c'est optimal dans la zone où le SNR tends vers l'infini et pour une distribution Gaussienne des symboles sources. D'autre part, pour une constellation discrète le précodage optimale en terme de débit consiste à maximiser l'information mutuelle entre les paires émetteur-récepteur.

Malgré la sous-optimalité du technique d'IA, elle est toujours intéressante pour les transmissions sous une constellation discrète, grâce à sa capacité de séparer les interférences et le signal désiré, ainsi que son pouvoir d'envoyer un nombre de symboles désirés plus important que celui envoyé en utilisant les techniques de multiplexage classiques.

Schéma de détection en présence du schéma d'alignement d'interférence

Dans la première partie de nos contributions, nous avons traité la gestion d'interférence dans un canal à interférence du côté émetteur . Dans la deuxième partie, nous penons en hypothèse un schéma d'alignement d'interférence, et nous adressons le schéma de détection du côté récepteur.

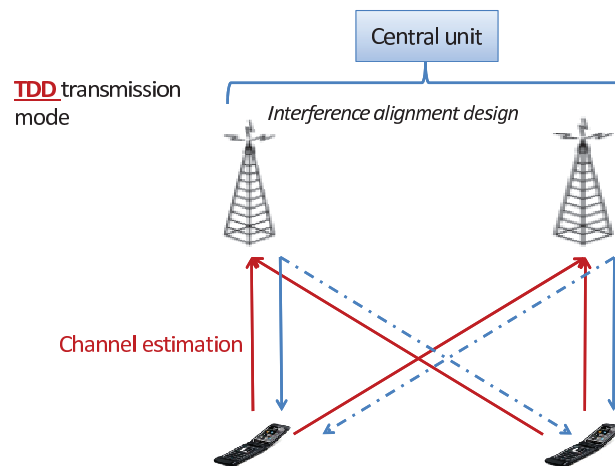


FIGURE 4: Communication mobile sans fil: transmission downlink.

L'exemple illustré par la figure 4 sert à définir le contexte. Deux stations de bases veulent se communiquer avec leur destinations (chacun avec son propre terminal mobile). Les terminaux mobiles envoient aux stations de bases afin d'estimer le canal. Cette estimation se fait via des séquences d'apprentissage de longueur

lié au nombre des canaux à estimer. Ces stations sont connectées par une unité centrale et donc pourront partager les connaissances des canaux, ce qui conduit à une réalisation possible du schéma d'AI. Notre contribution aborde le schéma de détection après l'application du schéma d'IA.

Le modèle mathématique est donné comme suit

$$\begin{aligned} \mathbf{y}_k &= \mathbf{H}_{kk} \mathbf{V}_k \mathbf{s}_k + \sum_{j \neq k} \mathbf{H}_{kj} \mathbf{V}_j \mathbf{s}_j + \mathbf{z}_k, \\ &= [\bar{\mathbf{H}}_k^k \quad \bar{\mathbf{H}}_I^k] [\mathbf{s}_k^T \quad \bar{\mathbf{s}}_k^T]^T + \mathbf{z}_k \end{aligned} \quad (2)$$

Le signal reçu s'exprime comme étant un terme désiré, plus un terme interférence plus un bruit. La matrice désignant le terme désiré est engendré par la matrice $\bar{\mathbf{H}}_k^k$ de dimension d , les matrices désignant les interférences alignés sont engendrés par la matrice $\bar{\mathbf{H}}_I^k$ de dimension $N - d$. Ces deux sous espaces constituent un espace de dimension N . En présence d'IA, le signal reçu s'exprime donc comme une matrice de mélange déterminée de rang plein multiplié par un vecteur source.

Le schéma de détection classique consiste à estimer en première étape le sous espace engendrant les interférences. Cette estimation se fait à partir d'une séquence d'apprentissage introduite dans chaque trame émis. Ensuite, les interférences sont supprimées par une simple projection sur le sous espace orthogonal aux interférences linéairement indépendant du signal désiré. Une fois les interférences sont éliminées, les symboles désirés peuvent s'extraire par l'utilisation des détecteurs sous les critères de forçage à zéro, de minimisation de l'erreur quadratique moyenne, de distance minimale ...

D'autres schémas de détection existent basés sur des techniques de séparation de source aveugle qui consistent extraire les symboles désirés sans aucune information a priori sur la matrice de mélange (i.e. matrice du canal). La seule hypothèse est l'indépendance des symboles superposés. Le modèle mathématique du signal reçu est équivalent au modèle mathématique de séparation de source avec bruit, avec un signal source contenant des symboles mutuellement indépendants et des symboles mutuellement dépendants. D'ailleurs, ça peut se montrer que les méthodes de séparation aveugle comme par exemple la technique de diagonalisation jointe des matrices propres (JADE), sont capables d'extraire les symboles indépendants du vecteur source. Dans ce contexte, il est possible de détecter le signal désiré par l'utilisation de technique JADE suite à leur propriété d'indépendance.

Par contre, quelques ambiguïtés résident sur l'échelle et l'ordre des symboles détectés. Afin de résoudre ces ambiguïtés, nous introduisons quelques symboles

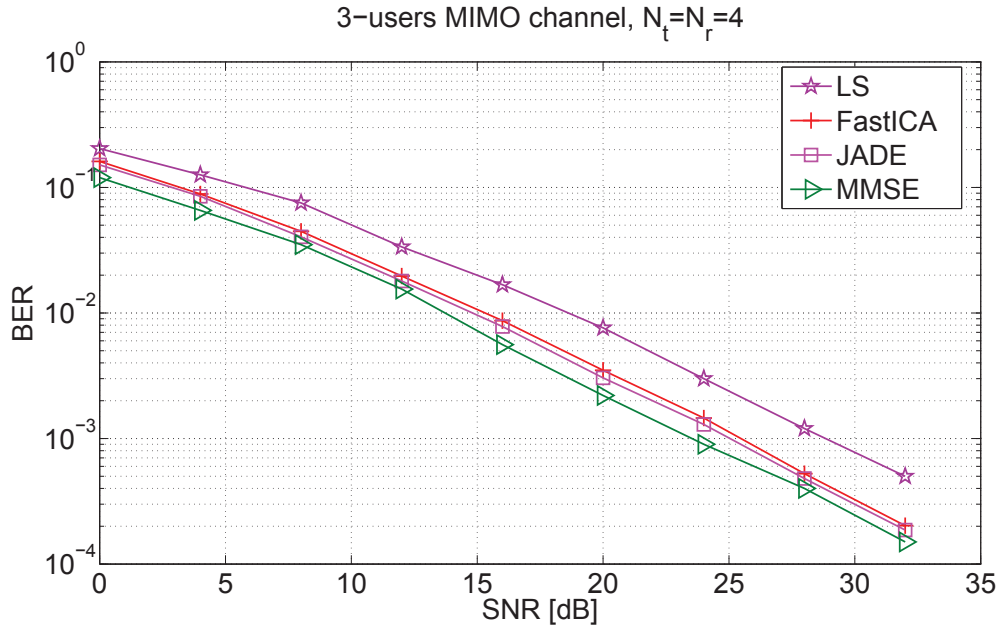


FIGURE 5: Taux d'erreur binaire en fonction de rapport signal sur bruit pour les détecteurs basé sur les techniques séparation de source, ainsi que le MMSE avec une connaissance d'interférence estimer et le MMSE à interférence parfaite pour $N_s = 8$ symboles d'apprentissage

connus, et nous cherchons à minimiser l'erreur quadratique moyenne normalisé avec les symboles détectés pour régler l'ordre des symboles, et à minimiser l'erreur quadratique moyenne non normalisé pour régler le facteur d'échelle.

Figures 5 et 6 illustrent les performances de taux d'erreur binaire (BER). La première figure, où le BER est tracé en fonction du SNR, compare les détecteurs basés sur les deux techniques de séparation de source JADE et ICA aux détecteurs: MMSE basé sur une connaissance parfaite de l'espace des interférences et MMSE basé sur une estimation de l'espace des interférences. Les détecteurs non classiques sont plus performants que ceux basés sur une estimation via des symboles d'apprentissage. Ces résultats s'interprètent à partir de la figure 6, qui montre que les performances des détecteurs classique et non classique se rapprochent quand le nombre des symboles de référence augmente. La supériorité des détecteurs non classique est due au fait que ces derniers ne sont pas très sensibles au nombre des symboles connus suite à une suppression aveugle des interférences.

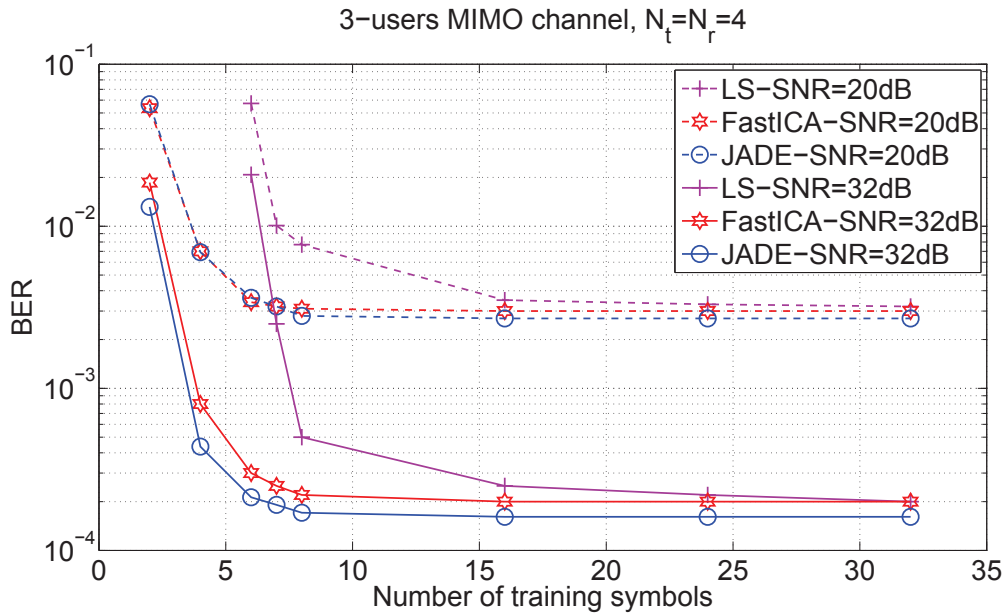


FIGURE 6: L'influence de nombre des symboles d'apprentissage sur le taux d'erreur binaire.

Schéma de détection en absence du schéma d'alignement d'interférence

Dans les deux parties précédentes, nous avons considéré un schéma d'IA à l'émission. Dans cette partie, nous nous sommes intéressés par le cas où les émetteurs n'ont pas une connaissance de l'état du canal, et par la suite l'IA n'est plus réalisable. Nous proposons deux schémas de détection itératifs, le premier est basé sur une minimisation d'une norme ℓ_1 et le deuxième basé sur une minimisation d'une fonction quadratique.

Le nouveau contexte est le suivant: les émetteurs ne connaissent pas l'état du canal et les récepteurs connaissent les canaux qui les lisent à tous les émetteurs, ce scénario est équivalent à une transmission uplink en communication mobile. Dans ce contexte, nous proposons de gérer les interférences de la façon suivante: chaque récepteur assume d'abord les interférences comme étant un signal désiré, une fois tout est décodé, le récepteur garde seulement les symboles désirés. De cette façon, les hypothèses à l'émission sont relâchées, et la complexité se reporte vers les stations de base. Nous nous mettons dans un cas MIMO avec une transmission de plusieurs symboles par utilisation de canal sur les différentes antennes, et nous considérons le cas pratique où l'alphabet de la constellation à l'émission appartient un ensemble fini.

Quand le nombre total des symboles à décoder est plus grand que le nombre des antennes à la réception, le système se rend sous déterminé. Pour une fiable détection des systèmes sous déterminé, il est proposé d'utiliser le critère de distance minimal. Cependant ce critère exige une recherche exhaustive avec un cot de calcul très élevé. Afin de réduire ce coût de calcul, nous montrons le modèle ici comme un modèle parcimonieux ¹.

La transition vers un modèle parcimonieux se résume dans l'exemple suivant. Un ensemble \mathcal{Q} constitué de trois éléments, et un vecteur \mathbf{q} inclue tous les éléments de cet ensemble. Nous définissons un dictionnaire comme dans la figure 7. Soit un vecteur \mathbf{x} ayant ses trois composantes appartenant à \mathcal{Q} . On attribue au premier composante le sous vecteur \mathbf{s}_1 , au deuxième composante le sous vecteur \mathbf{s}_2 et au troisième composante le sous vecteur \mathbf{s}_3 . Autrement dit, nous associons au vecteur \mathbf{x} de trois composantes un autre vecteur parcimonieux de dimension 9 qui ne contient que des composantes 0 et 1.

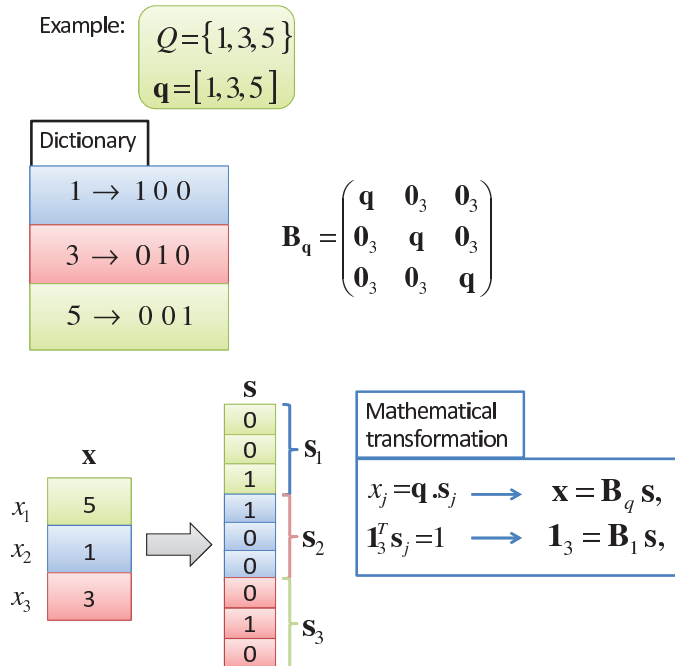


FIGURE 7: Décomposition parcimonieux du vecteur avec ses composantes appartenant sur un ensemble d'alphabet fini.

Suite à la transition vers un modèle parcimonieux comme dans la figure 7, le signal reçu s'exprime comme une nouvelle matrice de mélange sous-déterminée multipliée par un vecteur binaire source plus le vecteur bruit. Le problème sera

¹Un vecteur parcimonieux par définition est un vecteur qui a la majorité de ces éléments nuls.

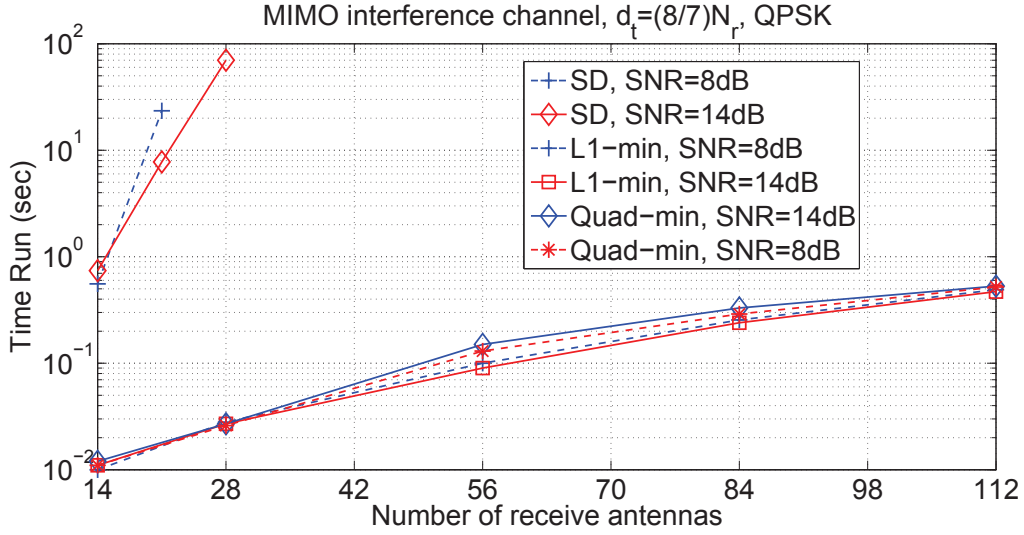


FIGURE 8: Comparaison du temps d'exécution des schémas de détection proposé contre le sphère décodeur pour différent valeurs de SNR sous une constellation discrète QPSK.

donc de chercher les composantes binaires d'un vecteur parcimonieux \mathbf{s} . Le nouveau problème de détection peut se résoudre soit par une minimisation d'une norme ℓ_1 bien défini sous des contraintes convexe linéaires et quadratiques, ou bien une minimisation d'une fonction quadratique défini par la distance euclidienne entre le signal reçu et les points de la constellation à la réception sous des contraintes convexe linéaires. L'avantage principal du deuxième problème est qu'il ne dépend d'aucun paramètre à optimiser. La contrainte quadratique dans le premier problème limite la zone de recherche dans une boule centrée de rayon constante. Les contraintes linéaires garantissent qu'au moins une composante non nulle existe dans chaque sous-vecteur. Les solutions des deux problèmes de détection proposés sont obtenues par l'utilisation des méthodes à complexité polynomiale comme la méthode du point intérieur.

Afin d'évaluer les performances, nous traçons d'abord le temps d'exécution en fonction du nombre des antennes à la réception comme montre la figure 8. La relation entre le nombre des antennes à la réception N_r et le nombre total des symboles émis d_t par utilisation de canal est donnée par la formule $N_r = \frac{7}{8}d_t$, ce qui rend le système sous-déterminé. Pour la comparaison de temps d'exécution des deux détecteurs proposés avec le sphère décodeur basé sur une recherche exhaustive dans une boule de rayon donné, nous observons une augmentation presque exponentielle du sphère décodeur tandis qu'avec les deux problèmes proposés l'augmentation est

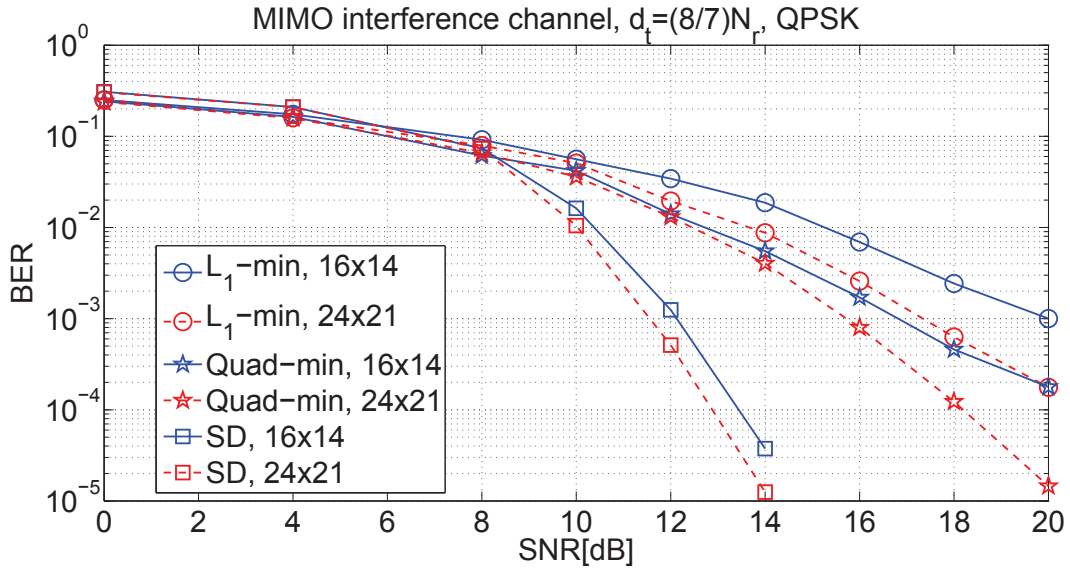


FIGURE 9: Comparaison des performances en taux d'erreur binaire pour les schémas de détection proposés contre le sphère décodeur sous une constellation QPSK.

presque linéaire.

Les performances de taux d'erreur binaire en fonction de SNR sont illustrés par la figure 9. Nous montrons les performances pour une configuration 24×21 , c. à d. un nombre total des symboles émis égal 24, ce qui implique une haute efficacité spectrale. Pour une probabilité d'erreur de 10^{-3} , nous observons une perte d'environ 4dB et 6dB de deux détecteurs basé sur la minimisation d'une fonction quadratique et basé sur la minimisation du norme ℓ_1 , respectivement, par rapport au décodeur par sphère.

Afin d'augmenter la fiabilité de transmission, nous intégrons le deuxième détecteur basé sur le problème de minimisation d'une fonction quadratique dans un schéma de turbo détection. Nous l'adaptions de façon à minimiser la probabilité d'erreur. Une connaissance à priori est que du côté émetteur, les composantes de chaque sous vecteur de vecteur parcimonieux \mathbf{s} représentent les poids de chaque symbole de la constellation. Autrement dit les probabilités de chaque symbole émis. Cette hypothèse est retenue au côté récepteur qui a les sorties du détecteur soft. Le détecteur adapté trouvé qui minimise la probabilité d'erreur nécessite une recherche exhaustive. C'est pourquoi, nous introduisons le nouveau critère basé sur l'approximation que la sortie du décodeur est Gaussienne.

Les performances de taux d'erreur binaire en fonction de SNR sont illustrés par la figure 10. Malgré les hypothèses inexacte, un gain très important accompagne

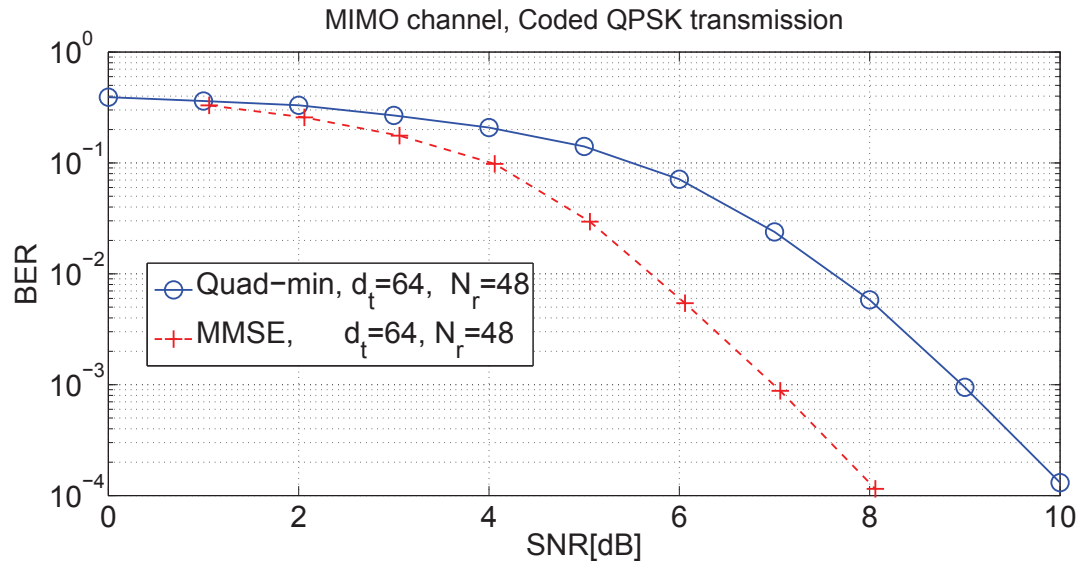


FIGURE 10: Performance en taux d'erreur binaire du schéma de turbo détection proposé pour une configuration large MIMO sous-déterminé sous une constellation QPSK et un rendement de code 1/2.

le schéma de turbo-détection intégré dans la chaîne de transmission. Par contre, une perte d'environ 2dB est obtenue par rapport au MMSE turbo égaliseur.

Abbreviations

AWGN	Additive white Gaussian noise
BC	Broadcast channel
BER	Bit error rate
BS	Base station
BSS	Blind source separation
CDM	Code division multiplexing
CSI	Channel state information
CSIT	Channel state information at the transmitter
DL	Downlink
DPC	Dirty paper coding
DoF	Degrees of freedom
FDM	Frequency division multiplexing
FEC	Forward error correction
IA	Interference alignment
IC	Interference channel
JADE	Joint approximate diagonalization of eigenmatrices
i.i.d.	Independent and identically distributed
KKT	Karush-Kuhn Tucker
LLR	Log-likelihood ratio
LTE	Long term evolution
LS	Least square
MAC	Multiple access channel
MAP	Maximum a posteriori
MI	Mutual information
MIMO	Multiple input multiple output
ML	Maximum likelihood
MD	Minimum distance
MMSE	Minimum mean square error
MSE	Mean square error
NMSE	Normalized mean square error

OFDM	Orthogonal frequency division multiplexing
PSK	Phase shift keying
QAM	Quadratic amplitude modulation
R_0	Cut-off rate
SD	Sphere decoder
SDM	Space division multiplexing
SISO	Single input single output
SNR	Signal-to-noise ratio
SINR	Signal to interference and noise ratio
SVD	Singular value decomposition
TDD	Time division duplexing
TDM	Time division multiplexing
TX-RX	Transmitter-receiver
UMTS	Universal mobile telecommunication system
UL	Uplink
V-BLAST	Vertical-Bell laboratories layered space-time
ZF	Zero forcing

Notations

x	Scalar x
\mathbf{x}	Vector \mathbf{x}
\mathbf{X}	Matrix \mathbf{X}
\mathbf{X}^T	Transpose of matrix \mathbf{X}
\mathbf{X}^*	Conjugate of matrix \mathbf{X}
\mathbf{X}^H	Hermitian of matrix \mathbf{X}
\mathbf{X}^{-1}	Inverse of matrix \mathbf{X}
$\text{trace}(\mathbf{X})$	Trace of matrix \mathbf{X}
$ \mathbf{X} $	Determinant of matrix \mathbf{X}
$\ \mathbf{a}\ _2$	ℓ_2 norm of vector \mathbf{a}
$\ \mathbf{a}\ _1$	ℓ_1 norm of vector \mathbf{a}
$\ \mathbf{a}\ _0$	ℓ_0 norm of vector \mathbf{a}
$\ \mathbf{A}\ _F$	Frobenius norm of matrix \mathbf{A}
\mathbf{I}_N	Identity matrix with N dimensions
$\mathbf{1}_M$	M -dimensional ones vector
$\mathbf{0}_M$	M -dimensional zeros vector
$\nu_{max}^l(\mathbf{A})$	Matrix of the l eigenvectors of \mathbf{A} corresponding to the l largest eigenvalues
$\nu_{min}^l(\mathbf{A})$	Matrix of the l eigenvectors of \mathbf{A} corresponding to the l smallest eigenvalues
$\mathbb{E}(\cdot)$	Expectation operator
\otimes	Kronecker products
$\min(a, b)$	Smallest element between a and b
$\max(a, b)$	Largest element between a and b

Contents

Abbreviations	xviii
Notations	xxi
List of Figures	xxvii
1 Introduction and motivations	1
1.1 Introduction	1
1.2 Motivations	2
1.3 Summary of the PhD contributions	3
2 State of the art on interference mitigation in wireless communications	7
2.1 Introduction	7
2.2 Radio propagation	7
2.2.1 Large-scale propagation models	8
2.2.2 Small-scale propagation models	9
2.3 Interference mitigation in mobile wireless communications	10
2.3.1 Multiplexing techniques	11
2.3.2 Achievable rate	12
2.4 Multi-user channel categories	13
2.5 Advanced techniques for data rate improvement under Gaussian input assumption	15
2.5.1 Broadcast channels	15
2.5.2 Multiple access channels	17
2.5.3 Interference channels	18
2.6 Optimality of the IA technique with respect to the input alphabet	20
2.7 Conclusion	22
3 Interference alignment for a multi-user SISO interference channel	23
3.1 Introduction	23
3.2 System model	24
3.3 IA design in a SISO interference channel	25
3.3.1 Precoding design	25

3.3.2	Linear decoding design	27
3.4	IA precoding subspaces optimization	28
3.4.1	MMSE-based decoder - Iterative solution	29
3.4.2	ZF-based decoder - Closed-form solution	30
3.4.3	Complexity and sum-rate performance	32
3.5	Precoding vectors design within IA subspaces	33
3.5.1	MMSE-based decoder	34
3.5.2	ZF-based decoder	35
3.5.3	Complexity and sum-rate performance	36
3.6	Convergence rate of the iterative solutions	36
3.7	Comparison of the proposed optimized designs to the state of art schemes	37
3.8	Conclusion	40
4	Linear detectors for downlink transmission with interference alignment	43
4.1	Introduction	43
4.2	Context and transmission network	45
4.3	System Model	45
4.4	Spatial IA design in a K-user MIMO IC	47
4.5	Traditional linear decoding in a spatial IA scheme	48
4.6	Desired signal extraction in a spatial IA scheme using high-cumulants order	50
4.6.1	Desired signal Extraction	50
4.6.2	Second-order information: Whitening	51
4.6.3	Joint Approximate diagonalization of Eigenmatrices	52
4.6.4	Semi-Blind separation	55
4.7	Simulation Results	56
4.8	Conclusion	63
5	Low complexity detectors based on sparse decomposition for up-link transmission	65
5.1	Introduction	65
5.2	System model	67
5.3	Joint decoding of interference and desired signal	68
5.4	Sphere decoding	69
5.5	Sparse decomposition	72
5.6	Iterative detection of sparse transformed MIMO via ℓ_1 -minimization	73
5.6.1	Noiseless MIMO channel	74
5.6.2	Noisy MIMO channel	75
5.7	Iterative detection of sparse transformed MIMO via minimum distance minimization	76
5.8	Complexity and bit error rate performance	79
5.9	Turbo detection of a sparse detected signal	82
5.9.1	Turbo detection concept	83

5.9.2	Turbo detection scheme	84
5.9.3	New detection criterion	86
5.9.4	Bit error rate performance	88
5.10	Conclusion	88
6	Conclusion and perspectives	91
6.1	Conclusion	91
6.2	Future works	92
A	Mutual information in the MIMO interference channels	95
B	Projected gradient method	99
C	Sum-rate gradient with respect to the combination matrix	101
D	Sphere Radius for the ℓ_1-minimization problem constraint	103
	Bibliography	105
	List of Publications	105

List of Figures

1	Canal à interférence mono-antenne entre trois utilisateurs en présence du schéma d'IA.	vii
2	Comparison du débit moyen par dimension pour plusieurs schéma de précodage quand $N = 3$	ix
3	Comparison du débit moyen par dimension pour plusieurs schéma de précodage quand $N = 5$	ix
4	Communication mobile sans fil: transmission downlink.	x
5	Taux d'erreur binaire en fonction de rapport signal sur bruit pour les détecteurs basé sur les techniques séparation de source, ainsi que le MMSE avec une connaissance d'interfèrnce estimer et le MMSE à interférence parfaite pour $N_s = 8$ symboles d'apprentissage	xii
6	L'influence de nombre des symboles d'apprentissage sur le taux d'erreur binaire.	xiii
7	Décomposition parcimonieux du vecteur avec ses composantes appartenant sur un ensemble d'alphabet fini.	xiv
8	Comparison du temps d'exécution des schémas de détection proposé contre le sphère décodeur pour different valeurs de SNR sous une constellation discrète QPSK.	xv
9	Comparison des performances en taux d'erreur binaire pour les schémas de détection proposés contre le sphère décodeur sous une constellation QPSK.	xvi
10	Performance en taux d'erreur binaire du schéma de turbo détection proposé pour une configuration large MIMO sous-déterminé sous une constellation QPSK et un rendement de code 1/2.	xvii
1.1	Mobile communication systems progress.	1
1.2	Multi-user mobile communication system transmission.	3
2.1	Multiplexing techniques for interference mitigation.	11
2.2	3-users MIMO Broadcast Channel	16
2.3	3-users MIMO Multiple-access Channel.	17
2.4	3-users MIMO Interference Channel.	19
2.5	Interference channel model studied in our work.	20
3.1	3-user SISO interference channel with IA scheme.	26
3.2	Average sum rate per dimension of the two proposed designs for subspace improvement with $N = 3$ and $N = 7$	33

3.3	Average sum rate per dimension of the proposed precoding vectors design using the combination matrices for $N = 3$ and $N = 7$	37
3.4	Convergence of the iterative algorithm in section 3.5.1 and the projected gradient method in section 3.4.1.	38
3.5	Comparison of the average sum rate per dimension for different precoding designs for $N = 3$	39
3.6	Comparison of the average sum rate per dimension for different precoding designs for $N = 5$	39
3.7	Comparison of the average sum rate per dimension for different precoding designs for $N = 7$	41
3.8	Evolution of the average sum rate per dimension with the precoding vectors length for the closed-form design with orthogonal precoding vectors, the iterative IA design [1], and the iterative design that maximizes the SINR [2].	41
4.1	Mobile interference network: transmission in downlink.	46
4.2	BER performance comparison using $N_s = 8$ training symbols	57
4.3	BER performance comparison using $N_s = 4$ training symbols	58
4.4	The influence of the training sequence length on the BER performance	58
4.5	NMSE for measuring the efficiency of the ICA algorithms	59
4.6	Effect of the IA imperfection on the BER performance $N_s = 8$	60
4.7	Effect of the IA imperfection on the BER performance $N_s = 8$	61
4.8	The channel estimation error for different SNR values using least square estimator	62
5.1	Sparse decomposition of a vector with components belonging to a finite alphabet set.	73
5.2	Time-run comparison of the proposed decoding schemes versus the sphere decoder for different SNR values under QPSK constellation inputs.	79
5.3	BER performance comparison of the proposed decoding schemes versus the sphere decoder under QPSK constellation inputs.	80
5.4	BER performance of the proposed decoding schemes for large antennas dimensions under QPSK constellation inputs.	81
5.5	Time-run comparison of the proposed decoding schemes versus the sphere decoder for different SNR values under 16-QAM constellation inputs.	81
5.6	BER performance of the proposed decoding schemes for large antennas dimensions under 16-QAM constellation inputs.	82
5.7	Turbo detection scheme	84
5.8	BER performance of the proposed turbo detector for large antennas dimensions under QPSK constellation inputs and code rate $1/2$	87
5.9	BER performance of the proposed turbo detector for underdetermined large MIMO under QPSK constellation inputs and code rate $1/2$	87

Chapter 1

Introduction and motivations

1.1 Introduction

Wireless communications have known an exponential growth and a fast progress over the past few decades. Nowadays, wireless mobile communications have evolved over time starting with the first generation primarily developed for voice communications. Later on, the second generation emerged and permitted data to be also processed. After a while, the third generation systems progressed due to the need of integrated voice, data and multimedia traffic. In the last few years, the fourth generation referred to as long term evolution has invaded the market and has attracted much attention as it offers an increasing capacity and speed using a different radio interface together with core network improvements.

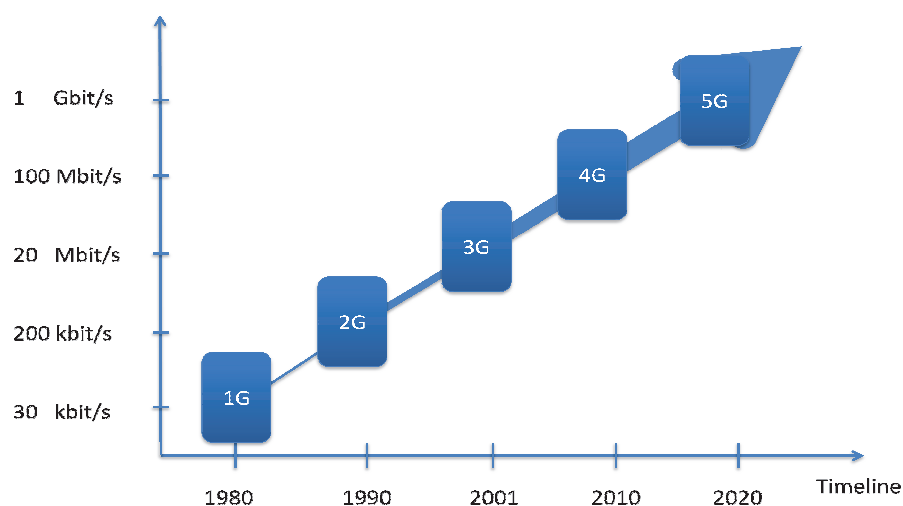


FIGURE 1.1: Mobile communication systems progress.

Overall throughput and transmission reliability are among the essential measures of the quality of service in a wireless system. Such measures are mainly subjected to interference management constraint in a multi-user network. The interference management is at the heart of wireless regulation and is essential for maintaining a desirable throughput while avoiding the detrimental impact of interference at the undesired receivers. Usually, interference incurring from undesired transmitters in a multi-user network is managed using some kind of multiplexing techniques. Such techniques commonly used in the previous and current generations of mobile communications, are based on the orthogonalization approach of the channel access by assigning the users orthogonal time/frequency/spatial resources. In single input single output channel, orthogonal access schemes can be used to divide the single degree of freedom among the users such that each user gets a fraction and the sum of these fractions is equal to one. Hence, the per-user throughput decreases as the number of users increases. Overcoming this inconvenient requires managing interference in different manner such that the per-user throughput remains independent of the number of active users.

Few years ago, a novel interference management technique appeared, known as interference alignment. Interference alignment has been initially proposed to deal with the interference caused by users sharing the same medium and using the same resources. The originality of this strategy of management is its efficiency for mitigating interference and for maximizing the overall throughput which can scale linearly with the number of users. Interference alignment technique has been introduced as an approach to maximize interference-free space for the desired signal. Its key idea is that all the interference can be concentrated roughly into one half of the signal space at each receiver, leaving the other half available to the desired signal and free of interference.

1.2 Motivations

In spite of its asymptotic optimality, interference alignment faces several practical challenges. One of the challenges is the sub-optimality in the finite signal-to-noise ratio region, since it does not achieve the channel capacity which in general is still not well defined. Another main challenge is to provide the knowledge of the perfect and full channel state information at the transmitters that links them to the receivers. Some designs based on distributed iterative algorithms do not require the full knowledge of the channels coefficients. However, these distributed

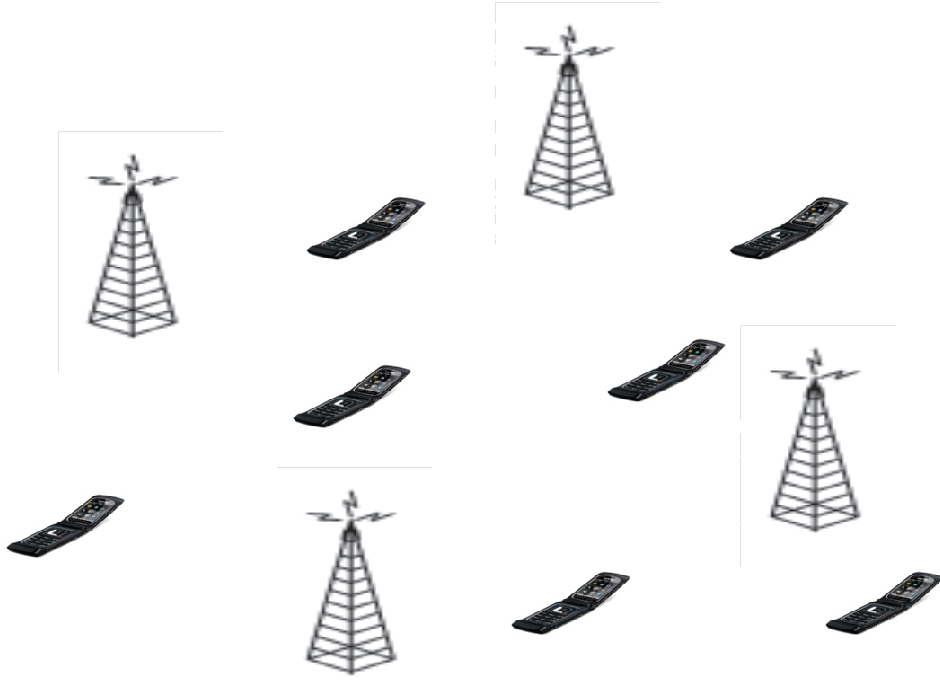


FIGURE 1.2: Multi-user mobile communication system transmission.

algorithms necessitate a high overhead signaling, which raises another challenge to deal with.

Our work is incorporated within the framework of interference channel where each node is equipped with single or multiple antennas. The goal is to resolve the challenges that the communications face in an interference network taking into account the computational efficiency and the complexity cost. We propose several solutions for the design at both the transmitter side and the receiver side, and we discuss some practical applications of the resulting schemes.

1.3 Summary of the PhD contributions

The first part of our work considers the single input single output interference channel. The goal is to show that although interference alignment is sub-optimal in the finite power region, it is able to achieve a significant overall throughput. We investigate the interference alignment scheme proposed for single input single output channel, which achieves a high multiplexing gain at any given signal dimension. Then, we try to modify the design in order to achieve an enhanced sum-rate performance in the practical SNR region. Firstly, we introduce a way

to optimize the precoding subspaces at all transmitters, exploiting the fact that channel matrices in the interference model of a single input single output channel are diagonal. Secondly, we propose to optimize jointly the set of precoder bases within their associated precoding subspaces. To this end, we combine each precoder with a new combination precoder, and this latter seeks the optimal basis that maximizes the network sum-rate.

Part of this work has been published in [3, 4, 5]

- Y. Fadlallah, A. Aissa-El-Bey, K. Amis and R. Pyndiah, “Interference Alignment : Improved Design via precoding Vectors,” in *In Proc. of IEEE Vehicular Technology Conference (VTC)-Spring*, Japan, May 2012.
- Y. Fadlallah, A. Aissa-El-Bey, K. Amis and R. Pyndiah, “Interference Alignment : Precoding Subspaces Design,” in *In Proc. IEEE International Workshop on Signal Processing Advances in Wireless Communications (SPAWC)*, Turkey, June 2012.
- Y. Fadlallah, K. Amis, A. Aissa-El-Bey and R. Pyndiah, “Formation de voie pour la maximisation du débit dans les schémas d’alignement d’interférence,” in *24eme édition du colloque GretsI*, Brest, France, Sept. 2013.

The second part assumes a K -user multiple input multiple output interference channel. We describe the interference alignment at the transmitter side, then we approach the linear decoding scheme at the receiver side. The interference are assumed to be aligned at each receiver, which transforms the decoding model into a determined linear model. Our approach of resolving the decoding problem is different from classical approaches based on interference subspace estimation. The main idea is to blindly separate the desired streams from the interference using higher-order cumulants. We show the equivalence between the problem to resolve and the determined blind source separation problem. Then, we propose to blindly extract the desired signal from the interference through a joint diagonalization of the fourth-order cumulants matrices [6]. We show that the separation ability is due to the independence between the desired signal and the interference.

Part of this work has been published in [7]

- Y. Fadlallah, A. Aissa-El-Bey, K. Abed-Meraim, K. Amis and R. Pyndiah, “Semi-blind source separation in a multi-user transmission system with interference alignment” *IEEE wireless communications letter*, to appear.

The last part assumes that the transmitters are not aware of the channel state information, and shows that decoding both desired signal and interference can achieve a full receive diversity. In this respect, we describe the joint optimal detector, which is characterized by a very high computational cost depending on the dimension of the decoding problem. Then, we try to find out alternative detectors that significantly reduce the computational cost at the detriment of error rate performance. The proposed detectors are robust even if the decoding problems are underdetermined. We also propose a channel coding scheme that employs a convolutional code at the transmitter side and a turbo-detector at the receiver side.

Part of this work has been published in [8] and submitted to

- Y. Fadlallah, A. Aissa-El-Bey, K. Amis, D. Pastor and R. Pyndiah, “New Decoding strategy for underdetermined MIMO transmission using sparse decomposition,” in *European Signal Processing Conference (Eusipco)*, Maroc, Sept. 2013.
- Y. Fadlallah, A. Aissa-El-Bey, K. Amis, D. Pastor and R. Pyndiah, “Iterative decoding strategy for underdetermined MIMO transmission using sparse decomposition” *Submitted to IEEE Transactions on Vehicular Technology*.
- A. Aissa-El-Bey, D. Pastors, S. M. Aziz-Sbai and Y. Fadlallah, “Recovery of Finite Alphabet Solutions of Underdetermined Linear System” *Submitted to IEEE Transactions on Information Theory*.

Another contribution is related to the non-optimality of the interference alignment under discrete constellation assumption. As such, we derive the mutual information under discrete constellation assumption, and we propose two ways to increase the data rate performance. One is by maximizing the joint cut-off rate that represents a lower bound on the mutual information. The other way is by approximating the mutual information using Taylor expansion. This contribution has been published in [9]

- Y. Fadlallah, A. Khandani, K. Amis, A. Aissa-El-Bey and R. Pyndiah, “Pre-coding and Decoding in the MIMO Interference Channels for Discrete Constellation,” in *IEEE International Symposium on Personal, Indoor and Mobile Radio Communications (PIMRC)*, UK, Sept. 2013.

Our thesis is organized as follows. Chapter 1 introduces our framework and contributions. Chapter 2 presents the well-known strategies for interference management in mobile wireless communications. In Chapter 3, we introduce the interference alignment concept for a multi-user single input single output interference channel. Then, Chapter 4 addresses the multi-user downlink transmission with interference alignment and proposes a linear detector based on blind source separation techniques. For uplink transmission when no precoding schemes are applied, we show in Chapter 5 the interest of decoding interference with the desired signal, and we propose low complexity detectors for high dimensional decoding problem. Finally, Chapter 6 concludes our thesis and proposes some perspectives.

Chapter 2

State of the art on interference mitigation in wireless communications

2.1 Introduction

This chapter deals with the usual techniques for interference mitigation in wireless systems. We first recall some features of transmission on the radio channel. Then we describe briefly orthogonal multiple access techniques and propose a classification of multi-user communication channels by giving the techniques used to deal with the multiple access interference.

2.2 Radio propagation

Wireless mobile communication systems suffer from performance limitations imposed by the propagation influences. In the mobile radio channel, the transmission path can vary from simple line-of-sight to the severely obstructed channel due to the motion of the mobile radio terminal, which makes the radio channels extremely random.

The information in a wireless channel is carried on an electromagnetic wave. This latter can be subjected to effects of the propagation environment such as reflection, diffraction and scattering. In order to characterize the propagation models, both empirical and analytical methods are used. The empirical approach results in a statistical model with an analytical description that recreates a set of measurements. In fact, propagation models are classified into two categories

[10]. The first category known as large-scale models, includes the models that predict the mean signal power for an arbitrary path separating a transmitter and a receiver. The second category known as small-scale fading, or fading models, includes the models that characterize the rapid fluctuations of the received signal power over short time duration.

2.2.1 Large-scale propagation models

Measurements-based propagation models have showed that average received signal power decreases logarithmically with distance separating a transmitter-receiver (Tx-Rx) pair. These models are used to estimate the received signal power as a function of distance and are called path loss models. The average path loss for an arbitrary Tx-Rx pair with distance d is expressed as [10]

$$\bar{P}L(d) \propto \left(\frac{d}{d_0}\right)^n, \quad \text{or} \quad \bar{P}L_{\text{dB}}(d) = \bar{P}L_{\text{dB}}(d_0) + 10n \log_{10} \left(\frac{d}{d_0}\right), \quad (2.1)$$

where n indicates the path loss exponent and d_0 the close-in reference distance. n depends on the propagation environment, e.g. in a free space environment n is equal to 2. The model in (2.1) considers that any distance d separating a Tx-Rx pair results in a constant path loss. However, two different Tx-Rx pairs at two different locations with the same separation distance may have the surrounding environment totally different. This implies that measured signals can be far away from the average value predicted in (2.1). Measurements have been derived in [11, 12], and have showed that at any distance d , the path loss PL at a particular location is random and log-normally distributed, i.e. Gaussian distributed when measured in dB [10]. That is,

$$PL_{\text{dB}}(d) = \bar{P}L_{\text{dB}}(d_0) + 10n \log_{10} \left(\frac{d}{d_0}\right) + X_\sigma, \quad (2.2)$$

where X_σ is a Gaussian distributed random variable with zero mean and variance σ^2 (in dB). The log-normally distributed random variable given in (2.2) describes the random shadowing effects. The close-in reference distance d_0 , the path loss exponent n and the standard deviation σ are the parameters that characterize the path model, which can be used to estimate the received power levels at a random location for communication system analysis purpose [10].

2.2.2 Small-scale propagation models

Small-scale fading, or simply fading, is a term used to describe the fluctuations of the parameters (phase, amplitude, frequency) of a radio signal over a small transmission distance. The most important effects in a fading channel are the fluctuation of the signal power, the fluctuation of the frequency modulation due to Doppler effect, and the time dispersion caused by the multipath propagation delays. For mobile wireless communications, fading effect usually occurs in urban areas where the mobile is surrounded by obstacles that prevent from a line-of-sight connection between the base station and the mobile terminal.

In a mobile radio channel, small-scale fading is influenced by the following major factors:

- Multipath propagation: the presence of reflecting objects and scatters in the channel disperses the signal parameters, and creates multiple modified versions of the transmitted signal displaced with respect to one another in time and phase.
- Terminal mobile motion: the movement of the destination causes a random modulation due to difference Doppler shifts on each of the multipath components. The frequency variation depends on the speed of the destination movement.
- Obstacles motion: when the obstacles of the propagation environment move, the multipath components undergo a time variation.
- Bandwidth of the transmitted signal: the small-scale fading strength depends on the transmitted signal bandwidth.

Slow and fast fading

The fading channel may be referred to as fast fading or slow fading channel depending on how fast the channel variations are compared to the transmitted baseband signal variations. If the coherence time T_c of the channel is smaller than the symbol period, i.e. the channel impulse response changes rapidly within the symbol duration, the channel is said fast fading. The coherence is used to characterize the time varying nature of the frequency variations of the channel in the time domain. It is inversely proportional to the Doppler spread D_s , i.e. $T_c \approx \frac{1}{D_s}$. If the symbol duration is much slower than the channel coherence time, i.e. $T \ll T_c$, the channel is supposed to be slow fading. In this case, the channel may be assumed to be static over one or several reciprocal bandwidths.

Flat and frequency selective fading

Frequency fading is mainly related to time dispersion due to multipath propagation. When the fading channel has a constant gain and linear phase response over a coherence bandwidth B_c that is greater than the bandwidth of the transmitted signal B_s , the radio channel is said flat fading channel. In a flat fading, the channel can be approximated with no excess delay, since the reciprocal bandwidth (symbol period) of the transmitted signal T is much larger than the channel time delay spread τ_{max} , i.e.

$$B_s \ll B_c, \quad \text{and } T \gg \tau_{max}. \quad (2.3)$$

Flat fading channels are also referred to as narrowband channels for which the transmission bandwidth is considered narrow when compared to the flat fading coherence bandwidth. On the other hand, if the fading channel has a constant gain and linear phase response over a bandwidth smaller than the transmitted signal bandwidth, the radio channel is called frequency selective fading channel. In such a case, the channel response has a time delay spread greater than the symbol period, i.e. $\tau_{max} > T$. This results in multipath effects, and multiple versions of the transmitted symbols are received attenuated and time-delayed which induces inter symbol interference. In the frequency domain, the transmitted components at different frequencies undergo different attenuation and phase shifts. Frequency selective fading channels are also referred to as wideband channels for which the signal bandwidth is supposed wide when compared to the coherence bandwidth.

The frequency selective fading channels can be transformed into adjacent flat fading subchannels by applying techniques such as orthogonal division frequency multiplexing (OFDM) that divides the wideband into many sub-bands much narrower than the coherence bandwidth. In our work, an OFDM scheme in a Rayleigh distributed channel. This assumption is commonly used in mobile radio channels to describe the envelope of an individual multipath component.

2.3 Interference mitigation in mobile wireless communications

In wireless communications, the ideal would be to allow the users in the same area to send information simultaneously in the same bandwidth to their intended receivers. Sending information at the same time in the same bandwidth will cause interference at the receiver side that, if dealt with as noise, enhances the noise

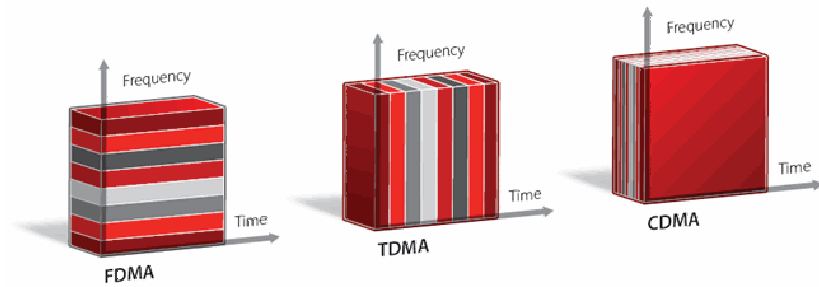


FIGURE 2.1: Multiplexing techniques for interference mitigation.

strength. Therefore, a wise management of interference is a challenging task so the users can share the same wireless medium. Multiplexing techniques used so far allocate the available resources in an orthogonal way. The three major multiplexing techniques used to share the available resources in wireless communication systems are: frequency division multiplexing (FDM) (orthogonal bandwidth allocation thanks to parallel sub-bands), time division multiplexing (TDM) (orthogonal time share thanks to successive time slots), and code division multiplexing (CDM) (orthogonal user signatures). Such techniques are applied for both narrowband and wideband systems.

2.3.1 Multiplexing techniques

Frequency division multiplexing: it assigns individual channels to individual users, i.e. each transmitter is allocated a unique frequency band that does not overlap with other user sub-bands. This requires the use of tight radio frequency filtering to eliminate the adjacent channel interference.

Time division multiplexing: it divides the transmission period into time slots, and each slot is allocated to one user. TDM consists in transmitting in a buffer-and-burst method, which means that for any user the transmission is discontinuous. The use of TDM requires an accurate time synchronization for interference elimination. This can be achieved using guard interval between different slots.

Code division multiplexing: it encodes the information by a pseudo random signature with very large bandwidth taken in a subset of near-orthogonal sequences. This technique allows the users to use the whole spectrum at the same time using different dedicated signatures. For detection of the desired information, the receiver correlates the received signal with the code of the desired user. When

the inter-correlation is high, i.e. the code matches the received signal, the desired signal is found and can be extracted.

As an analogy, we give the problem of people that want to talk to each other in a room. For a successful communication, each one can wait for his turn (TDM), or speak at different pitches (FDM), or use a different language (CDM).

Another multiplexing technique known as spatial division multiplexing (SDM), where users that transmit simultaneously in the same frequency band on multiple antennas aim at dividing the channel space into parallel channels. The concept of this technique is similar to the TDM that divides the time up to time slices and to the FDM that divides the spectrum into frequency bands, the SDM divides the space into parallel channels and information streams are sent independently and simultaneously in the same frequency band.

2.3.2 Achievable rate

The division multiplexing techniques described above succeed in avoiding interference induced from other users sharing the available resources. Such techniques result in a constant channel capacity, and a per user channel capacity that decreases with the increase of the number of users. When a single transmitter sends information in an additive white Gaussian noise (AWGN) channel with bandwidth B_s and average power p in watt, the channel capacity which represents the maximum rate of information that can be reliably transmitted over a communication channel is analytically expressed as [13]

$$C = B_s \log_2 \left(1 + \frac{p}{N_0 B_s} \right), \quad (2.4)$$

where N_0 is the noise power spectral density. When several transmitters want to share the same medium and apply the orthogonal division multiplexing techniques for network communication management, the total channel capacity between all Tx-Rx pairs is equal to the one given in (2.4). However, the channel capacity per user varies from one multiplexing technique to another. Using TDM technique, the capacity is equally-distributed between all users having equal time slot duration and equal average power. The capacity per user is given by [14]

$$C = \left(\frac{1}{K} \right) B_s \log_2 \left(1 + \frac{Kp}{N_0 B_s} \right), \quad (2.5)$$

where K is the total number of users sharing the same medium. A same expression is also obtained using FDM technique, for which the total bandwidth is divided into K sub-bands and equally-distributed between users. When the CDM is applied, the channel capacity depends on whether the transmitters can cooperate to exchange their pseudo-random sequence or not. When the cooperation is not allowed, the signals from other users are considered as noise, and hence the achievable capacity is upper bounded by a constant equal to $\frac{1}{\log_e(2)}$. When the cooperation is allowed, the total achievable rate for the K users assuming equal average power for each user is similar to that obtained for TDM and FDM, and the rate region is defined by the following equations

$$\begin{aligned} R_i &< B_s \log_2 \left(1 + \frac{p}{B_s N_0} \right) \quad \forall 1 \leq i \leq K, \\ R_i + R_j &< B_s \log_2 \left(1 + \frac{2p}{B_s N_0} \right) \quad \forall 1 \leq i, j \leq K \\ &\vdots \\ \sum_{i=1}^K R_i &< B_s \log_2 \left(1 + \frac{Kp}{B_s N_0} \right) \quad , \end{aligned} \quad (2.6)$$

where R_i represents the rate of the i^{th} user. From (2.6) one can notice that when the per user rates are identical, the CDM does not yield a higher rate than TDM and FDM. However, if the rates of the K users are selected to be unequal such that the inequations in (2.6) are satisfied, then it is possible to find an achievable per user rate that exceeds the per user capacity of FDM or TDM techniques.

Despite their ability to avoid interference and to provide a reliable communication over a wireless communication channel, the division multiplexing techniques result in a strong limitation for reaching the maximum achievable rate when applied for interference management in the multi-user interference channel (IC). Other techniques that involve precoding, i.e multi-stream beamforming, are able to deliver a higher data rate performance when applied for interference management, specially when the number of users is finite and both ends of a Tx-Rx pair are equipped with multiple antennas. The remaining of this chapter introduces the precoding concept for different multi-user single input single output (SISO) and multiple inputs multiple outputs (MIMO) channels.

2.4 Multi-user channel categories

As mentioned in Section 2.2, we consider a flat fading transmission channel. Denoting by \mathbf{y} the vector of symbols collected on the received antennas at a given

time instant, we can write

$$\mathbf{y} = \mathbf{H}\mathbf{x} + \mathbf{z}, \quad (2.7)$$

where \mathbf{H} is the channel matrix between the transmit antennas and the receive antennas, \mathbf{x} is the transmitted data vector from the transmit antennas at the same time instant, and \mathbf{z} is the white complex Gaussian distributed noise vector. Despite its simplicity, the model is extremely rich and describes several situations of interest in wireless communications. Depending on the transmitter and the receiver features, the different transmission channel types described by (2.7) are classified into the following categories

- When all antennas at the transmitter and the receiver are allowed to cooperate, i.e. full antennas cooperation, the channel can be viewed as a **single user MIMO channel**. The single user MIMO channel arises in multiple antenna wireless communications, e.g. LTE network.
- When no cooperation is allowed in the system and each antenna transmit to only one receive antenna, the channel is called a **SISO interference channel**.
- When the antennas are divided into groups and within each group the antennas fully cooperate, the channel is called a **MIMO interference channel (IC)**. The IC arises for example in peer to peer communication wireless networks.
- When only the receive antennas are allowed to cooperate and the transmit antennas are constrained to encode their signals independently, the model represents a **multiple access channel (MAC)**. The MAC arises in the uplink of cellular communications where multiple mobile terminals send data to a base station equipped with an antenna array.
- When only the transmit antennas can cooperate and the receive antennas are constrained to decode their messages independently, the model represents a **broadcast channel (BC)**. The BC represents the downlink of cellular communications where a base station equipped with an antenna array sends to multiple mobile terminals.

2.5 Advanced techniques for data rate improvement under Gaussian input assumption

The transmission model given by (2.7) is degraded by the co-channel interference effect. That is, the transmission from each antenna causes interference at the unintended antennas. Many techniques exist to struggle against this effect. In the case of a single user MIMO channel, one of the most efficient schemes is the singular value decomposition (SVD) based scheme. It consists in applying a unitary linear precoder and a unitary linear decoder that transform the channel into independent sub-channels. The SVD-based scheme is capacity-achieving and yields a minimum mean squared error (MMSE) at the receiver [15]. Designing such a scheme requires the knowledge of the channel state information (CSI) at the transmitter which is done using a feedback link from the receiver. Therefore, the channel estimation methods are of significant importance.

2.5.1 Broadcast channels

Similarly to MIMO single user channel, the knowledge of the channel state information at the transmitter (CSIT) in a MIMO BC allows the use of advanced processing techniques that increase the total channel throughput. Dirty paper coding (DPC) is a non-linear precoding technique that characterizes the capacity of a BC. DPC is based on the fact that a destination wants its private message free of interference. This principle has been introduced by Costa *et al.* in [16]. The authors have shown that with the idea of interference cancellation in mind, the capacity of a channel where the transmitter knows the interfering signal is the same as if there were no interference. A proposed analogy was that from an information theory point of view, writing on dirty paper is equivalent to writing on clean paper when one has a priori knowledge of the dirt place. In [17], this concept has been applied to downlink transmission in a multi-user MIMO channel. When the CSI is available at the base station (BS), this latter knows the interference that the first user will produce at the second user, and hence can design a signal that avoids the known interference at the second user. This concept has been used to characterize the capacity region of the MIMO BC [18]. The proposed DPC technique for the MIMO BC uses a QR decomposition of the channel matrix between the BS and the users. This channel matrix can be decomposed as the product of an unitary matrix with an upper-triangular matrix, or equivalently as the product of a lower triangular matrix \mathbf{L} with a unitary matrix \mathbf{Q} , i.e. $\mathbf{H} = \mathbf{LQ}$.

The transmitted signal from the BS is precoded with the Hermitian transpose of \mathbf{Q} . At the end users, the effective channel seen is \mathbf{L} . The first user of this system sees no interference from signal transmitted to the other users, therefore its signal may be processed without those coming from the other users. The second user sees interference only from the signal transmitted to the first user, therefore this interference is known and can be overcome using DPC. Subsequent users are dealt with in a similar manner.

Another precoding concept is the linear precoding, which is a linear transformation of the data vector by a matrix \mathbf{P} at the transmitter. When the CSIT is available, the precoder can be sought to fulfill many criteria. A well known criterion is to reduce the inter-user interference by imposing the constraint that all interference terms are zero. When K is less than or equal to the number of transmit antennas N_t , this can be accomplished by multiplying the data vector by the pseudo inverse of the channel matrix, known as channel inversion precoding [19]. However, this method faces a real problem when the channel matrix is ill-conditioned and the transmitter is allocated a limited power. It results in a dramatically degraded SNR at the receiver, hence poor data rate performance.

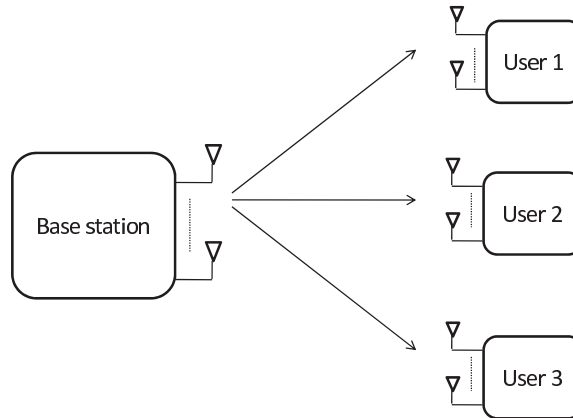


FIGURE 2.2: 3-users MIMO Broadcast Channel

Allowing some interference level at the receiver is usually better in terms of sum-rate improvement. A simple way of precoding that derives from the linear MMSE criterion is to select the precoder as $\mathbf{P} = (\mathbf{H}^H \mathbf{H} + \alpha \mathbf{I})^{-1}$, referred to as regularized channel inversion [20]. This simple procedure results in a sum-rate that grows linearly with $\min(N_t, K)$, the DoF of the MIMO BC, but at a rate that is somewhat slower than the capacity. If some receivers are equipped with more than

one antenna, the channel inversion technique can still be applied but with a lower efficiency than in the single receive antenna case, since antennas for the single user can cooperate and jointly detect the desired symbols. Therefore, the channel inversion is replaced by the block channel inversion or block diagonalization [21]. As for channel inversion, this approach does not achieve capacity, but offers a relatively low computational cost. Now, when a linear decoder is applied at the receivers and is known to the transmitter, the optimal linear precoder depends on the optimal linear decoder. Consequently, some arbitrary precoding and decoding vectors can be chosen for the transmitter and the receiver, and then iteratively optimized until a convergence criterion is satisfied. This iterative processing is characterized by its high computational cost in favor of the best performance.

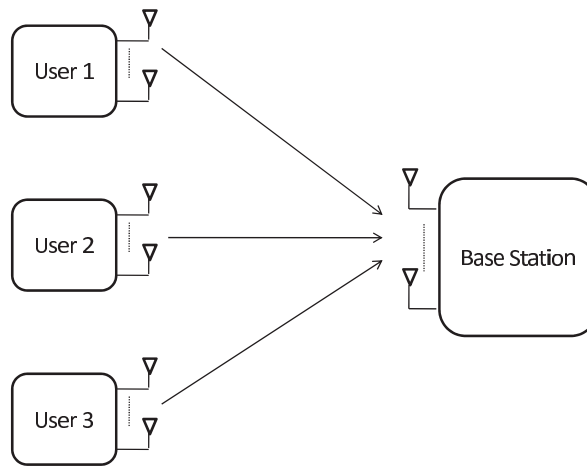


FIGURE 2.3: 3-users MIMO Multiple-access Channel.

2.5.2 Multiple access channels

In a MIMO MAC, the precoding has no interest when the users cannot cooperate with each other in the uplink transmission. The capacity region of the MAC reaches its upper limit for Gaussian distributed input and depends only on the input covariance [22]. In the cases where the joint design (i.e. cooperation) is possible, the optimal input covariance matrix is obtained by maximizing the channel weighted sum rate, which is a convex optimization problem under Gaussian input assumption. When only sum rate criterion is considered, the problem is optimized using iterative water-filling algorithm developed in [22]. Precoding design can also

be applied taking into account other criteria. For instance, in [23] the mean square error (MSE) is minimized under the assumption of a linear receiver. In [24], the signal-to-interference and noise ratio (SINR) is maximized assuming an iterative linear receiver.

2.5.3 Interference channels

As explained previously, the BC and MAC model the downlink and uplink transmissions, respectively, in a mobile wireless communication. In a cellular environment, one cell is not isolated from the others, and therefore the effects of the cell interaction must be taken into consideration in the received signal model. This case arises when many point-to-point links sharing a same medium need to establish communication simultaneously. IC is the situation in which multiple transmitters send their messages independently to their intended receiver, and transmitters and receivers are not aware of the interference caused by each other.

The main difference between the IC and the multiple access and broadcast channels lies in their channel capacity characterization. For the BC and MAC, the capacity region is well-defined (see [18] and [22]), and optimal transmit-receive designs have been derived for capacity achieving. However, in the IC where no cooperation is allowed between the transmitters and the receivers, the characterization of the channel capacity, until recently, was an open problem and very little was known about its region. An important step in this direction is the characterization of the degree of freedom (DoF) of a K -user interference network. The DoF represents the asymptotical rate of growth of the network capacity with the \log_2 of the signal to noise ratio (SNR). The spatial DoF turns out to be the number of non-interfering paths that can be created in a wireless network through signal processing at the transmitters and receivers. The definition of the DoF was first introduced by Host-Madsen *et al.* in [25] as follows

$$\lim_{snr \rightarrow \infty} \frac{C(snr)}{\log_2(snr)} = DoF, \quad (2.8)$$

The DoF of an interference network has been demonstrated by Cadambe *et al.* in [26] to be equal to $\frac{K}{2}$ using a new approach of interference management proposed first by Maddah *et al.* in [27] and known as interference alignment (IA) approach. With the innovative idea of IA, the authors in [26] have closed the gap with the upper bound on the DoF $\frac{K}{2}$ obtained by the authors in [25]. IA consists of linear precoding at the transmitters and zero forcing (linear decoding) at the receivers,

and can be applied for SISO and MIMO IC [26, 27, 28], in the quasi-static and the time-varying fading cases [26, 29]. This process is very efficient in terms of computational cost. However, it requires a heavy signaling to communicate all channel coefficients between transmitters and receivers to the transmitters in order to complete the IA design. Another IA achieving strategy is to communicate to each transmitter the coefficients of the channels that link it to all receivers, and then to seek the IA precoders iteratively using distributed algorithms between each Tx-Rx pair. Such an algorithm is described in [2] in the case of MIMO IC. The authors have proposed to seek the precoders iteratively so that the interference leakage power is minimized. Other algorithms have been later proposed taking into account other criteria such as minimum mean square error (MMSE), network sum-rate, power minimization [1, 30, 31] and so on. Some closed form solutions that achieve optimized DoF have also been derived among which we can quote [26] and [32].

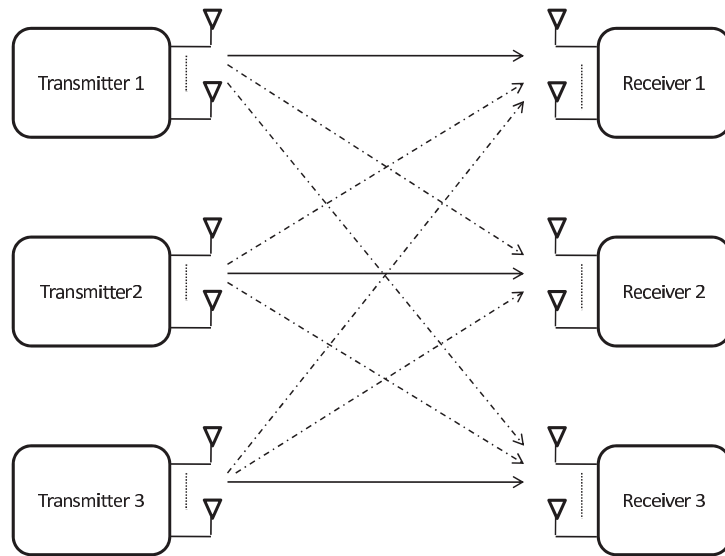


FIGURE 2.4: 3-users MIMO Interference Channel.

Several IA schemes have been introduced since the first proposed for SISO time-varying channels in [26]. In all these schemes, the received subspace is the sum of the linearly independent desired and interference subspaces to which noise subspace is superposed. This decomposition also holds in the case of multiplexing techniques described in section 2.3.1, but the dimension of the desired subspace is smaller. For example, assuming a K -user SISO IC, when the dimension of the

received signal vector is of order K , the dimensions of the desired subspace and the interference subspace are 1 and $K - 1$ respectively. When the IA technique is used instead, the desired subspace dimension tends asymptotically to $\frac{K}{2}$.

2.6 Optimality of the IA technique with respect to the input alphabet

The preceding paragraph has introduced the IA design as an asymptotic capacity-achieving ; i.e. for Gaussian-distributed channel input (continuous input constellation). However, does IA keep this asymptotic rate optimality under practical assumptions, e.g. under discrete input constellation assumption? Not necessarily, since the maximum rate-achieving linear precoding design is the one that maximizes the mutual information (MI).

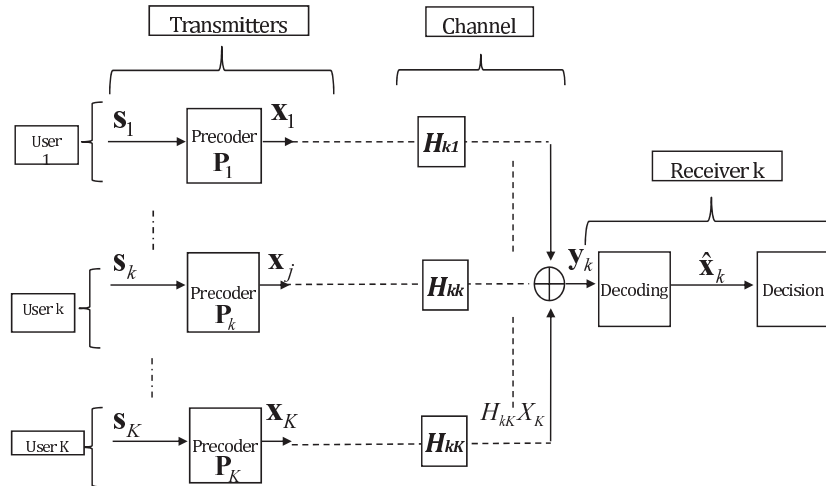


FIGURE 2.5: Interference channel model studied in our work.

In most research works, the MI has been maximized under the assumption of Gaussian input distribution. Unfortunately, this assumption seems to be far away from the practical systems that employ a discrete input constellation such as phase shift keying (PSK) modulation and quadratic amplitude modulation (QAM). Several papers have discussed the precoding optimization under finite alphabet constellation in single user and multi-user channels. For instance, the linear precoding scheme that maximizes the MI for discrete constellation in a single user MIMO

channel has been addressed in [33]. The authors have proved that the MI is a concave function of a matrix which is itself a quadratic function of the precoding matrix. For multi-user channels, other schemes have been defined such as [34] and [35], where the MI expression has been derived for both BC and MAC. In the multi-user IC, the maximum rate-achieving linear precoding scheme is also the one that maximizes the MI expression which have to be derived. In this section, we are interested in this general case where the model is represented as

$$\mathbf{y}_k = \sum_{j=1}^K \mathbf{H}_{kj} \mathbf{P}_j \mathbf{x}_j + \mathbf{z}_k, \quad (2.9)$$

where $\mathcal{K} = \{1, \dots, K\}$ is the set of all users, \mathbf{y}_k is the received signal vector at receiver k , \mathbf{H}_{kj} is the complex channel matrix between the j^{th} transmitter and the k^{th} receiver, \mathbf{P}_j is the precoding matrix of the j^{th} transmitter. The j^{th} transmitted information \mathbf{x}_j is defined as a $d_j \times 1$ vector from a discrete constellation. \mathbf{z}_k is the $N \times 1$ circularly symmetric complex Gaussian noise vector at the receiver k , with independent and identically distributed (i.i.d.) components and zero mean and $\sigma^2 \mathbf{I}_N$ variance; i.e. $\mathbf{z}_k \sim \mathcal{N}_c(0, \sigma^2 \mathbf{I}_N)$.

For such a case, the MI can be expressed as (see Appendix A for more details)

$$\begin{aligned} I(\mathbf{x}_k; \mathbf{y}_k) &= \log_2(M^{d_k}) + \frac{1}{M^{Kd_k}} \sum_{a_1, \dots, a_K} \mathbb{E} [\log_2 (J_k(\mathbf{y}_k, a_1, \dots, a_K))] \\ &- \frac{1}{M^{Kd_k}} \sum_{a_1, \dots, a_K} \mathbb{E} [\log_2 (J_k(\mathbf{y}_k, a_1, \dots, a_{k-1}, a_{k+1}, \dots, a_K))] \end{aligned} \quad (2.10)$$

where

$$J_k(\mathbf{y}_k, a_1, \dots, a_K) = \sum_{a'_1, \dots, a'_K} \exp \left(- \frac{\|\mathbf{z}_k + \sum_{j=1}^K \hat{\mathbf{H}}_{kj} (\mathbf{x}_j^{a_j} - \mathbf{x}_j^{a'_j})\|^2}{\sigma^2} \right),$$

$$\begin{aligned} J_k(\mathbf{y}_k, a_1, \dots, a_{k-1}, a_{k+1}, \dots, a_K) &= \\ &\sum_{a''_1, \dots, a''_{k-1}, a''_{k+1}, \dots, a''_K} \exp \left(- \frac{\|\mathbf{z}_k + \sum_{j \neq k}^K \hat{\mathbf{H}}_{kj} (\mathbf{x}_j^{a_j} - \mathbf{x}_j^{a''_j})\|^2}{\sigma^2} \right), \end{aligned}$$

where $\hat{\mathbf{H}}_{kj} = \mathbf{H}_{kj} \mathbf{P}_j$, and the indexes a_j, a'_j, a''_j are in the set $\mathcal{M}_{d_j} = \{1, \dots, M^{d_j}\}$ for all j with M the constellation set length for one symbol. $\mathbf{x}_j^{a_j}$ is a symbol

vector from the j^{th} transmitter belonging to the set \mathcal{Q}^{d_j} . The MI expression given in 2.10 is a one-dimensional integration that can be resolved using Monte-Carlo simulation.

Seeking the linear precoding scheme that maximizes the MI expression in a closed-form is non trivial. Therefore, iterative algorithm for multi-variable optimization can be employed, where at each iteration the optimization is based on the gradient descent. On the other hand, a huge computational cost may pursue this iterative process since the calculation of the MI is required many times ; i.e. Monte-Carlo simulations might be required many times. Other solutions can be proposed for computational cost reduction by replacing the MI criterion by another criterion such as cut-off rate which represents a tight lower bound on the MI. A criterion modification might result in a sub-optimal performance but more efficiency in term of computational cost.

2.7 Conclusion

In this chapter, we have described the constraints imposed by the wave propagation environment on the mobile wireless communication systems. Then, the commonly used multiplexing techniques for interference avoidance have been briefly presented with a focus on the achievable rate. Applied in a multiple access case and given an average SNR value, limitations of these techniques for reliable communications are twofold: Either the target data rate imposes the maximum tolerable number of users or the number of users being fixed and the per user data rate cannot exceed a maximum value. Higher achievable rates can be obtained by applying at the transmitter a precoding concept optimized with this regard. A brief description of precoding techniques for different multi-user channel categories has been presented assuming Gaussian-distributed inputs. In next chapter, we come back to the interference alignment scheme and consider the case of SISO interference channel.

Chapter 3

Interference alignment for a multi-user SISO interference channel

3.1 Introduction

In most existing wireless communication systems, interference is avoided either by coordinating the users to orthogonalize the channel access, or by treating interference from other transmitters as noise. However, until recently, the capacity region of the IC remained unknown, except for some special cases such as strong and very strong interference [36, 37]. In [27], Maddah *et al.* have proposed a new approach in order to show that the N -antennas MIMO X -channels can offer as much as $\frac{4N}{3}$ DoF. This new approach of interference management has been named IA.

The key idea of IA is to jointly design all transmitted signals such that interfering signals at each receiver overlap and remain distinct from the desired signal. This approach has been exploited by Cadambe *et al.* in [26]. The authors have shown that the maximum achievable DoF in the K -user time-varying SISO IC, in the N -dimensional Euclidean space, is $\frac{K}{2}$, and is achieved thanks to an IA scheme. Later on, Motahari *et al.* have addressed the achievable DoF of a quasi-static IC. They have extended the idea of IA from space/time/frequency dimensions to the signal level dimensions, and have shown that based on the field of Diophantine approximation in number theory [29], the interference can be aligned in the rational spaces, achieving a maximum DoF of $\frac{K}{2}$.

The first IA scheme for SISO transmissions has been proposed in [26] for the

time/frequency varying channel. This scheme has been designed to achieve the asymptotic capacity in the IC, i.e. when both the SNR and the signal dimensions tend to infinity. In contrast, Choi *et al.* have introduced another IA design that aims to achieve a higher multiplexing gain at any given signal dimension [38]. In this chapter, we adopt the IA scheme proposed by Choi *et al.* for SISO transmission, and we try to modify the design in order to achieve higher sum-rate performance in the practical SNR region. Firstly, we introduce a way to optimize the precoding subspaces at all transmitters, exploiting the fact that channel matrices in the IA model are diagonal. Two solutions are derived. The first is achieved iteratively using projected gradient descent method. The second is a closed-form solution that avoids the numerical computation, thus, resulting in a very low computational complexity. Secondly, we propose to optimize the precoding vectors at each transmitter within its precoding subspace. To this end, we combine each IA precoder with a new combination precoder. The combination precoder seeks the optimal basis that maximizes the network sum-rate assuming an individual transmit power constraint. However, a closed-form solution seems non trivial. Therefore, we apply an iterative process based on the simple gradient descent method, and converges to a local maximum due to the non-concavity of the objective function.

This chapter is organized as follows. Section 3.2 describes the system model. Then, Section 3.3 presents the IA design in SISO IC. In Section 3.4, we propose to optimize the network sum-rate through a diagonal matrix \mathbf{W} . The precoding vectors optimization within the IA subspaces is presented in Section 3.5. In section 3.6, we present the convergence rate of the proposed iterative algorithms. Section 3.7 evaluates the sum-rate performance of the proposed optimization. Finally, Section 3.8 concludes the chapter.

3.2 System model

Let us assume a K -user SISO IC with K transmitter-receiver pairs. A wireless channel links each receiver to each transmitter, but a given transmitter intends to have its signal decoded by a single dedicated receiver only. User j transmits a symbol vector of length d_j . This symbol vector is then precoded using an $N \times d_j$ precoding matrix, and transmitted through a frequency/time-varying complex channel. In a SISO transmission, the vector of symbols is transmitted using channel extensions or realizations. For instance, in a frequency selective (frequency varying)

channel, each symbol occupies one frequency slot. The received signal at the k^{th} receiver can be modeled as

$$\mathbf{y}_k = \sum_{j=1}^K \mathbf{H}_{kj} \mathbf{V}_j \mathbf{s}_j + \mathbf{z}_k, \quad \forall k \in \mathcal{K}, \quad (3.1)$$

where $\mathcal{K} = \{1, \dots, K\}$ is the set of all users, $\mathbf{H}_{kj} \in \mathbb{C}^{N \times N}$ is the diagonal channel matrix between the j^{th} transmitter and the k^{th} receiver, $\mathbf{V}_j \in \mathbb{C}^{N \times d_j}$ is the precoding matrix of the j^{th} transmitter. The j^{th} transmitted information \mathbf{s}_j is defined as a $d_j \times 1$ vector belonging to a Gaussian continuous constellation. \mathbf{z}_k is the $N \times 1$ circular symmetric complex Gaussian noise vector at the receiver k , with i.i.d. components; i.e. $\mathbf{z}_k \sim \mathcal{N}_c(0, \sigma^2 \mathbf{I}_N)$. We also consider the following hypothesis in this chapter:

1. Users do not cooperate.
2. Non-precoded user symbols are Gaussian continuously distributed and mutually independent.
3. The set of channel matrices \mathbf{H}_{kj} is entirely and perfectly known at all transmitters and all receivers.
4. All diagonal components of $\mathbf{H}_{kj} \forall k, j \in \mathcal{K}$ are independent and identically distributed (i.i.d.) and continuously distributed, with absolute values upper-bounded with a finite value.

The maximum achievable DoF in the K -user SISO IC is equal to

$$\lim_{snr \rightarrow \infty} \frac{C(snr)}{\log_2(snr)} = \frac{K}{2}, \quad (3.2)$$

where $C(snr)$ represents the channel capacity.

3.3 IA design in a SISO interference channel

3.3.1 Precoding design

The essence of the IA scheme is to design the transmit beamforming matrices in a way that the interference-free stream number at each receiver is maximized.

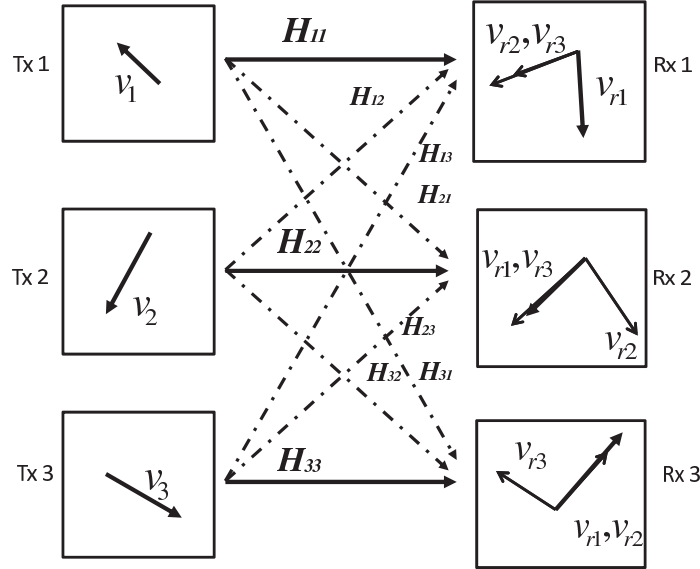


FIGURE 3.1: 3-user SISO interference channel with IA scheme.

The IA design conditions have been defined as follows

$$\begin{aligned} \text{rank}(\mathbf{U}_k \mathbf{H}_{kk} \mathbf{V}_k) &= d_k, \\ \mathbf{U}_k \mathbf{H}_{kj} \mathbf{V}_j &= 0, \forall j \neq k, \end{aligned} \quad (3.3)$$

where \mathbf{U}_k is the decoding matrix at the k^{th} receiver. In other words, the desired signal belongs to the subspace generated by the vectors of $\mathbf{G}_k = \mathbf{U}_k \mathbf{H}_{kk} \mathbf{V}_k$, while the interference is completely eliminated. The feasibility of the linear system in (4.3) is conditioned to the following: i) the linear system has to be proper, i.e. the number of variables is more than or equal to the number of equations, ii) the linear system has to be generic [28]. In some particular case, the genericity is satisfied by providing a channel matrix with random and independent coefficients.

An example on the IA design is given in Figure 3.1. A particular case where three users sharing the same resources are communicating. Each transmitter has one symbol to transmit to its dedicated receiver. All channel coefficients are supposed known at all transmitters¹. In order to achieve the IA linear precoding design, each transmitter k transmits its symbol in the direction of a two-dimensional vector \mathbf{v}_k , and the precoding vectors at all transmitters are conceived in such a way that at all receivers the vectors carrying the two interfering symbols are aligned

¹This hypothesis is very optimistic, but it is taken by many research works in the literature.

and linearly independent of the vector that carry the desired symbol. Then, the interference are eliminated by a simple projection on the interference null space.

One precoding design that provides IA at all receiver nodes and fulfills the conditions in (3.3) in the SISO interference channel is proposed by Choi et al as [38]

$$\begin{aligned}
\mathbf{V}_1 &= \left\{ \prod_{k,l \in \mathcal{K} \setminus \{1, k \neq l, (k,l) \neq (2,3)\}} ((\mathbf{T}_{23})^{-1} \mathbf{T}_{kl})^{n_{kl}} \mid \sum_{k,l \in \mathcal{K} \setminus \{1, k \neq l, (k,l) \neq (2,3)\}} n_{kl} \leq m^* + 1 \right\}, \\
\mathbf{V}_3 &= \left\{ (\mathbf{T}_{23})^{-1} \prod_{k,l \in \mathcal{K} \setminus \{1, k \neq l, (k,l) \neq (2,3)\}} ((\mathbf{T}_{23})^{-1} \mathbf{T}_{kl})^{n_{kl}} \mid \sum_{k,l \in \mathcal{K} \setminus \{1, k \neq l, (k,l) \neq (2,3)\}} n_{kl} \leq m^* \right\}, \\
\mathbf{V}_j &= \mathbf{H}_{1j}^{-1} \mathbf{H}_{13} \mathbf{V}_3, \\
\mathbf{T}_{kl} &= (\mathbf{H}_{k1})^{-1} \mathbf{H}_{kl} (\mathbf{H}_{1l})^{-1} \mathbf{H}_{13}.
\end{aligned} \tag{3.4}$$

where m^* is any non-negative integer which defines the number of transmitted symbols and the length of the precoding vectors, and \mathbf{T}_{kl} is an $N \times N$ diagonal matrix. In the IA design described above, the achievable DoF per user can be obtained using the following combinations

$$d_1 = \binom{m^* + M + 1}{M} \quad \text{and} \quad d_3 = \binom{m^* + M}{M},$$

where M is a parameter depending on the user number, $M = (K-1)(K-2) - 1$, d_i is the DoF of the i^{th} user i.e. the number of transmitted symbols, and N is defined as $N = d_1 + d_2$. In the particular scheme above, the IA conditions can be satisfied by providing $d_i = d_3$, $d_1 > d_3$, $i \in \mathcal{K} \setminus \{1, 3\}$. For example, in a 3-user SISO multi-user IC, we have $d_1 = n + 1$, $d_2 = d_3 = n$, $N = 2n + 1$, and n can be any non negative integer.

3.3.2 Linear decoding design

In the aforementioned transmission model, the received signal given in (3.1) can be rewritten as

$$\mathbf{y}_k = \underbrace{\bar{\mathbf{H}}_k^k \mathbf{s}_k}_{\text{Desired subspace}} + \underbrace{\sum_{j \neq k} \bar{\mathbf{H}}_j^k \mathbf{s}_j}_{\text{Interference subspace}} + \mathbf{z}_k, \tag{3.5}$$

where $\bar{\mathbf{H}}_j^k = \mathbf{H}_{kj} \mathbf{V}_j$. We assume that the IA conditions are satisfied. Let $\bar{\mathbf{H}}_I^k \in \mathbb{C}^{N \times (N-d_k)}$ denotes the $N-d_k$ matrix spanning all interference subspaces ; i.e. $\bar{\mathbf{H}}_j^k$ for $j \in \{1, \dots, K\}$, $j \neq k$ are all spanned by $\bar{\mathbf{H}}_I^k$. Before going further into the description, we introduce the following lemma.

Lemma 1. Let $\mathbf{A}_1 \in \mathbb{C}^{N \times n}$ and $\mathbf{A}_2 \in \mathbb{C}^{N \times n}$ ($N > n$), where $\text{rank}(\mathbf{A}_1) = n$ and $\text{rank}(\mathbf{A}_2) = m$, ($m \leq n$) and $\text{span}(\mathbf{A}_2) \subset \text{span}(\mathbf{A}_1)$. Then, for every $\mathbf{s}_2 \in \mathbb{C}^{n \times 1}$, $\exists \mathbf{s}_1 \in \mathbb{C}^{n \times 1}$ such that $\mathbf{A}_1 \mathbf{s}_1 = \mathbf{A}_2 \mathbf{s}_2$

Using Lemma 1 at the receiver k , the interference subspace from the j^{th} transmitter can be expressed in terms of $\bar{\mathbf{H}}_I^k$ as

$$\bar{\mathbf{H}}_j^k \mathbf{s}_j = \bar{\mathbf{H}}_I^k \mathbf{s}_{jI}, \text{ where } \mathbf{s}_{jI} = \left(\bar{\mathbf{H}}_I^{kH} \bar{\mathbf{H}}_I^k \right)^{-1} \bar{\mathbf{H}}_I^{kH} \bar{\mathbf{H}}_j^k \mathbf{s}_j. \quad (3.6)$$

Substituting (3.6) into (3.5) yields

$$\begin{aligned} \mathbf{y}_k &= \bar{\mathbf{H}}_k^k \mathbf{s}_k + \bar{\mathbf{H}}_I^k \bar{\mathbf{s}}_k + \mathbf{z}_k \\ &= \begin{bmatrix} \bar{\mathbf{H}}_k^k & \bar{\mathbf{H}}_I^k \end{bmatrix} \begin{bmatrix} \mathbf{s}_k^T & \bar{\mathbf{s}}_k^T \end{bmatrix}^T + \mathbf{z}_k \\ &= \mathbf{B}_k \tilde{\mathbf{s}}_k + \mathbf{z}_k, \end{aligned} \quad (3.7)$$

where $\bar{\mathbf{s}}_k = (\mathbf{s}_{1I} + \dots + \mathbf{s}_{(k-1)I} + \mathbf{s}_{(k+1)I} + \dots + \mathbf{s}_{KI})$, $\mathbf{B}_k \in \mathbb{C}^{N \times N}$ is a full rank matrix that spans the union of the desired and the interference subspaces, and $\tilde{\mathbf{s}}_k$ is the $N \times 1$ vector consisting of the d_k desired streams and the $N-d_k$ interference streams. Equation (3.7) gives the mathematical formulation of a linear determined decoding problem, where an N -length source data vector $\tilde{\mathbf{s}}_k$ is mixed by a constant mixing matrix \mathbf{B}_k to produce a vector \mathbf{y}_k of N observations. Such a decoding problem can be resolved using classical criteria such as Zero-Forcing (ZF), MMSE, Maximum Likelihood (ML)...

3.4 IA precoding subspaces optimization

In this section, we aim to optimize the IA precoding subspaces in the scheme described above. From (3.3), it can be noted that the modified precoding matrices defined as

$$\mathbf{V}_k = \mathbf{W} \mathbf{V}_k^{IA} \quad \forall k \in \mathcal{K}, \quad (3.8)$$

where \mathbf{V}_k^{IA} is the original matrix derived with respect to the IA conditions and \mathbf{W} is any diagonal matrix, satisfy the IA conditions. That is, the projection of all

precoding matrices of the IA scheme on a common diagonal matrix \mathbf{W} keeps the IA conditions respected.

The precoding subspaces can be optimized by judiciously selecting the components of \mathbf{W} in (3.8). This diagonal matrix \mathbf{W} determines the interference and the desired subspaces design, while maintaining the IA conditions at the receivers. We assume both MMSE and ZF based detection schemes, widely used due to their simplicity for implementation, and we derive two different optimized designs that maximize the network sum-rate for both cases.

3.4.1 MMSE-based decoder - Iterative solution

Assuming an MMSE decoder, the mutual information between the k^{th} transmitter and its intended receiver k can be expressed as

$$R_k(\mathbf{w}) = \log_2 \frac{|\mathbf{I}_N + p \sum_j \mathbf{H}_{kj} \mathbf{W} \mathbf{V}_j \mathbf{V}_j^H \mathbf{W}^H \mathbf{H}_{kj}^H|}{|\mathbf{I}_N + p \sum_{j \neq k} \mathbf{H}_{kj} \mathbf{W} \mathbf{V}_j \mathbf{V}_j^H \mathbf{W}^H \mathbf{H}_{kj}^H|}, \quad (3.9)$$

where p is the user average transmit power over the average noise power assumed equal at all receivers. Using the Sylvester's determinant theorem [39], the fact that all channel matrices are diagonal, and the definition of \mathbf{B}_k and \mathbf{A}_k as

$$\begin{aligned} \mathbf{B}_k &= \sum_{j=1, j \neq k}^K \mathbf{H}_{kj} \mathbf{V}_j \mathbf{V}_j^H \mathbf{H}_{kj}^H \\ \mathbf{A}_k &= \mathbf{B}_k + \mathbf{H}_{kk} \mathbf{V}_k \mathbf{V}_k^H \mathbf{H}_{kk}^H, \end{aligned} \quad (3.10)$$

(3.9) can be reformulated in the following compact form as

$$R_k(\tilde{\mathbf{w}}) = \log_2 \frac{|\mathbf{I}_N + p \tilde{\mathbf{W}} \mathbf{A}_k|}{|\mathbf{I}_N + p \tilde{\mathbf{W}} \mathbf{B}_k|}, \quad (3.11)$$

where $\tilde{\mathbf{W}} = \mathbf{W} \mathbf{W}^H$ is a diagonal matrix with positive elements $\tilde{w}_i \forall i$. One can notice from (3.10) that matrices \mathbf{A}_k and \mathbf{B}_k are written as the sum of semi-definite positive matrices, and hence are positive semi-definite. Consequently, the Cholesky decomposition² can be applied, and the matrices \mathbf{A}_k and \mathbf{B}_k can be rewritten as

$$\mathbf{A}_k = \mathbf{L}_{A_k}^H \mathbf{L}_{A_k} \quad \text{with} \quad \mathbf{L}_{A_k}^H = [\mathbf{L}_{B_k}^H \quad \mathbf{H}_{kk} \mathbf{V}_k] \quad \text{and} \quad \mathbf{B}_k = \mathbf{L}_{B_k}^H \mathbf{L}_{B_k}. \quad (3.12)$$

²It is important to note that the Cholesky decomposition, originally defined for a positive definite matrix, can be extended to the positive semi-definite case [40].

Substituting (3.12) into (3.11) yields the k^{th} user rate

$$R_k(\tilde{\mathbf{w}}) = \log_2 \frac{|\mathbf{I}_N + p \mathbf{L}_{A_k} \tilde{\mathbf{W}} \mathbf{L}_{A_k}^H|}{|\mathbf{I}_N + p \mathbf{L}_{B_k} \tilde{\mathbf{W}} \mathbf{L}_{B_k}^H|}. \quad (3.13)$$

Our goal is to seek $\tilde{\mathbf{w}}$; the vector of positive components defining the diagonal of $\tilde{\mathbf{W}} = \mathbf{W}\mathbf{W}^H$, that maximizes the total mutual information (i.e. network sum-rate) in the IC under the constant total transmit power linear constraint. The maximization problem is then defined as

$$\arg \max_{\tilde{\mathbf{w}}} \frac{1}{N} \sum_{k=1}^K \log_2 \frac{|\mathbf{I}_N + p \mathbf{L}_{A_k} \tilde{\mathbf{W}} \mathbf{L}_{A_k}^H|}{|\mathbf{I}_N + p \mathbf{L}_{B_k} \tilde{\mathbf{W}} \mathbf{L}_{B_k}^H|},$$

subject to the total transmit power constraint

$$\sum_{k=1}^K \text{tr}(\mathbf{V}_k(\mathbf{w})\mathbf{V}_k(\mathbf{w})^H) = K, \quad \tilde{w}_i \geq 0, \quad i \in \{1, \dots, N\}. \quad (3.14)$$

It is not obvious whether a closed-form solution can be obtained or not, therefore, one can search for the solution iteratively. However, the convergence towards the global maximum is not guaranteed unless the objective function is concave. The proof of the concavity with respect to the variable vector $\tilde{\mathbf{w}}$, requires the objective function to be twice differential and its Hessian matrix to be negative semi-definite [41]. Indeed, a similar problem has been treated in [42] for the 3-user IA scheme. The authors have demonstrated that a function having the form of (3.14) is concave if \mathbf{A}_k and \mathbf{B}_k are defined as in (3.12) (see Appendix B in [42]). The solution that approaches the optimum can be obtained using the projected gradient method with an optimized variable step size (details are given in Appendix B). Other algorithms can also be used such as simple gradient descent method using Lagrange multipliers.

3.4.2 ZF-based decoder - Closed-form solution

In the previous subsection, we have proposed to optimize the precoding subspaces using iterative processing when MMSE is applied at the receiver. In this section, we apply a ZF criterion at the receiver. Then, we propose a closed-form solution for \mathbf{w} that is asymptotically optimal. This solution is obtained from the network sum-rate maximization problem approximation for very high SNR, and under the hypothesis of a ZF applied at all receivers. It also avoids the need for

a numerical solver that requires a matrix inversion at each iteration, and thus increases the processing time and computational cost.

Assuming a ZF criterion at all receiver nodes and an IA design at all transmitters, the mutual information between the k^{th} transmitter and its intended receiver k is expressed as

$$R_k = \log_2 |\mathbf{I}_N + p \mathbf{U}_k \mathbf{H}_{kk} \mathbf{W} \mathbf{V}_k \mathbf{V}_k^H \mathbf{W}^H \mathbf{H}_{kk}^H \mathbf{U}_k^H| \quad (3.15)$$

where \mathbf{U}_k is the interference canceler at the k^{th} receiver. Assuming well-conditioned channel matrices and using Sylvester's determinant theorem [39], the k^{th} user rate can be approximated for high SNR values by

$$R_k \underset{SNR \gg 1}{\approx} \log_2 |p \mathbf{H}_{kk} \mathbf{W} \mathbf{V}_k \mathbf{V}_k^H \mathbf{W}^H \mathbf{H}_{kk}^H \mathbf{U}_k^H \mathbf{U}_k|. \quad (3.16)$$

Now, we intend to maximize the sum-rate approximation $\sum_k R_k$ with respect to \mathbf{w} under the total transmit power constraint. Using the following equivalence

$$\arg \max_{\tilde{\mathbf{w}}} \sum_{k=1}^K R_k(\tilde{\mathbf{w}}) \equiv \arg \max_{\tilde{\mathbf{w}}} |\tilde{\mathbf{W}}|^K \prod_{k=1}^K |\mathbf{H}_{kk} \mathbf{V}_k \mathbf{V}_k^H \mathbf{H}_{kk}^H| |\mathbf{U}_k^H \mathbf{U}_k| \quad (3.17)$$

and the fact that $\prod_{k=1}^K |\mathbf{H}_{kk} \mathbf{V}_k \mathbf{V}_k^H \mathbf{H}_{kk}^H| |\mathbf{U}_k^H \mathbf{U}_k|$ is positive, the optimization problem in (3.17) can also be reduced to

$$\begin{aligned} & \arg \max_{\tilde{\mathbf{w}}} |\tilde{\mathbf{W}}|, \\ & \text{subject to } \sum_k \text{tr}(\tilde{\mathbf{W}} \mathbf{V}_k \mathbf{V}_k^H) = KN, \tilde{w}_i > 0 \forall i. \end{aligned} \quad (3.18)$$

We notice that the objective function in (3.18) is a simple determinant of a diagonal matrix, hence, a concave function. Introducing Lagrange multiplier λ , the convex dual of this problem is formulated as follows [41]

$$\arg \max_{\tilde{\mathbf{w}}} \arg \min_{\lambda} L(\tilde{\mathbf{w}}, \lambda). \quad (3.19)$$

where the Lagrangian function is defined as

$$\begin{aligned} L(\tilde{\mathbf{w}}, \lambda) &= |\tilde{\mathbf{W}}| - \lambda \left(\text{tr}(\sum_k \tilde{\mathbf{W}} \mathbf{V}_k \mathbf{V}_k^H) - KN \right), \\ & \text{with } \text{tr}(\sum_k \tilde{\mathbf{W}} \mathbf{V}_k \mathbf{V}_k^H) = \sum_{i=1}^N c_i \tilde{w}_i, \text{ and } c_i = \sum_{k=1}^K \|\mathbf{v}_{ki}\|^2, \end{aligned} \quad (3.20)$$

and \mathbf{v}_{ki} stands for the i^{th} row of the matrix \mathbf{V}_k . Since the objective function is

concave, the Karush Kuhn-Tucker (KKT) conditions are sufficient to determine the global optimum. The KKT conditions of the problem in (3.19) are given by

$$\begin{aligned} \nabla_{\tilde{\mathbf{w}}} L(\tilde{\mathbf{w}}, \lambda)|_{\tilde{\mathbf{w}}=\tilde{\mathbf{w}}^*} &= 0, \quad \lambda > 0, \\ \sum_{i=1}^N c_i \tilde{w}_i &= K N \end{aligned} \quad (3.21)$$

The solution of the linear problem in (3.21) is given by

$$\tilde{w}_i^* = \frac{K}{c_i}, \quad i \in \{1, \dots, N\}. \quad (3.22)$$

Hence, the components of \mathbf{w} are obtained as $w_i^* = \sqrt{\tilde{w}_i^*}$ for all i . It is worth noting that beside maximizing the sum-rate, the problem of maximizing the individual rate using the approximation in (3.16), has the same solution obtained in (3.22).

A major advantage of the proposed solution is the fact that it has an analytic simple expression making its implementation complexity very low. Indeed, the other algorithms proposed for sum-rate maximization and interference power minimization in SISO and MIMO³ transmissions, achieve the optimum using singular value decomposition (SVD) [43] and/or iterative algorithm that requires hundreds to thousands iterations to converge [1, 2, 30].

3.4.3 Complexity and sum-rate performance

The computational complexity is a major bottleneck for the practical implementation that is considered in system designs. In the following, we discuss the complexity of the precoding schemes proposed above.

The first optimized design that maximizes the sum-rate assuming an MMSE detector is obtained using the projected gradient descent method. This iterative method requires at each iteration the computational cost of the first order derivative of the objective function. Looking at the expression given in (B.2), one can notice that the derivative is calculated using matrix multiplications and matrix inversions with dimensions $N \times N$. Therefore, the computational complexity at each iteration can be considered of order $\mathcal{O}(N^3)$. On the other hand, the design based on a closed-form solution requires the computation of a Frobenius norm and a division of N real numbers. Thus, the complexity order is $\mathcal{O}(N)$.

Figure 3.2 compares the average sum-rate per dimension performance of both designs W-MMSE and W-ZF that symbolize the designs based on the solutions

³The IA schemes proposed for MIMO transmission can also be used in SISO systems.

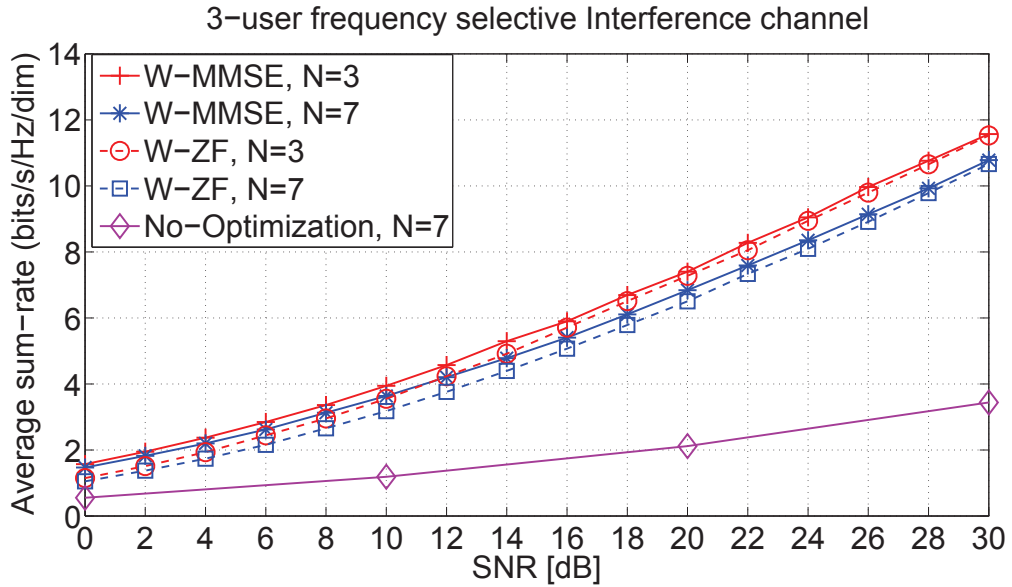


FIGURE 3.2: Average sum rate per dimension of the two proposed designs for subspace improvement with $N = 3$ and $N = 7$.

of the problems in (3.14) and (3.18), respectively. It can be observed that for $N = 3$ and $N = 7$, the W-MMSE design outperforms the W-ZF design with the closed-form solution in the low SNR region. However, when the SNR becomes very high, the sum-rate performance for both designs get very close.

It is important to note that the proposed designs result from the optimization of the original designs proposed in [38], and not the optimal IA design that maximizes the sum-rate. This explains why when we compare the designs for different dimensions N , a higher sum-rate is obtained for $N = 3$ compared to the design for $N = 7$.

3.5 Precoding vectors design within IA subspaces

The previous section has addressed the optimization of the IA precoding subspaces at once using a diagonal matrix \mathbf{W} . On the other hand, there was no discussion on the optimality of the precoding vectors within IA subspaces. In this section, we propose to maintain the IA subspaces design at the transmitters, and we aim to optimize the precoding vectors within each subspace. We consider both cases: MMSE and ZF criterion at the receiver, and we attempt to maximize the network sum-rate in each case.

The precoding matrices defined in (3.4) are of size $N \times d_k$ with $N > d_k, \forall k$. Thus, introducing a new combination matrix $\mathbf{C}_k \in \mathbb{C}^{d_k \times d_k}$ at each transmitter node as follows

$$\mathbf{P}_k = \mathbf{V}_k \mathbf{C}_k, \forall k \in \mathcal{K}, \quad (3.23)$$

will modify the basis of \mathbf{V}_k within its own subspace without modifying the subspace itself. These variables can later be defined taking into account different criteria such as MSE, BER, sum-rate, transmit power... Next, we show how to optimize the additional combination matrices so as to maximize the network sum-rate.

3.5.1 MMSE-based decoder

Assuming an MMSE at all receivers, the mutual information between the k^{th} transmitter and its dedicated receiver k can be written as a function of the combination matrices $\mathbf{C}_k \forall k$ as follows

$$R_k = \log_2 \frac{|\mathbf{I}_N + p \sum_{j=1}^K \mathbf{H}_{kj} \mathbf{P}_j \mathbf{P}_j^H \mathbf{H}_{kj}^H|}{|\mathbf{I}_N + p \sum_{j \neq k}^K \mathbf{H}_{kj} \mathbf{P}_j \mathbf{P}_j^H \mathbf{H}_{kj}^H|}. \quad (3.24)$$

Now, in order to maximize the sum-rate under the individual transmit power constraint, we propose the following maximization problem

$$\begin{aligned} \arg \max_{\mathbf{C}_k, k \in \mathcal{K}} \quad & \frac{1}{N} \sum_{k=1}^K \log_2 \frac{|\mathbf{I}_N + p \sum_{j=1}^K \bar{\mathbf{H}}_{kj} \mathbf{C}_j (\bar{\mathbf{H}}_{kj} \mathbf{C}_j)^H|}{|\mathbf{I}_N + p \sum_{j \neq k}^K \bar{\mathbf{H}}_{kj} \mathbf{C}_j (\bar{\mathbf{H}}_{kj} \mathbf{C}_j)^H|} \\ \text{subject to} \quad & \text{tr}(\mathbf{V}_k \mathbf{C}_k \mathbf{C}_k^H \mathbf{V}_k^H) = N, \forall k \in \mathcal{K}. \end{aligned} \quad (3.25)$$

where $\bar{\mathbf{H}}_{kj} = \mathbf{H}_{kj} \mathbf{V}_j$. It is well-known that the optimal solution is the one that nullifies the gradient of the sum-rate expression. However, a closed-form solution is not obvious due to a complicated expression of the first order derivative as shown in (C.5) in Appendix B. Therefore, we attempt to get close to the solution iteratively. We use an iterative algorithm that optimizes the cost function with respect to one variable while the others remain fixed. In our reasoning, each variable is considered as one of the precoding matrices. This technique results in a non-convex optimization due to the dependence between the precoding matrices. At each iteration, the optimization is based on the gradient descent widely used in MIMO multi-user channel. The iterative algorithm for the sum-rate maximization is detailed in algorithm 3.1.

Algorithm 3.1 IA precoding vectors optimization

-
- 1: Initialize randomly all precoding matrices $\mathbf{C}_1, \dots, \mathbf{C}_K$.
 - 2: Start loop with $l = 1$
 - 3: **for** $k = 1$ **to** K **do**
 - 4: Calculate the gradient, $\nabla_{\mathbf{C}_k} f(\mathbf{C}_1^l, \dots, \mathbf{C}_K^l)$.
 - 5: Update $\mathbf{C}_k^{(l+1)} = \mathbf{C}_k^l + \lambda \nabla_{\mathbf{C}_k} f(\mathbf{C}_1^l, \dots, \mathbf{C}_K^l)$.
 - 6: if $\text{trace}(\mathbf{V}_k \mathbf{C}_k^{(l+1)} \mathbf{C}_k^{(l+1)H} \mathbf{V}_k^H) > N$ update $\mathbf{C}_k^{(l+1)} = \frac{\sqrt{\frac{N}{d_k}} \mathbf{C}_k^{(l+1)}}{\sqrt{\text{trace}(\mathbf{V}_k \mathbf{C}_k^{(l+1)} \mathbf{C}_k^{(l+1)H} \mathbf{V}_k^H)}}$.
 - 7: **end for**
 - 8: If $f(\mathbf{C}_1^{(l+1)}, \dots, \mathbf{C}_K^{(l+1)}) - f(\mathbf{C}_1^l, \dots, \mathbf{C}_K^l) > \epsilon$, set $l = l + 1$ and go back to step 3), otherwise stop the processing.
-

In this algorithm the gradient is defined in (C.5) in Appendix B, f describes the objective function given in (3.25), and the precoding matrices are supposed to be of unit Frobenius norm. The step size λ is updated using the backtracking search, which is an effective and quite simple method [41]. Despite the non-convexity of the multi-variable objective function, as long as the variable is steered in the gradient direction, the algorithm converges to a local maximum. In our simulations, the convergence of this iterative algorithm is supposed to be achieved either when

$$\sum_k \|\nabla_{\mathbf{C}_k^{(l)}} R\| < \epsilon \quad (3.26)$$

or when a maximum number of iterations is reached, and ϵ is defined as a tolerance value that could be e.g. 10^{-6} (taken in our simulation results).

3.5.2 ZF-based decoder

Given the k^{th} user rate, the ZF-based detector uses a matrix \mathbf{U}_k to cancel the interference, yielding an equivalent $d_k \times d_k$ MIMO transmission model. Many options exist to find the best family of combination matrices $\{\mathbf{C}_j\}$ in order to maximize the sum-rate. The channel model after interference suppression at receiver k is obtained as

$$\begin{aligned} \mathbf{y}_k &= \mathbf{U}_k \mathbf{H}_{kk} \mathbf{V}_k \mathbf{C}_k \mathbf{s}_k + \mathbf{U}_k \mathbf{z}_k, \\ &= \tilde{\mathbf{H}}_k \mathbf{C}_k \mathbf{s}_k + \mathbf{U}_k \mathbf{z}_k, \end{aligned} \quad (3.27)$$

where \mathbf{U}_k is the decoding matrix at the k^{th} receiver. It is defined as the $d_k \times N$ interference null space. The model defined in (3.27) is a typical MIMO single

user model with channel matrix $\tilde{\mathbf{H}}_k$ and precoding matrix \mathbf{C}_k . One optimized form of \mathbf{C}_k is the one composed of the right singular vector of the new channel matrix $\tilde{\mathbf{H}}_k$. Such a precoding scheme achieves the channel capacity as described in [44]. Another form that requires less computational complexity is the one that orthonormalizes the columns of the original precoding matrix \mathbf{V}_k . In [45], the authors have shown that this last form gets close to the maximum information rate when the SNR becomes high.

3.5.3 Complexity and sum-rate performance

The algorithm that optimizes the solution iteratively in section 3.5.1 is based on the gradient descent method. At each iteration, the iterative algorithm requires the gradient of the objective function that needs itself inversion of $N \times N$ full rank matrices. Thus, the total computational complexity depends mainly on the number of iterations and on the precoding matrices dimensions. The complexity cost is of order $\mathcal{O}(nb_i N^3)$ where nb_i is the number of iterations.

Figure 3.3 illustrates the sum-rate per dimension of the design CW-MMSE which represents the solution W-MMSE optimized with the algorithm 3.1, and the solution OW-ZF that represents the W-ZF design with orthogonal precoding vectors. For the subspace optimization, we use the closed form solution derived in section 3.4.2. One can observe a sum-rate performance loss in the case of OW-ZF compared to the CW-MMSE for low SNR values, whereas when the SNR increases both sum rates become very close. However, in terms of complexity cost, less operations are required, of order $\mathcal{O}(Nd_k^2)$ at each transmitter, and no joint processing is required for the optimization design.

3.6 Convergence rate of the iterative solutions

In section 3.4.1 and section 3.5.1, we have proposed two iterative solutions, one aims to optimize the IA subspaces and the other optimizes the precoding vectors within each IA subspace without modifying the subspace itself.

The first iterative solution to the problem in (3.14) for the IA subspaces optimization is reached using the projected gradient method. We have mentioned that the objective function is concave, thus, the convergence towards the global optimum is guaranteed. On the other hand, the iterative solution proposed for the IA precoding vectors optimization is reached using an algorithm based on the gradient descent method for a multi-variable objective function. Thereby, the objective

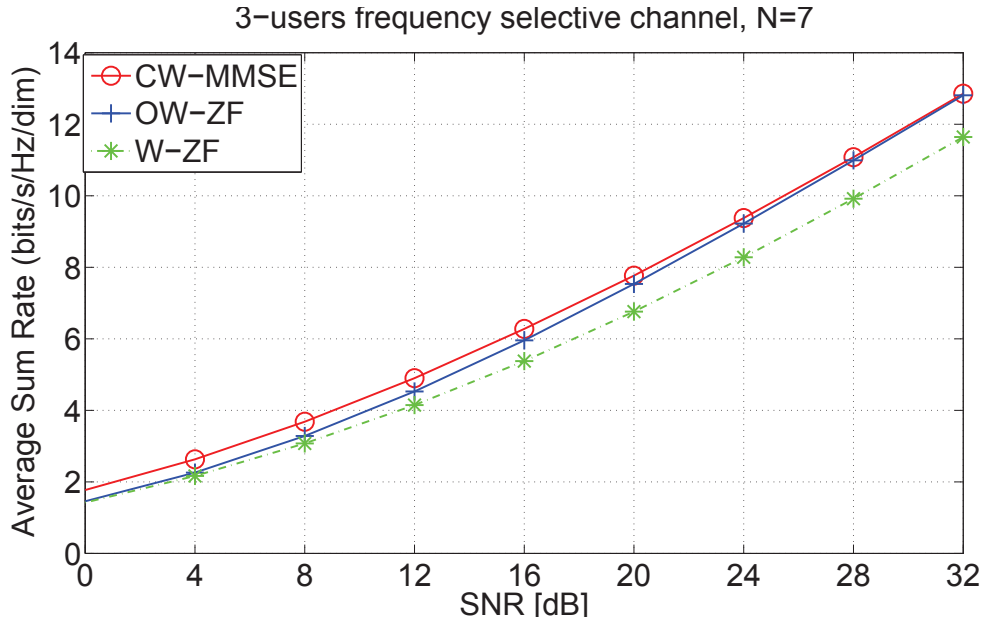


FIGURE 3.3: Average sum rate per dimension of the proposed precoding vectors design using the combination matrices for $N = 3$ and $N = 7$.

function changes at every iteration yielding a non convex optimization problem. However, as long as the iterative method is based on the gradient descent and the variable follows the direction of the gradient using an optimized step size, a convergence towards a local optimum is guaranteed.

The convergence rates of the discussed iterative solutions above are shown in Figure 3.4. For the projected gradient descent method, the convergence towards either the optimal solution or a neighboring optimal solution requires hundreds of iterations. This slow convergence rate shifts the attention to the closed-form solution obtained in section 3.4.2. Now, looking at the design for precoding vectors optimization within their subspace, the convergence rate seems fast. For example, almost 10 to 15 iterations are required to achieve a near-optimal value at 15dB and 25dB when $N = 7$.

3.7 Comparison of the proposed optimized designs to the state of art schemes

In this section, we compare the proposed designs to the distributed designs proposed in [1, 2] in terms of sum-rate per dimension. We consider a 3-user frequency selective SISO IC, with the model proposed in section 3.2. The total

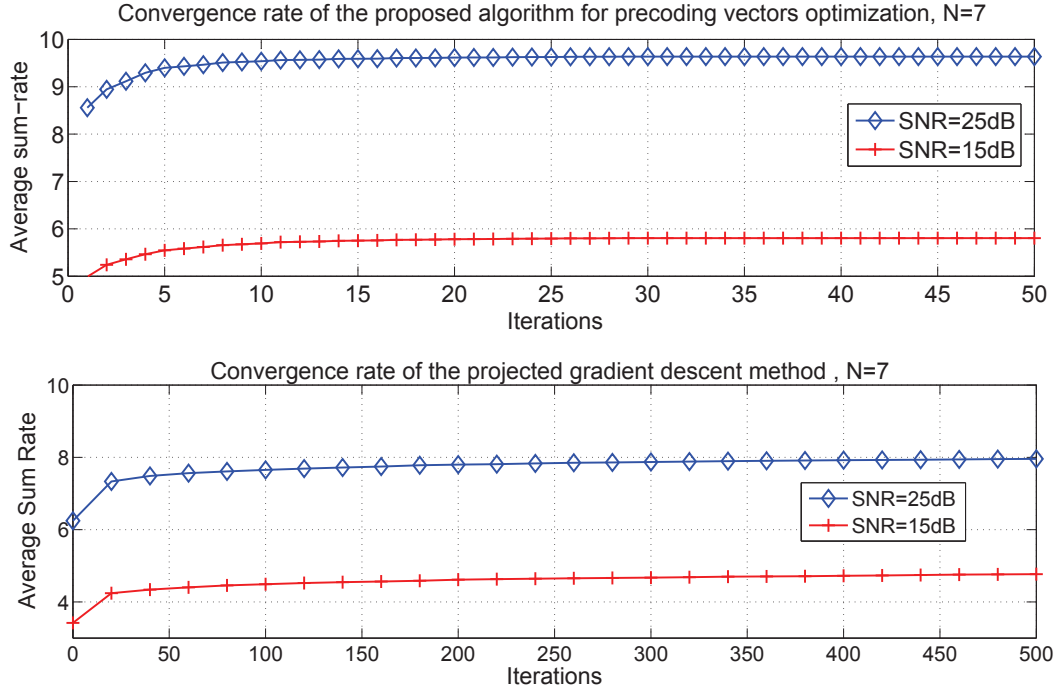


FIGURE 3.4: Convergence of the iterative algorithm in section 3.5.1 and the projected gradient method in section 3.4.1.

independent stream number from all users is equal to $\text{DoF}_T = 3n + 1$, and the precoding vectors length is $N = 2n + 1$ for all users, and n can be any non negative number. The transmit constellation is Gaussian continuously distributed, and the channel coefficients are circularly symmetric complex Gaussian distributed with zero mean and unit variance. The following abbreviations are used for the compared designs:

- OW-ZF : the proposed IA design with the closed-form solution derived in section 3.4.2 that uses orthogonal precoding vectors.
- CW-MMSE : the IA design with the two iterative proposed optimization in section 3.4.1 and section 3.5.1.
- IA-Iter: the IA design obtained with the distributed algorithm proposed in [1]
- Max-SINR: the beamforming design proposed in [2] that maximizes the signal to interference and noise ratio (SINR) of all streams.

Figures 3.5, 3.6 and 3.7 illustrate the average sum-rate per dimension performance of the OW-ZF, the CW-MMSE, the IA-Iter and the Max-SINR for $N = 3$,

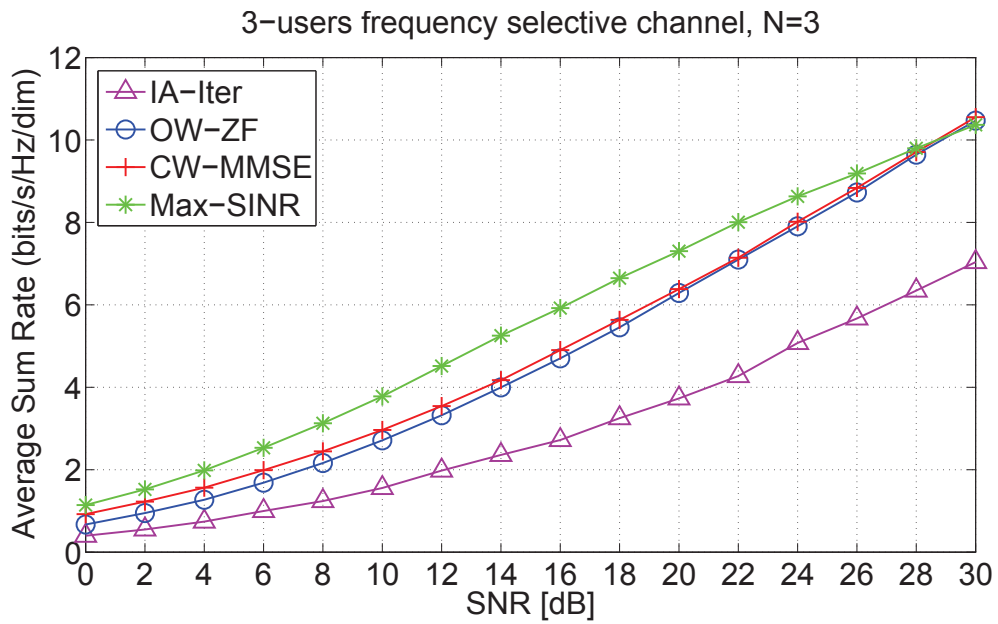


FIGURE 3.5: Comparison of the average sum rate per dimension for different precoding designs for $N = 3$.

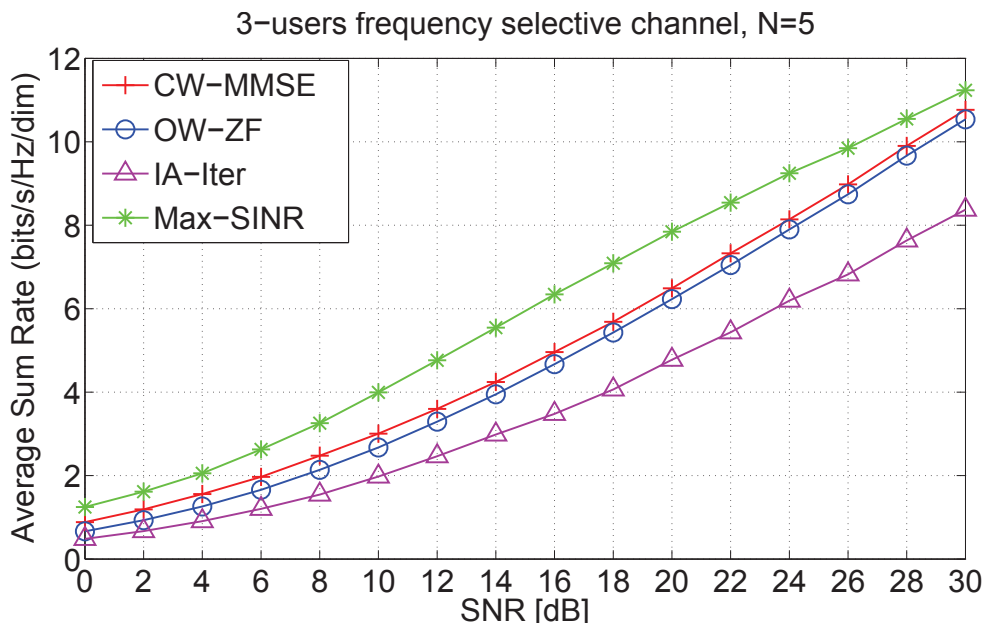


FIGURE 3.6: Comparison of the average sum rate per dimension for different precoding designs for $N = 5$.

$N = 5$ and $N = 7$, respectively. The iterative algorithm IA-Iter and Max-SINR are evaluated under $n_i = 800$ maximum number of iteration. Compared to the CW-MMSE, the OW-ZF performs similarly for all configurations with a slight loss for low and medium SNR values. This is due to the fact that a ZF criterion becomes equivalent to an MMSE when the SNR becomes very high, and that the OW-ZF design is based on an approximation for high SNR. On the other hand, an important gain is obtained over the IA-Iter design over the whole SNR region when $N = 3$ and $N = 5$, e.g. at 20dB a gain of about 2.2 – 2.5 bits/s/Hz and 1.7 – 2 bits/s/Hz is obtained for $N = 3$ and $N = 5$ respectively. It is worth noting that in addition to this gain, the OW-ZF design is a closed-form, thus, it exhibits a much less computational complexity than the other designs. It also does not require any iterative processing to achieve the solution, and thus exhibits a reasonable complexity order when N increases. Now, considering the beamforming optimization design that maximizes the SINR referred to as Max-SINR, this last outperforms the proposed designs in the low and medium SNR region. However, this resulting gain decreases as the SNR increases in the medium to high SNR region. For example, the OW-ZF design and the Max-SINR design reach the same sum-rate value of about 10.4 bits/s/Hz at 30dB for $N = 3$. This result can show that in some particular cases, the proposed designs are very close to one of the most efficient designs when the SNR is high enough while keeping a low complexity level such as the OW-ZF design.

Next, Figure 3.8 evaluates the performance of the following designs: OW-ZF, IA-Iter and Max-SINR, as a function of the precoding vectors sizes. At 15dB and 30dB, the OW-ZF outperforms the IA-Iter for $N \leq 9$ and $N \leq 11$. On the other hand, it can be observed that the two iterative designs IA-Iter and Max-SINR result in an increasing sum-rate with the vectors sizes, however, the closed-form design OW-ZF results in a decreasing sum-rate with the vectors sizes. This means that OW-ZF is close to the optimal for small precoding dimensions, and starts moving away when N increases.

3.8 Conclusion

In this chapter, we have introduced three optimized designs for the IA scheme proposed in [38] in a K -user SISO IC. The first and the second consider optimizing the precoding subspaces at the IA transmitters through a common diagonal matrix assuming an MMSE and ZF linear detector, respectively. The third assumes an

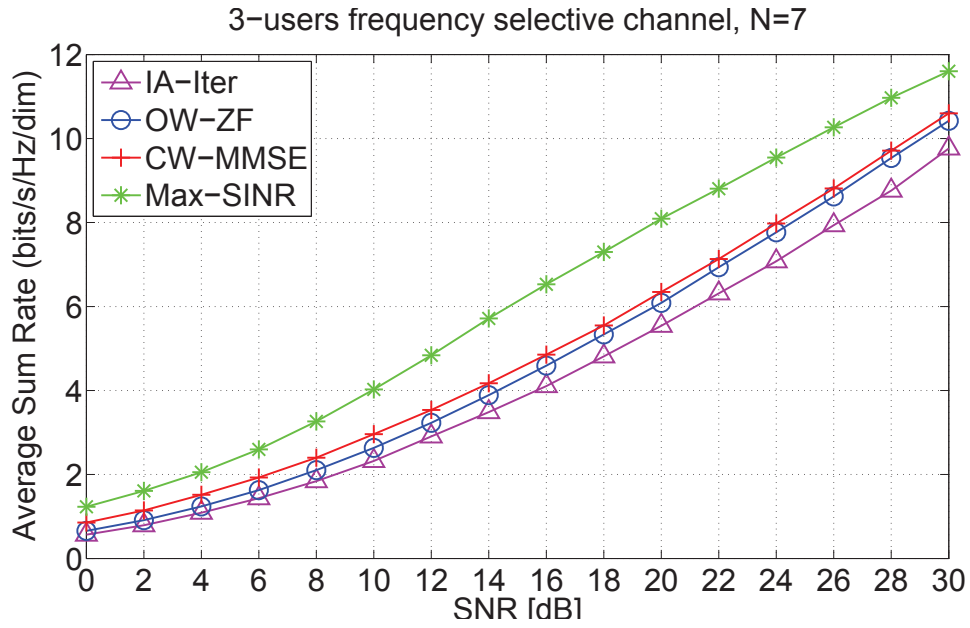


FIGURE 3.7: Comparison of the average sum rate per dimension for different precoding designs for $N = 7$.

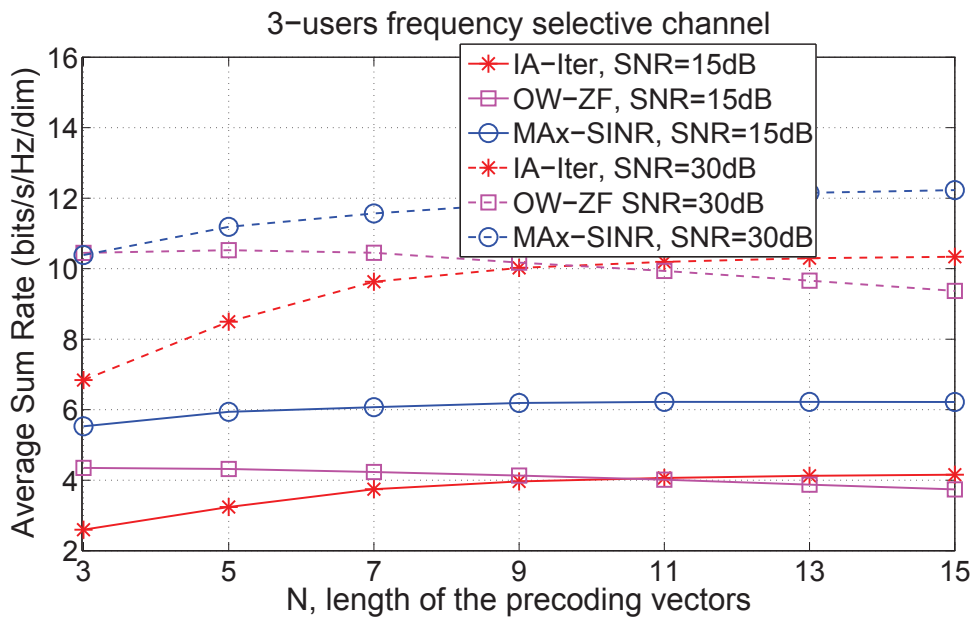


FIGURE 3.8: Evolution of the average sum rate per dimension with the precoding vectors length for the closed-form design with orthogonal precoding vectors, the iterative IA design [1], and the iterative design that maximizes the SINR [2].

MMSE linear detector, and seeks the optimal precoding vectors within a predefined subspace at each transmitter. The first and the third designs referred to as W-MMSE and C-MMSE, respectively, require iterative algorithms to converge to their optimum, whereas the second design referred to as W-ZF, is obtained from a closed-form solution. Comparing to other IA distributed designs, the proposed designs show a significant sum-rate performance, and much less computational complexity when the closed-form solution is applied. To enhance the sum-rate performance, we have introduced an orthogonalization of the precoding vectors in the W-ZF design, which enables to achieve a trade-off between complexity and data rate.

In the next chapter, we introduce the spatial IA concept in the MIMO IC. We address the detection problem at the receivers, where we consider transmitters with full CSI knowledge and receivers with no CSI knowledge. Such a situation appears when each transmitter estimates the CSI between itself and all receivers in the IC through feedback links, then shares it with the other transmitters via a centralized coordinator.

Chapter 4

Linear detectors for downlink transmission with interference alignment

4.1 Introduction

The previous chapter has addressed the transmission in a multi-user SISO IC. The interference alignment scheme has been presented with some proposed optimization for the precoding design. This chapter addresses the transmission in a multi-user MIMO IC, i.e. the transmitters and the receivers are equipped with multiple antennas. We assume a network where the transmitters have a limited cooperation on CSI exchange level i.e. the IA can be applied, and the receivers cannot cooperate. This context is similar to the downlink transmission in mobile communication network, where the base stations (BS) that cooperate through a central unit transmit to their independent terminal users simultaneously.

Similarly to the SISO IC, in a K -user MIMO systems where different users are equipped with multiple antennas, the IA results in a linearly scaling network sum-rate with the number of users sharing a common transmission medium. The achievable DoF¹ has been studied in many papers using the IA concept in signal scale and signal vector space [26, 28, 46, 47, 48]. Also, different schemes have been proposed in space/frequency/time/rational dimensions to characterize the DoF by defining new inner and upper bounds.

¹The degrees of freedom (DoF) of wireless interference networks represent the number of interference-free signaling dimensions in the network.

On the other hand, IA in spatial dimensions are desirable for their analytical tractability, for the useful insights they offer in the finite SNR region, and for their robustness to practical limitations such as frequency offsets due to mismatched synchronization. The feasibility of the spatial IA design for MIMO transmissions has been studied [28], and distributed IA-achieving algorithms have been derived, e.g. [1, 2, 30]. These algorithms are based on an iterative processing at the transmitter when the full-CSI is available at the transmitters, and on information exchange with the receiver when only the local CSI is available at the transmitters and the receivers.

In this chapter, we assume a linear spatial IA design at the transmitters and approach the decoding problem. That is, the interfering signals are aligned in a subspace linearly independent of the desired signal subspace. The traditional linear decoders can estimate the decoding matrices, defined as the interference null space, using the basic Least Square (LS) method essentially based on a training sequence within each frame. Herein, our contribution regarding the decoding scheme pursues a different approach. The main idea consists in separating each desired streams (desired signal) from the interference using higher-order cumulants, and then the desired signal can be identified using a few training symbols. This approach has the advantage of allowing to decode the received signal even when the number of training symbols is low, and thus result in a more robust decoding scheme for a given training sequence length. We first show the equivalence between the MIMO IC model with IA at the transmitters and a determined Blind Source Separation (BSS) model. Then, we demonstrate the feasibility of solving the BSS problem to separate the desired signal from the interference through a joint diagonalization of the fourth-order cumulants matrices [6]. The separation ability is due to the existing independence between the desired signal and the interference. The joint diagonalization is able to extract the desired streams blindly up to a permutation and scaling ambiguities. These ambiguities can be solved using a few training symbols within each transmitted frame, hence, the term semi-blind is invoked.

The remaining of this chapter is organized as follows. In Section 4.3, the assumed MIMO IC is described. The distributed IA in MIMO IC is reviewed in Section 4.4. The traditional linear decoding is derived in Section 4.5. In Section 4.6, we link the IC model associated with IA design to the determined blind source separation model, and show the ability of the joint diagonalization technique to decode the desired signal. Section 4.7 evaluates the performance of the

BSS techniques. Finally, Section 4.8 concludes the paper.

4.2 Context and transmission network

In this chapter, we consider a downlink transmission in mobile network where the BSs (Base stations) transmit to the mobile terminals. The communication starts when each mobile terminal provide all BSs in a given area with training symbols for CSI estimation. The transmission is assumed in TDD mode. The channel is firstly estimated at the BS using an L_s -length uplink reference signal sent from the mobile terminals assuming a reciprocal channel supposed constant during one frame transmission. This strategy is employed in the TDD-uplink transmission scheme in the 3GPP-LTE network [49]. Once all CSI linking each BS to all terminal mobiles are estimated at each BS, they can be shared with the other BSs through a central unit. Hence, the IA scheme can be designed between all transmitters (BS) based on the total CSIT knowledge. In the second phase, the downlink transmission begin. At the receiver side, the mobile terminal knows a priori that the interference and the desired signal are separated. In order to extract the desired signal, classical detection methods propose to estimate the interference subspace based on a training sequence, and then to project the total received signal on the interference null space. In our work, we show that the interference can be suppressed blindly with no need of the training symbols using the BSS techniques.

4.3 System Model

We consider a K -user quasi static IC with K transmit-receive pairs and $N = N_t = N_r$ antennas at each side of the link. A given transmitter intends to have its signal decoded by a single dedicated receiver. Each transmitter sends d_k symbols at one channel use. Without loss of generality, we assume $d = d_1 = \dots = d_K$. The received signal at the k^{th} receiver node and at instant l is given by

$$\mathbf{y}_k(l) = \mathbf{H}_{kk} \mathbf{V}_k \mathbf{s}_k(l) + \sum_{j \neq k} \mathbf{H}_{kj} \mathbf{V}_j \mathbf{s}_j(l) + \mathbf{z}_k(l), \quad l = 0, \dots, T-1 \quad (4.1)$$

where T represents the frame length, $\mathbf{H}_{kj} \in \mathbb{C}^{N \times N}$ is the fading channel matrix between the j^{th} transmitter and the k^{th} receiver, $\mathbf{V}_j \in \mathbb{C}^{N \times d}$ is the precoding matrix

at the j^{th} transmitter, and $\mathbf{z}_k(l) \in \mathbb{C}^{N \times 1}$ is the circular symmetric complex Gaussian noise vector at the k^{th} receiver, with i.i.d. components; i.e. $\mathbf{z}_k \sim \mathcal{N}_c(0, \mathbf{I}_N)$. $\{\mathbf{s}_j(l) \in \mathcal{Q}^{d \times 1} | l = 0, \dots, T-1\}$ represents the d streams from the j^{th} transmitter during a T -symbol duration interval. The symbols of \mathbf{s}_j are supposed i.i.d. from a finite constellation \mathcal{Q} . Each T -length frame is decoded at once and assumed time invariant over the duration of a frame.

The K precoders are jointly designed to satisfy the IA conditions, which can be achieved using different solutions without channel extensions [1, 2, 26]. At the receiver side, the intended signal can be detected by projecting the received signal on the interference null space. The l^{th} decoded signal vector is given by

$$\begin{aligned} \tilde{\mathbf{y}}_k(l) &= \mathbf{U}_k \mathbf{y}_k(l) \\ &= \mathbf{U}_k \mathbf{H}_{kk} \mathbf{V}_k \mathbf{s}_k(l) + \sum_{j \neq k} \mathbf{U}_k \mathbf{H}_{kj} \mathbf{V}_j \mathbf{s}_j(l) + \mathbf{U}_k \mathbf{z}_k(l), \end{aligned} \quad (4.2)$$

where \mathbf{U}_k is the decoding matrix at the k^{th} receiver. In the upcoming sections, we present the spatial IA design for the adopted channel model, and we show the ability of extracting the desired signal using higher-order cumulants.

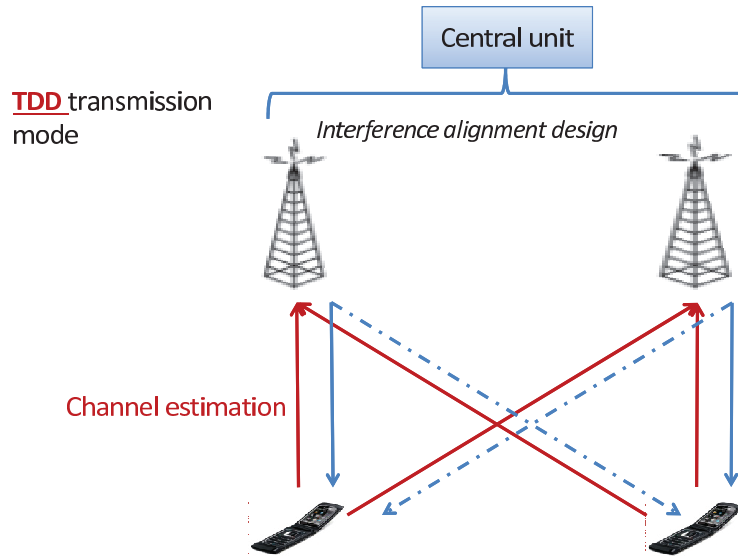


FIGURE 4.1: Mobile interference network: transmission in downlink.

4.4 Spatial IA design in a K-user MIMO IC

Many solutions have been proposed to align the interference in a K -user MIMO IC. Some of them are computed numerically from a closed form [26, 32, 46]. Others require an iterative processing and try to converge to a solution for which the interference are aligned at each receiver. For example, in [2] the proposed scheme consists in seeking iteratively the precoding and decoding matrices that minimize the interference leakage under the assumption of channel reciprocity. In [1], the criterion has been generalized to minimize the interference caused at all undesired receivers. In [30], the same criterion has been considered under the sum rate maximization and the constant transmit power constraints. Other criteria have also been investigated such as the maximization of the chordal distance preserving aligned interference [43], the maximization of the received power in the interference-free subspaces [30] and so on. In the following, a brief description of the iterative IA-achieving concept is exhibited. At receiver k , the conditions to align interference from other transmitters into the null space of \mathbf{U}_k are given by [2]

$$\begin{aligned} \text{rank}(\mathbf{U}_k \mathbf{H}_{kk} \mathbf{V}_k) &= d_k, \\ \mathbf{U}_k \mathbf{H}_{kj} \mathbf{V}_j &= 0, \forall j \neq k. \end{aligned} \quad (4.3)$$

In other words, the desired signal belongs to the subspace generated by the vectors of $\mathbf{G}_k = \mathbf{U}_k \mathbf{H}_{kk} \mathbf{V}_k$, while the interference is completely eliminated. The feasibility of the linear system in (4.3) is conditioned to the following: i) the linear system has to be proper, i.e. the number of variables is more than or equal to the number of equations, ii) the linear system has to be generic [28]. In some particular case, the genericity is satisfied by providing a channel matrix with random and independent coefficients.

When both conditions are satisfied, the IA scheme is achieved by only minimizing the total interference leakage expressed as

$$IL = \sum_{k=1}^K \sum_{j \neq k} \|\mathbf{U}_k^H \mathbf{H}_{kj} \mathbf{V}_j \mathbf{V}_j^H \mathbf{H}_{kj}^H \mathbf{U}_k\|. \quad (4.4)$$

The IA design consists in defining the precoding and the decoding matrices that minimize the interference leakage at all users. The proposed IA-achieving distributed algorithms start with arbitrary transmit and receive filters \mathbf{V}_k and \mathbf{U}_k for

all k , and iteratively update these filters to minimize the interference leakage. The interference leakage is the metric for the quality of alignment. The basic algorithm is described as in 4.1. This algorithm above is guaranteed to converge, however, a convergence to a global minimum is not guaranteed due to the non-convex nature of the interference optimization problem [2].

Algorithm 4.1 Distributed IA design

- 1: Set \mathbf{V}_k to an arbitrary matrix such as $\mathbf{V}_k^H \mathbf{V}_k = \mathbf{I}_{d_k}$.
 - 2: Compute the interference covariance as $\mathbf{Q}_k = \sum_{j \neq k}^K \mathbf{H}_{kj} \mathbf{V}_j \mathbf{V}_j^H \mathbf{H}_{kj}^H$.
 - 3: Compute \mathbf{U}_k that minimizes the interference covariance as $\mathbf{U}_k = \nu_{min}^{d_k}(\mathbf{Q}_k)$, where $\nu_{min}^{d_k}(\cdot)$ denotes the eigenvectors corresponding to the d_k^{th} smallest eigenvalues.
 - 4: Exchanging the roles of the precoders and decoders in the reciprocal network.
 - 5: Compute the new interference covariance as $\bar{\mathbf{Q}}_k = \sum_{j \neq k}^K \mathbf{H}_{kj}^H \mathbf{U}_j \mathbf{U}_j^H \mathbf{H}_{kj}$.
 - 6: Compute $\bar{\mathbf{V}}_k$ that minimizes the new interference covariance as $\bar{\mathbf{V}}_k = \nu_{min}^{d_k}(\bar{\mathbf{Q}}_k)$.
 - 7: Exchanging the roles of the precoders and decoders in the reciprocal network.
 - 8: Repeat 2 – 7 until convergence.
-

4.5 Traditional linear decoding in a spatial IA scheme

The application of the IA design at the transmitters allows a linear detection² using criteria such as ZF and MMSE. The reason is that the interference signals are all aligned in a subspace linearly independent from the subspace that contains the desired signal. Hence, seeking the null space of the interference signal can separate the desired signal and the interference, and then the signal can be linearly detected. In this section, we derive the ZF and the MMSE detector applied at the receivers in a K -user MIMO IC.

We apply the distributed algorithm proposed in section 4.4. The interference canceler is given by $\mathbf{U}_{c,k}$. It is calculated using the singular value decomposition of the interference subspace as

$$\mathbf{U}_k^0 \mathbf{S}_k \mathbf{V}_k = \sum_{j \neq k} \mathbf{H}_{kj} \mathbf{P}_j \quad (4.5)$$

²In the new model, IC with IA, the number of observations is equal to the number of variables.

where $\mathbf{U}_k^0 = [\mathbf{U}_k^1, \mathbf{U}_{c,k}]$ consists of the interference space $\mathbf{U}_k^1 \in \mathbb{C}^{N_r \times (N_r - d_k)}$ and the interference null space $\mathbf{U}_{c,k} \in \mathbb{C}^{N_r \times d_k}$, respectively.

Assuming a perfect knowledge of the interference subspace at each receiver, the received signal after applying the interference canceler $\mathbf{U}_{c,k}$ is obtained as

$$\tilde{\mathbf{y}}_k(l) = \mathbf{U}_{c,k} \mathbf{H}_{kk} \mathbf{V}_k \mathbf{s}_k(l) + \mathbf{U}_{c,k} \mathbf{z}_k(l). \quad (4.6)$$

The system in (4.6) with \mathbf{s}_k variable is a determined linear system with d_k equations and d_k variables, and the matrix $\mathbf{G}_k = \mathbf{U}_{c,k} \mathbf{H}_{kk} \mathbf{V}_k$ has full rank with dimensions $d_k \times d_k$. A ZF-based decoding matrix is then defined as \mathbf{G}_k^{-1} , and the decoded signal yields

$$\begin{aligned} \hat{\mathbf{y}}_k(l) &= \mathbf{G}_k^{-1} \mathbf{G}_k \mathbf{s}_k(l) + \mathbf{G}_k^{-1} \mathbf{U}_{c,k} \mathbf{z}_k(l), \\ &= \mathbf{s}_k(l) + \bar{\mathbf{z}}_k(l). \end{aligned} \quad (4.7)$$

where $\bar{\mathbf{z}}_k(l) = \mathbf{G}_k^{-1} \mathbf{U}_{c,k} \mathbf{z}_k(l)$. It is well-known that a ZF-based receiver increases the level of noise due to the non-unitary matrix \mathbf{G}_k^{-1} . Therefore an MMSE can be used instead. The MMSE use the a priori information of the noise distribution to decrease the mean square errors (MSE).

One can notice that the interference canceler is a unitary matrix, thus, it keeps the noise level unchanged. Consequently, the MMSE detector can be directly applied to the interference-free signal $\tilde{\mathbf{y}}_k(l)$ given in (4.6). The MMSE criterion looks for the matrix $\tilde{\mathbf{G}}_k$ that minimizes the MSE between the estimated signal and the original signal. The MSE is defined as follows

$$MSE_k = \mathbb{E} [\|\tilde{\mathbf{G}}_k \tilde{\mathbf{y}}_k(l) - \mathbf{s}_k(l)\|^2] \quad (4.8)$$

Deriving MSE_k with respect to $\tilde{\mathbf{G}}_k$, the solution that makes the derivative zero is obtained as

$$\tilde{\mathbf{G}}_k = (\mathbf{G}_k \mathbf{G}_k^H + \sigma^2 \mathbf{I}_{d_k})^{-1} \mathbf{G}_k^H, \quad (4.9)$$

and the decoded signal becomes

$$\hat{\mathbf{y}}_k(l) = \tilde{\mathbf{G}}_k \mathbf{G}_k \mathbf{s}_k(l) + \tilde{\mathbf{G}}_k \mathbf{U}_{c,k} \bar{\mathbf{z}}_k(l). \quad (4.10)$$

The described receivers need a perfect CSI knowledge for an accurate estimation of the decoding matrix. In practice, the CSI is estimated at each receiver using a training sequence. Several estimators have been proposed among which the least

square (LS) and the MMSE estimators [50]. In this chapter, we pursue a different approach. We exploit the statistical independence of the transmitted streams, and we blindly seek the decoding matrix, at each receiver, that maximizes the statistical independence between the components of the mixed received signal. Then, we introduce a few training symbols in order to remove the residual scaling and permutation ambiguities inherent in the blind separation.

4.6 Desired signal extraction in a spatial IA scheme using high-cumulants order

The blind and semi-blind source separation using high-cumulants order has been exploited in single user MIMO systems [51, 52]. Here, we want to show that the blind source separation techniques can be extended to the downlink of a multi-user MIMO IC when the IA scheme is applied at the transmitters.

4.6.1 Desired signal Extraction

The standard Blind Source Separation (BSS) standard instantaneous model is defined as

$$\mathbf{y}(l) = \mathbf{A}\mathbf{s}(l), \quad l = 0, \dots, T - 1 \quad (4.11)$$

where $\mathbf{s}(l) \in \mathbb{C}^{N \times 1}$ is the vector of N statistically independent latent variables called independent components, $\mathbf{y}(l) \in \mathbb{C}^{N \times 1}$ is the observation vector, and $\mathbf{A} \in \mathbb{C}^{N \times N}$ is a full rank unknown mixing matrix. The BSS technique seeks the demixing matrix \mathbf{U}_{bss} that maximizes the statistical independence between the estimated components $\hat{\mathbf{s}}(l) = \mathbf{U}_{bss}\mathbf{A}\mathbf{s}(l)$, $\forall l$. For the sake of simplicity, the time index will be ignored in the remaining of this section.

It is shown in [53] that, under mild assumptions, the estimated variables $\hat{\mathbf{s}}$ are similar to the original sources \mathbf{s} up to a permutation and scaling by a complex constant, i.e.

$$\mathbf{U}_{bss}\mathbf{A} = \mathbf{P}\mathbf{\Lambda}, \quad (4.12)$$

where \mathbf{P} is a permutation matrix and $\mathbf{\Lambda}$ is a diagonal matrix.

Back to the MIMO IC model with IA technique applied at the transmitters, the model is formulated as (3.7)

$$\begin{aligned}\mathbf{y}_k &= [\bar{\mathbf{H}}_k^k \quad \bar{\mathbf{H}}_I^k] [\mathbf{s}_k^T \quad \bar{\mathbf{s}}_k^T]^T + \mathbf{z}_k \\ &= \mathbf{A}_k \tilde{\mathbf{s}}_k + \mathbf{z}_k.\end{aligned}\tag{4.13}$$

where \mathbf{A}_k is a full rank square matrix and $\bar{\mathbf{s}}_k = (\mathbf{s}_{1I} + \cdots + \mathbf{s}_{(k-1)I} + \mathbf{s}_{(k+1)I} + \cdots + \mathbf{s}_{KI})$. All components of $\bar{\mathbf{s}}_k$ are mutually dependent. This model is similar to the BSS model except that some mutual dependencies exist between some components of $\tilde{\mathbf{s}}_k$. The first d components of $\tilde{\mathbf{s}}_k$ are mutually independent and represent the desired streams \mathbf{s}_k . The other $(N-d)$ -components of $\tilde{\mathbf{s}}_k$ are mutually dependent and represent the interference part $\bar{\mathbf{s}}_k$. This situation of dependent sources has been considered in certain recent studies, e.g. [54, 55, 56]. Several algorithms have been proposed for source separation such as bounded component analysis algorithm. In our case, there is no need for such algorithms, and the desired signal can be extracted using a simple joint block diagonalization of the high order cumulants as explained in the following subsection. The received signal is whitened first before applying the blind source separation algorithm.

4.6.2 Second-order information: Whitening

For the model in (4.11), the whitening matrix that decorrelates the received signal is denoted by \mathbf{W}_k . Its derivation requires the estimation of the correlation matrix $\mathbf{R}_{y_k} = \mathbb{E}(\mathbf{y}_k^H \mathbf{y}_k)$. \mathbf{W}_k is obtained as the solution of the following equation

$$\mathbf{W}_k \mathbf{R}_{y_k} \mathbf{W}_k^H = \mathbf{I}_N.\tag{4.14}$$

For independent and equally power distributed streams, \mathbf{R}_y can be decomposed as $\mathbf{R}_{y_k} = \mathbf{A}_k \mathbf{A}_k^H$. This means that for \mathbf{W}_k satisfies (4.14), there exists a unitary matrix \mathbf{B}_k such that $\mathbf{W}_k \mathbf{A}_k = \mathbf{B}_k$. In other words, the whitening reduces the determination of the random matrix \mathbf{A}_k to the unitary matrix \mathbf{B}_k .

In the MIMO IC with IA, the k^{th} whitened received signal yields

$$\mathbf{y}_k^w = \mathbf{W}_k \mathbf{y}_k = \mathbf{W}_k \mathbf{A}_k \tilde{\mathbf{s}}_k + \mathbf{W}_k \mathbf{z}_k,\tag{4.15}$$

and the k^{th} decoded signal is obtained as

$$\hat{\mathbf{y}}_k = \mathbf{U}_k^H \mathbf{W}_k \mathbf{y}_k = \mathbf{U}_k^H \mathbf{W}_k \mathbf{A}_k \tilde{\mathbf{s}}_k + \mathbf{U}_k^H \mathbf{W}_k \mathbf{z}_k,\tag{4.16}$$

where \mathbf{U}_k is the unitary matrix that will separate the desired signal, i.e. the independent streams in (4.13).

4.6.3 Joint Approximate diagonalization of Eigenmatrices

JADE is a well known statistical technique for solving linear determined BSS problems. It is based on the fact that the fourth order cross-cumulants of independent variables are zeros. That is, demixing a mixed signal as in (4.11) involves looking for the decoding matrix that minimizes the sum of all the squared cross-cumulants of \mathcal{C}_e [57], and \mathbf{e} represents any vector of N mixed random variables. The sum of all the squared cross-cumulants of \mathcal{C}_e is given by

$$C_{cross} = \sum_{i \neq j} |cum(e_i, e_j^*, e_p, e_l^*)|^2, \quad (4.17)$$

where the cumulant set of all components (streams) of an observed data vector \mathbf{z} is defined as

$$\mathcal{C}_z = \{cum(e_i, e_j^*, e_p, e_l^*) \mid i, j, p, l \in \{1, \dots, N\}\}, \quad (4.18)$$

and cum refers to the fourth order cumulant and e_i^* is the complex conjugate of the i^{th} entry of \mathbf{e} .

In our transmission model, the observed vector is transformed to \mathbf{y}_k^w after being whitened. \mathbf{y}_k^w is then decoded using the unitary matrix \mathbf{U}_k . In [53], the authors have proposed to find \mathbf{U}_k that maximizes the sum of the squared auto-cumulants defined as

$$C_{auto}(\mathbf{U}_k) = \sum_{i=1}^N |cum(\hat{y}_{k,i}, \hat{y}_{k,i}^*, \hat{y}_{k,i}, \hat{y}_{k,i}^*)|^2, \quad (4.19)$$

and they have showed that it is equivalent to minimizing the sum of the squared cross-cumulants in $\mathcal{C}_{\hat{y}_k}$. Maximizing the criterion in (4.19) under unitary decoding matrix constraint can be done using Givens rotations based method. However, for the complex case, the Givens angles cannot be formulated in a closed-form.

In [6], the authors have modified the criterion in (4.19), and have proposed to seek \mathbf{U}_k as the unitary maximizer of the following criterion

$$c(\mathbf{U}_k) = \sum_{i,k,l=1}^N |cum(\hat{y}_{k,i}, \hat{y}_{k,i}^*, \hat{y}_{k,p}, \hat{y}_{k,l}^*)|^2. \quad (4.20)$$

This is equivalent to minimizing the sum of the squared cross-cumulants with distinct first and second indices. The modified criterion allows an efficient optimization by the use of the term "joint diagonalization". In our case, due to the existence of some mutual dependencies between the undesired signal, we show that the term becomes joint block diagonalization.

Now, for resolving the maximization problem of the function in (4.20) under the constraint of a unitary demixer, let us first define the cumulant matrices of the observed whitened signal as follows. To any $N \times N$ matrix \mathbf{M}_r with elements $m_{r,lp}$, $\forall p, l \in \{1, \dots, N\}$, is associated a cumulant matrix denoted $\mathbf{Q}_{\mathbf{y}_k^w}(\mathbf{M}_r)$ defined entrywise by

$$q_{ij} = \sum_{k,l=1}^N cum(\mathbf{y}_{k,i}^w, \mathbf{y}_{k,j}^{w*}, \mathbf{y}_{k,p}^w, \mathbf{y}_{k,l}^{w*}) m_{r,lp}, \quad \forall i, j \in \{1, \dots, N\}. \quad (4.21)$$

Also, defining the parallel set of all cumulant slices for $p, l \in \{1, \dots, N\}$ as

$$\mathcal{N}^p = \{\mathbf{Q}_{\mathbf{y}_k^w}(\mathbf{b}_p \mathbf{b}_l^T) | p, l \in \{1, \dots, N\}\} \quad (4.22)$$

where \mathbf{b}_p is the vector with only one non-zero element equal to one at the p^{th} position. Thus, $\mathbf{Q}_{\mathbf{y}_k^w}(\mathbf{b}_p \mathbf{b}_l^T)$ represents the (p, l) parallel cumulant slice whose $(i, j)^{th}$ entry is $cum(\mathbf{y}_{k,i}^w, \mathbf{y}_{k,j}^{w*}, \mathbf{y}_{k,p}^w, \mathbf{y}_{k,l}^{w*})$. It has been shown in [6] that for the set \mathcal{N}^p , the unitary matrix \mathbf{U}_k that maximizes $c(\mathbf{U}_k)$ is equivalent to the joint diagonaliser of the set \mathcal{N}^p given by

$$C_{diag}(\mathbf{U}_k, \mathcal{N}^p) = \sum_{k,l=1}^N \|\text{diag}(\mathbf{U}_k^H \mathbf{Q}_{\mathbf{y}_k^w}(\mathbf{b}_k \mathbf{b}_l^T) \mathbf{U}_k)\|^2, \quad (4.23)$$

where $\|\text{diag}(\cdot)\|^2$ is the norm of the vector built from the diagonal of the matrix. The joint diagonaliser of the set \mathcal{N}^p is also proven to be essentially equal to $\mathbf{W} \mathbf{A} = \mathbf{B}$ when all the variable components are independent. The joint diagonaliser can be obtained using the Jacobi technique.

In order to increase the computational efficiency, it has been demonstrated that for any N -dimensional complex random vector \mathbf{e} with fourth-order cumulants, there exist N^2 real numbers $\lambda_1, \dots, \lambda_{N^2}$ and N^2 matrices $\mathbf{M}_1, \dots, \mathbf{M}_{N^2}$ called eigenmatrices satisfying

$$\mathbf{Q}_e(\mathbf{M}_n) = \lambda_n \mathbf{M}_n, \quad \text{trace}(\mathbf{M}_n \mathbf{M}_r^H) = \delta(n, r) \quad \forall n, r \in \{1, \dots, N^2\}, \quad (4.24)$$

and for a unitary demixing matrix, $N(N - 1)$ eigenvalues of \mathbf{Q}_e are zeros and the rest N eigenvalues are equal to the kurtosis of the sources. Consequently, the joint diagonalization can be performed on the set made from the N most significant eigenpairs

$$\mathcal{N}_e = \{\lambda_n, \mathbf{M}_n \mid n \in \{1, \dots, N\}\} \quad (4.25)$$

The joint diagonalization is performed using the extended Jacobi technique.

Let us now summarize the steps of the algorithm JADE as follows

1. Step 1: Compute the whitening matrix \mathbf{W}_k as the inverse square root of the sample covariance matrix of the received data. As shown in [6], \mathbf{W}_k transforms \mathbf{A}_k into a unitary matrix $\mathbf{B}_k = \mathbf{W}_k \mathbf{A}_k$.
2. Step 2: Form the sample fourth order cumulant matrix³ $\mathbf{Q}_{\mathbf{y}_k^w}$ of the whitened data $\mathbf{y}_k^w = \mathbf{W}_k \mathbf{y}_k$
3. Step 3: Compute the N most significant eigenpairs of $\mathbf{Q}_{\mathbf{y}_k^w}$: $\{\lambda_n, \mathbf{M}_n \mid n = 1, \dots, N\}$
4. Step 4: Perform the approximate joint diagonalization of matrices $\{\lambda_n \mathbf{M}_n \mid n = 1, \dots, N\}$ by an unitary matrix \mathbf{U}_k
5. Step 5: An estimate of the source vector is $\hat{\mathbf{s}} = \mathbf{U}_k \mathbf{y}_k^w$

As described above and in [6], when all streams are statistically independent JADE is able to separate the original streams through joint diagonalization of the cumulant matrices. Let us now show that even in the presence of some mutually dependent components, as in (3.7), JADE is able to separate the mutual independent streams. For our considered problem, the $(N - d)$ interference sources are dependent in which case the set of matrices $\{\lambda_n \mathbf{M}_n \mid n = 1, \dots, N\}$ are not anymore jointly diagonalizable but are jointly block-diagonalizable. In other words, for $n = 1, \dots, N$, we have the following joint matrix structure:

$$\lambda_n \mathbf{M}_n = \mathbf{B}_k \begin{bmatrix} \mathbf{M}_{n,1} & \mathbf{0} \\ \mathbf{0} & \mathbf{M}_{n,2} \end{bmatrix} \mathbf{B}_k^H \quad (4.26)$$

where $\mathbf{M}_{n,1}$ are $d \times d$ diagonal matrices, $\mathbf{M}_{n,2}$ are $(N - d) \times (N - d)$ unstructured matrices and $\mathbf{B}_k = \mathbf{W}_k \mathbf{A}_k$. In [58], it is shown that the joint diagonalization algorithm used in the standard BSS method JADE can be used as well for the joint

³ $\mathbf{Q}_{\mathbf{y}_k^w}(i, j, k, l) = cum(y_{k,i}^w, y_{k,j}^{w*}, y_{k,p}^w, y_{k,l}^{w*})$.

block diagonalization of a set of matrices. Consequently, the final transformation given by the whitening matrix and unitary transform \mathbf{U} leads to:

$$\mathbf{U}_k \mathbf{W}_k \mathbf{A}_k = \begin{bmatrix} \mathbf{D}_1 & \mathbf{0} \\ \mathbf{0} & \mathbf{D}_2 \end{bmatrix}$$

where \mathbf{D}_1 is a $d \times d$ diagonal matrix and \mathbf{D}_2 a $(N - d) \times (N - d)$ given matrix. Hence, the first d entries of $\hat{\mathbf{s}}_k = \mathbf{U}_k \mathbf{y}_k^w$ represent the desired source signals while its remaining $N - d$ entries represent linear mixtures of the (non-desired) interference signals.

4.6.4 Semi-Blind separation

The ambiguities on the scale and permutation of the estimated streams can be solved using a few training symbols inserted within each data frame. We denote $\mathbf{s}_{j,tr} \in \mathbb{C}^{1 \times N_s}$ the j^{th} training sequence for $j \in \{1, \dots, d\}$, and $\hat{\mathbf{s}}_{i,N_s}$ the first N_s symbols of the i^{th} estimated independent stream with $i \in \{1, \dots, d\}$. We define the Normalized Minimum Mean Squared Error (NMSE), widely used to evaluate the efficiency of the BSS techniques, as

$$\text{NMSE}(\hat{\mathbf{s}}_{i,N_s}, \mathbf{s}_{j,tr}) = \log_{10} \left[1 - \frac{|\hat{\mathbf{s}}_{i,N_s} \mathbf{s}_{j,tr}^H|^2}{\|\hat{\mathbf{s}}_{i,N_s}\|^2 \|\mathbf{s}_{j,tr}\|^2} \right]. \quad (4.27)$$

The ambiguity on the permutation order can be solved by minimizing the NMSE according to the training sequence

$$\underset{i,j \in \{1, \dots, d\}}{\text{argmin}} \text{NMSE}(\hat{\mathbf{s}}_{i,N_s}, \mathbf{s}_{j,tr}), \quad (4.28)$$

Next, the scale ambiguity can be solved by looking for the complex variable α that minimizes the MMSE between the estimated variables and the training sequence

$$\text{MMSE} = \mathbb{E} [|\alpha \hat{\mathbf{s}}_{j,N_s} - \mathbf{s}_{j,tr}|^2]. \quad (4.29)$$

The $1 \times N_s$ vector $\hat{\mathbf{s}}_i$ used in (4.27), (4.28), and (4.29) is formed by the first N_s estimated symbols of the stream \mathbf{s}_k .

Remark 4.1: The proposed technique requires the receiver to wait for all samples within one frame. Therefore, the authors in [51] have proposed an adaptative semi-blind high order separation technique. This technique can be adapted to our case

since we have showed that the dependency between interference streams does not affect the desired source extraction.

Remark 4.2: As will be shown by our simulation results, the semi-blind approach results in a slight performance loss as compared to the standard (data-aided) MMSE. However, it is shown in [59], that in such cases one can compensate for this performance loss using a decision-directed MMSE detection in a two step approach, the first step being the semi-blind approach proposed previously (see [59] for further details).

4.7 Simulation Results

In this section, we evaluate the Bit Error Rate (BER) of the JADE and FastICA in a 3-user 2×2 and 4×4 MIMO IC with an IA design. The IA scheme is achieved using the distributed iterative solution proposed in [2] and described in section 4.4. We only treat the cases where the algorithm converges to a solution that guarantees an average interference power level of 10^{-4} . Each user sends $d = 2$ data streams. The symbols are QPSK modulated. The channel is supposed flat fading Rayleigh distributed, and remains constant over one frame with length $L = 2000$ symbols. We consider a naive training sequence, where the training symbols are selected randomly for all compared algorithms. Before starting we introduce the basic estimation method LS. The estimated channel matrix is given by

$$\mathbf{H}_{LS} = \mathbf{y}_{k,N_s} \mathbf{s}_{k,tr}^H (\mathbf{s}_{k,tr} \mathbf{s}_{k,tr}^H)^{-1}, \quad (4.30)$$

where $\mathbf{y}_{k,N_s} \forall k$ are the N_s^{th} first received signal vectors, and $\mathbf{s}_{k,tr}$ is the training sequence vector.

Fast ICA is a BSS technique characterized by its low computational complexity and fast convergence. It also performs close to the JADE in terms of robustness. The implementation of FastICA is based on the algorithm described in [60] (see [60] section V). Regarding the implementation of JADE, it is based on the algorithm proposed in [61], for which the matlab function can be found at [62].

Fig. 4.2 illustrates the BER performance of the MMSE-based detector with full and perfect CSI, the BSS-based detectors (JADE and FastICA), and the MMSE-based detector with LS-CSI estimation. We use $N_s = 8$ training symbols to resolve the scale and the permutation ambiguities, and to estimate the CSI for the LS method. As shown, JADE and FastICA have close BER performance in the entire

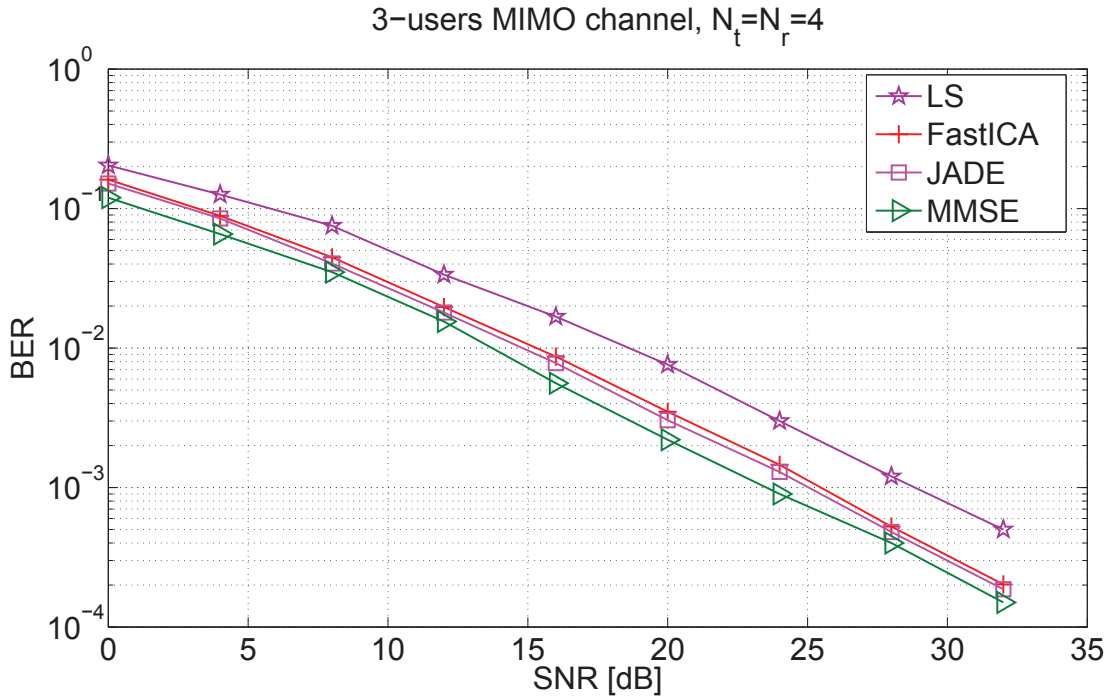


FIGURE 4.2: BER performance comparison using $N_s = 8$ training symbols

- JADE: proposed decoding scheme that uses JADE-based detector.
- FastICA: proposed decoding scheme that uses FastICA-based detector.
- LS: the MMSE-based detector with LS-CSI estimation.
- MMSE: the MMSE-based detector with perfect CSI.

SNR region. They also perform close to the MMSE-based with full and perfect CSI with a gap of about 1dB - 2dB over the entire SNR region. On the other hand, compared to the LS, a gain between 1dB - 4dB over all SNR values is obtained. Similar comparison is obtained for the 2×2 MIMO IC configuration, where $N_s = 4$ training symbols are introduced, as illustrated in Fig 4.3. In addition, the JADE-based detector and the FastICA-based detector performs the same. Compared to the MMSE-based with full CSI, a slight loss between 1dB and 2dB is obtained over the whole SNR region.

The scale and the permutation ambiguities can be resolved by inserting a few training symbols. Fig. 4.4 describes the BER behavior of the JADE and FastICA algorithm as a function of the training sequence length. The MMSE-based with LS-CSI estimation requires at least $N_s = \sum_{j=1}^3 d_j = 6$ to separate the sources. The JADE and FastICA techniques can separate the independent sources without any

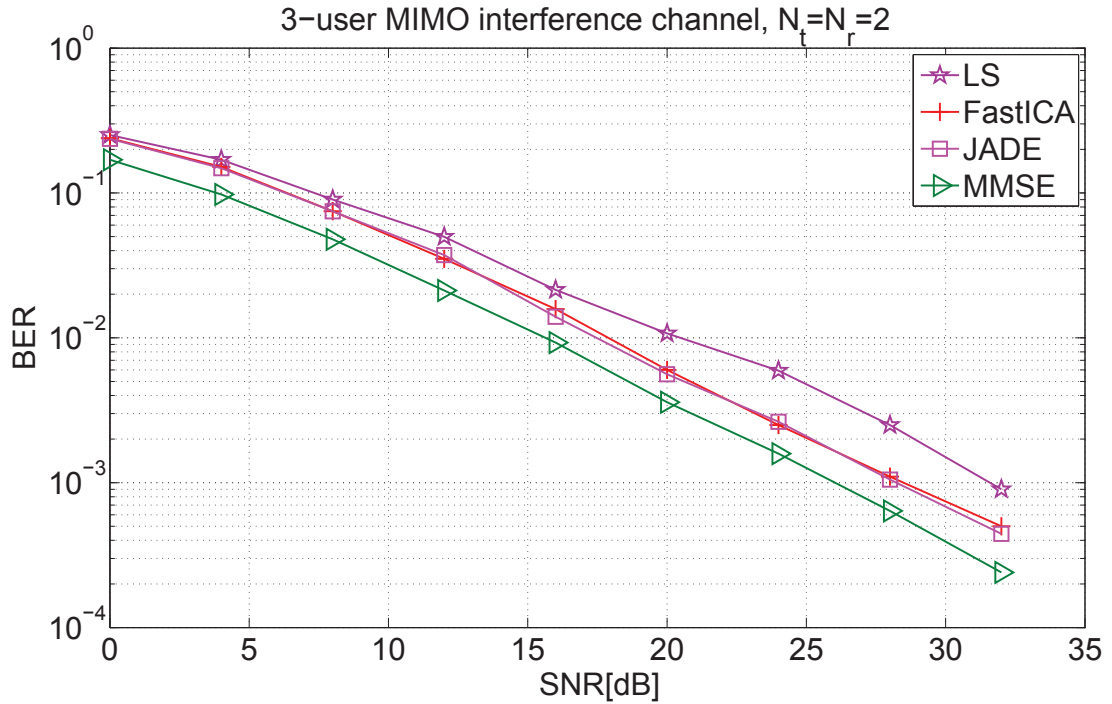
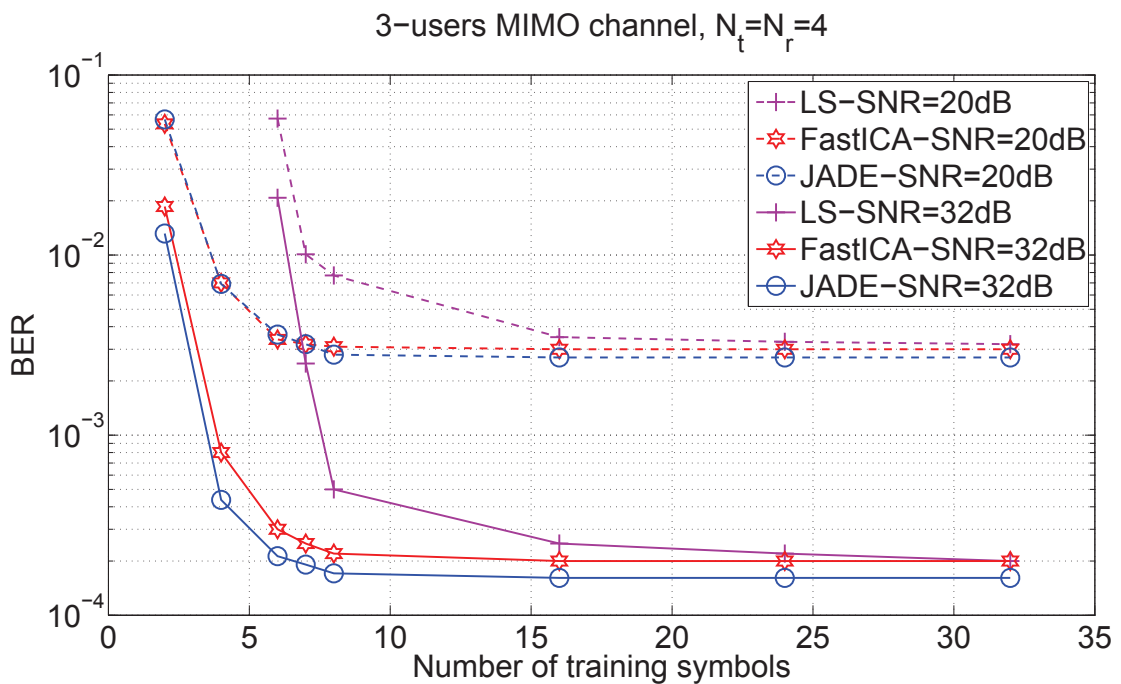
FIGURE 4.3: BER performance comparison using $N_s = 4$ training symbols

FIGURE 4.4: The influence of the training sequence length on the BER performance

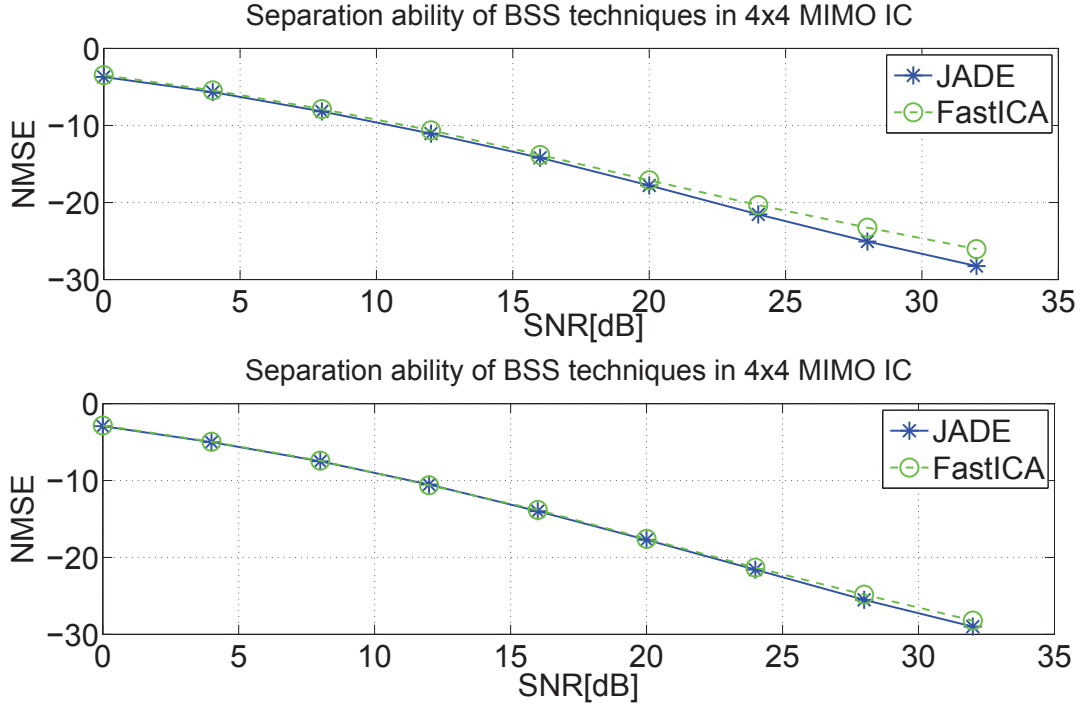


FIGURE 4.5: NMSE for measuring the efficiency of the ICA algorithms

training symbols. Then, the scaling and the permutation problem can be solved using $N_s = 1$ symbol for the case of one desired stream (i.e. one stream per user, $d = 1$) and more for the other cases, depending on the number of desired streams. For example, when $d_1 = d_2 = d_3 = 2$, $N_s = 2$ symbols is required. At 20dB, the BER of both techniques improves with N_s to reach $3 \cdot 10^{-3}$ for $N_s = 8$, and remains roughly unchanged when N_s increases. Comparing to the LS, an important BER gain is obtained for $N_s < 16$. This gain decreases when N_s increases and becomes negligible at $N_s = 32$. This BER behavior comparison is similar for SNR= 32dB.

Next, the Normalized Minimum Squared Error (NMSE) of the FastICA and the JADE algorithms is shown in Fig. 4.5. The NMSE defined below is similar to the one defined in (4.27) except that here we consider it over the whole frame, whereas in (4.27), it is considered over the duration of the training sequence. The NMSE of the j^{th} stream at the receiver k is given by

$$\text{NMSE}(\mathbf{s}_{j,N_s}, \hat{\mathbf{s}}_j) = \log_{10} \left[1 - \frac{|\hat{\mathbf{s}}_{j,N_s} \mathbf{s}_j^H|^2}{\|\hat{\mathbf{s}}_{j,N_s}\| \|\mathbf{s}_j\|} \right]. \quad (4.31)$$

One can notice that the NMSE decreases when the SNR increases, which means that the desired signals, composed from independent components, can be separated

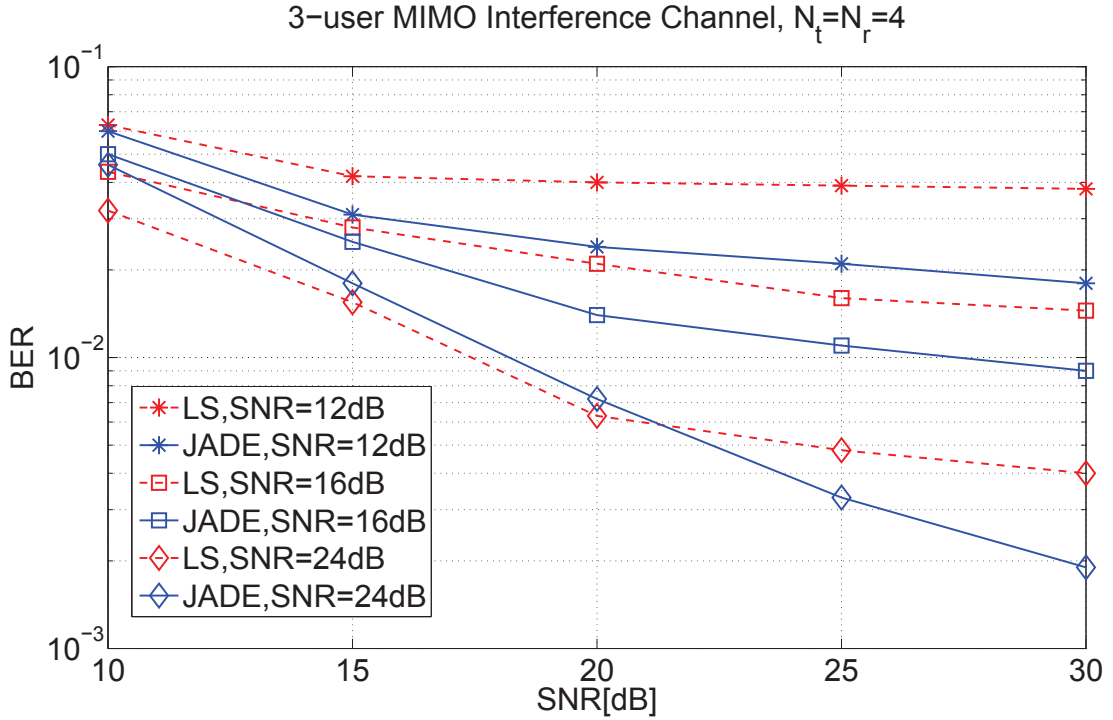
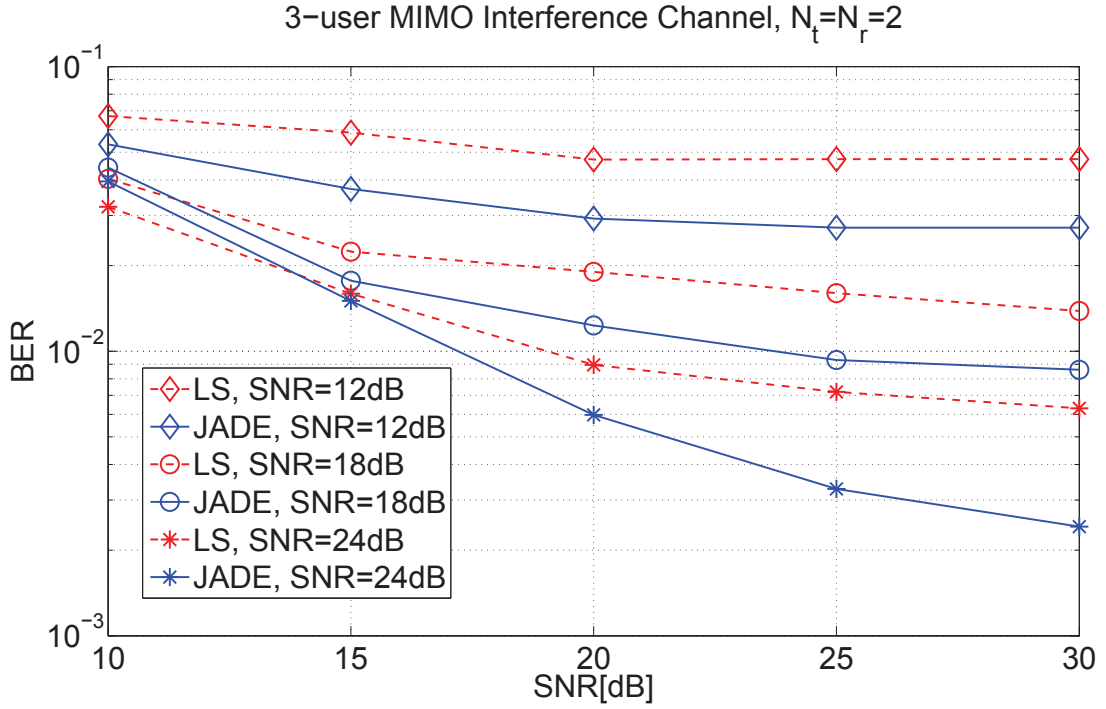


FIGURE 4.6: Effect of the IA imperfection on the BER performance $N_s = 8$

from the signal mixed with interference using high order cumulants concept.

In practice, in order to perform the IA design, channel matrices have to be estimated. There exists two strategies for channel estimation at the transmitters. In the first, the channel is estimated at each transmitter using an L_s -length uplink reference signal sent from the receivers assuming a reciprocal channel supposed constant during one frame transmission. This strategy is employed in the TDD-uplink transmission scheme in the 3GPP-LTE network [49]. The second strategy is when each receiver estimates the channels connecting him with the transmitter, and feeds it back quantized to the transmitter. The reliability of this strategy depends on the channel estimator at the receiver, the channel quantizer, and the feedback link quality. Research works carried out, e.g. in [63, 64], and have studied the IA achievability using a limited feedback link. They have defined a channel quantizer over the composite Grassmannian manifold, that achieves a full DoF in the IC when the feedback bit rate scales sufficiently fast with the SNR. In our study, we assume the first strategy in a TDD-uplink transmission scheme where the receiver sends to the transmitter an L_s -length reference signal in a reciprocal channel for CSI estimation, and we want to study the robustness of the proposed detector for a given channel estimation error. The estimated channel matrices are

FIGURE 4.7: Effect of the IA imperfection on the BER performance $N_s = 8$

modeled as [65]

$$\tilde{\mathbf{H}}_{kj} = \mathbf{H}_{kj} + \mathbf{E}_{kj}; \quad \forall k, j \quad (4.32)$$

where \mathbf{E}_{kj} is the channel estimation error $\forall k, j$. The coefficients of \mathbf{E}_{kj} are symmetric complex Gaussian distributed with zero mean and σ_e^2 variance. In Fig. 4.6 and 4.7, the BER performance of both LS and JADE methods is illustrated in presence of a channel estimation error. For the configuration 2×2 MIMO IC, it can be observed that JADE tends to the performance with perfect IA design when:

- SNR= 12dB and the imperfection is beyond $\sigma_h^2/\sigma_e^2 = 20$ dB,
- SNR= 18dB and the imperfection is beyond $\sigma_h^2/\sigma_e^2 = 25$ dB,
- SNR= 24dB and the imperfection is beyond $\sigma_h^2/\sigma_e^2 = 30$ dB.

JADE also results in better BER performance than the LS. Now, for the configuration 4×4 MIMO IC, it can be observed that JADE tend to the performance with perfect IA design when the imperfection is beyond $\sigma_h^2/\sigma_e^2 = 20$ dB for the three SNR values 12dB, 16dB and 24dB. Additionally, in the region where $\sigma_h^2/\sigma_e^2 < 10$ dB, both of the detectors result in a degraded BER. However, our

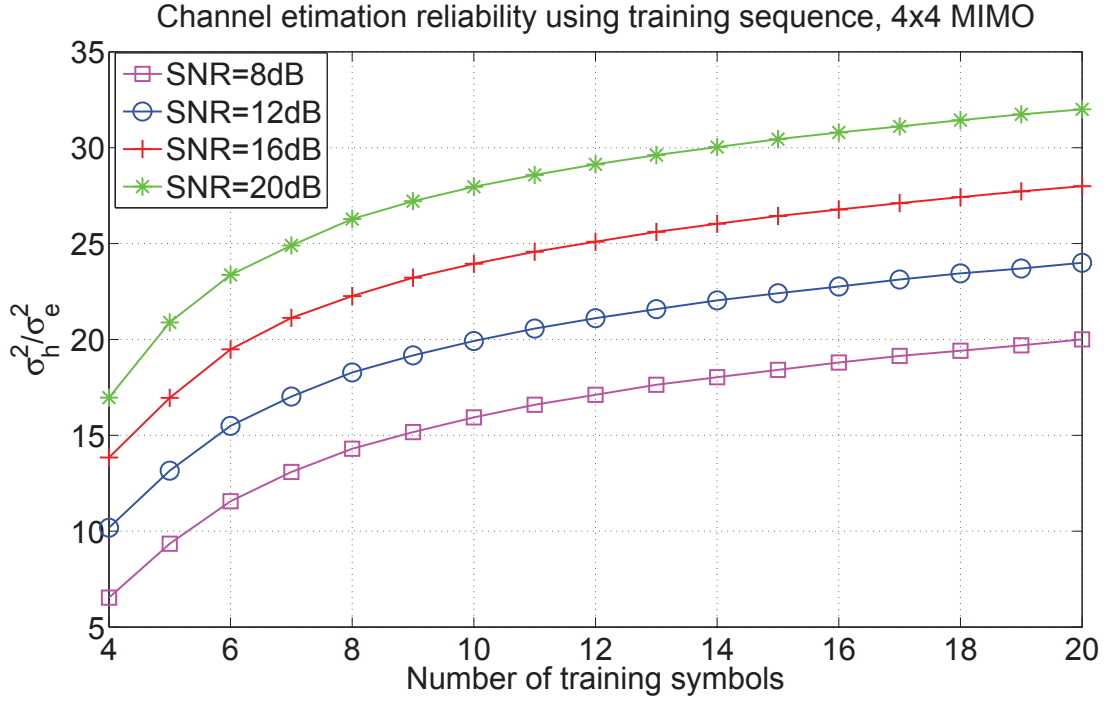


FIGURE 4.8: The channel estimation error for different SNR values using least square estimator

proposed decoder outperforms the LS: i) beyond $\sigma_h^2/\sigma_e^2 = 10\text{dB}$ when SNR=12dB, ii) beyond $\sigma_h^2/\sigma_e^2 = 14\text{dB}$ when SNR=16dB, and iii) beyond $\sigma_h^2/\sigma_e^2 = 21\text{dB}$ when SNR=20dB.

In a practical system, the training symbol number is a tradeoff between channel estimation accuracy and spectral efficiency loss. It is necessary to study the influence of the training sequence length on the performance of the proposed scheme. Fig. 4.8 illustrates the variation of estimation reliability in terms of the training sequence length. One can observe that high values, i.e. $\sigma_h^2/\sigma_e^2 > 20\text{dB}$, can be achieved using:

- $L_s = 5$ training symbols sent to the transmitter when SNR= 20dB,
- $L_s = 7$ training symbols sent to the transmitter when SNR= 16dB,
- $L_s = 11$ training symbols sent to the transmitter when SNR= 12dB,
- $L_s = 20$ training symbols sent to the transmitter when SNR= 8dB.

Which means that reliable channel estimation can be achieved with a reasonable training sequence length, even when the SNR is not too high.

Remark 4.3: The results shown above are for the basic scheme proposed in this chapter. It is worth noticing that the introduction of the training sequence is not the only way for solving the permutation and scaling problem. However, it is one of the simplest method. For example, when a receiver has only one desired stream to extract, the ambiguity is the limited to the scale only. Such ambiguity can be resolved using ACMA algorithm (analytical constant modulus algorithm) as proposed in [59].

4.8 Conclusion

In this chapter, we have addressed the problem of detection for the downlink of a multi-user MIMO system using IA scheme at the transmitters. The problem has been formulated as a blind source separation problem, and we have shown the efficiency of the BSS methods, e.g. the joint diagonalization technique (JADE), for blindly detecting the desired signals. Training sequences have been introduced to resolve the permutation and scaling ambiguities. The proposed scheme performs close to full-CSI MIMO IC-IA schemes. We have also showed by simulations that it outperforms the traditional MMSE using LS for interference estimation method when using the same training sequence length.

In the next chapter, we assume that in the multi-user MIMO IC the transmitters cannot cooperate and do not have any knowledge of the CSI. We address the problem of detection with a spatial multiplexing scheme assumption as IA cannot be applied due to a lack of CSI at the transmitters.

Chapter 5

Low complexity detectors based on sparse decomposition for uplink transmission

5.1 Introduction

In chapter 3 and 4, we have addressed the K -user MIMO and SISO interference networks where the transmitters have knowledge of the full CSI and apply the IA concept. In this chapter, we address a K -user MIMO interference network and consider the only possible CSI knowledge ; the one between each transmitter and its destination. In such a context, IA and joint designs cannot be applied. This context is similar to the transmission in an uplink mode when the transmitters (mobile end users) cannot exchange information and have knowledge of only the CSI between them and their intended destinations. Herein, we do not study the precoding design at the transmitters, but rather we focus on a detection scheme that utilizes ML criterion for signal reconstruction. We show first that decoding the interference jointly with the desired signal using ML joint detector can achieve the maximum receive diversity that is equal to the number of independent observations at the receiver side. Then, we propose alternative solutions to the ML that highly increase the computational efficiency for high signal and constellation dimensions.

Basically, ML joint detection has been proposed as an optimal strategy that detects simultaneously the transmitted signals [66]. ML detector has been proved to minimize the probability of error for medium and high SNR values. However, its complexity grows exponentially with the antenna dimensions and the constellation size, which makes it impractical. Alternative solutions have been proposed,

among which the sphere decoder (SD) which achieves near-optimal performance assuming that the spherical search is well designed [67]. However, SD exhibits a variable computational complexity that depends heavily on the SNR value, the signal dimension, and the sphere radius initialization. The computational complexity order has been upper-bounded by $\mathcal{O}(M^\gamma)$, where $\gamma \in (0, 1]$, N is the signal dimension, and M is the constellation size [68].

The aforementioned detectors are based on an exhaustive search of the desired signal. This implies a high computational complexity order that does not suit the practical systems. Sub-optimal MIMO detection schemes have been studied such as fixed sphere decoder and the K-best sphere decoding scheme [69, 70]. However, these detectors still require very high computational complexity for very high signal and constellations dimensions. In this chapter, we assume a finite transmit constellation size, and propose iterative strategies to detect the desired signal. This iterative detection aims to maintain a low computational cost even with the increase of the signal and/or constellation size. We rewrite the MIMO channel model with inputs selected from a finite alphabet set as a MIMO channel with sparse inputs belonging to the binary set $\{0, 1\}$. Then, we propose two ways for the signal detection. In the first, we exploit the knowledge of the number of non-zero elements of the vector to be recovered and formulate the problem of detection as a minimization problem of the norm ℓ_0 within a well-defined sphere. The ℓ_0 -norm minimization can be relaxed by an ℓ_1 -norm minimization problem [71]. This relaxation makes it possible to use iterative algorithms proposed for sparse source recovering with polynomial time complexity [41, 72]. The proposed ℓ_1 -minimization problem seeks a solution that lies in the intersection of a sphere with radius ϵ and of a well-defined plane.

The first minimization problem is highly dependent on ϵ , and does not necessarily ensure a low error probability for very high SNR when the number of observations is less than the number of decoded symbols. Therefore, we propose an alternative minimization problem for signal detection equivalent to the ML detection problem. This alternative problem looks for a solution that minimizes the euclidean distance with the received signal subject to the constant norm ℓ_0 . For the same reasons as previously, and with the aim of reducing the computational complexity, we relax the ℓ_0 -norm constraint by the ℓ_1 -norm constraint. This relaxation imposes a solution lying in the intersection of a lozenge with a unit diameter and a predefined plane. Unfortunately, the equality constraint of the ℓ_1 -norm is not convex. Therefore, we demonstrate that for our specified problem the relaxed

ℓ_1 -norm constraint is satisfied by only ensuring that all components of the variable vector are positive. This reduces our problem to a quadratic minimization problem under linear equality and positive variable constraints, i.e. under convex constraints. Such a problem can be solved iteratively using first order optimization algorithms (i.e. gradient descent) and other polynomial time algorithms e.g. primal-dual point interior method [41].

The last part of this chapter incorporates the minimum distance (MD) based detector in a turbo detection scheme. The goal is to improve the joint detection iteratively by modifying the minimization criterion of the detector at each iteration depending on the extrinsic information at the output of the channel decoder. The main points addressed in this chapter are summarized as follows:

- Highlighting the receive diversity when an ML joint detector is applied for detecting the desired signal and the interference signal simultaneously.
- Transforming the decoding problem into a sparse input recovering problem.
- Detecting the desired signal via ℓ_1 -minimization under linear and quadratic constraints.
- Detecting the desired signal via quadratic minimization under linear equality constraints.
- Integrating the minimum distance based detector in a turbo detection scheme.

This chapter is organized as follows. Section 5.2 describes the MIMO transmission model. In section 5.3, we show the receive diversity gain when interference is jointly decoded with the desired signal. The sphere decoding scheme is described in section 5.4. The MIMO model with finite alphabet input is transformed into a model with sparse input in section 5.5. Section 5.6 proposes the iterative decoding scheme based on ℓ_1 -norm minimization. Section 5.7 proposes an alternative decoding scheme that minimizes the euclidean distance with the received signal preserving a constant norm ℓ_1 . The complexity and the error rate performance are assessed in Section 5.8. The last contribution of the turbo detection is proposed in 5.9. Finally, Section 5.10 concludes the chapter.

5.2 System model

We consider a K -user MIMO interference channel, where each transmitter and each receiver are equipped with N_t and N_r antennas, respectively. We assume a

perfect CSI knowledge at the receiver. Our system model does not necessitate any joint design at the transmitters and do not consider any precoding scheme. The received signal is defined as follows

$$\mathbf{y}_k = \mathbf{H}_{kk}\mathbf{x}_k + \sum_{j \neq k} \mathbf{H}_{kj}\mathbf{x}_j + \mathbf{z}_k, \quad (5.1)$$

where $\mathbf{H}_{kj} \in \mathbb{C}^{N_r \times N_t}$ is the random channel matrix between the j^{th} transmitter and the k^{th} receiver, \mathbf{x}_k is the $d_k \times 1$ data vector from the k^{th} transmitter with symbols selected from a finite alphabet constellation, and \mathbf{z}_k is the $N_r \times 1$ circularly symmetric additive Gaussian noise vector with zero mean and covariance matrix equals to $\sigma^2 \mathbf{I}$ at the k^{th} receiver. The components of \mathbf{x}_k belong to a finite alphabet constellation defined as $\mathcal{Q} = \{q_1, q_2, \dots, q_M\}$. For example, assuming a 4-QAM constellation yields $M = 4$ and $\mathcal{Q} = \{\frac{1+i}{\sqrt{2}}, \frac{1-i}{\sqrt{2}}, \frac{-1+i}{\sqrt{2}}, \frac{-1-i}{\sqrt{2}}\}$.

In the previous chapters, we have assumed an IA design, which allows the use of linear receivers for the desired signal detection. In this chapter, we do not assume any specific precoding design, which means that linear receivers are not efficient for desired signal detection and interference suppression. In this respect, we propose to consider the interference as a useful signal, and to jointly decode the desired signal plus the interference signal. We show that decoding the interference jointly with the desired signal can achieve a full receive diversity equal to the number of observations.

5.3 Joint decoding of interference and desired signal

Let us first rewrite the received signal in (5.1) as follows

$$\begin{aligned} \mathbf{y}_k &= \mathbf{H}_{k1}\mathbf{x}_1 + \dots + \mathbf{H}_{kK}\mathbf{x}_K + \mathbf{z}_k \\ &= (\mathbf{H}_{k1}, \dots, \mathbf{H}_{kK}) \begin{pmatrix} \mathbf{x}_1 \\ \vdots \\ \mathbf{x}_K \end{pmatrix} + \mathbf{z}_k, \\ &= \bar{\mathbf{H}}_k \mathbf{x} + \mathbf{z}_k, \end{aligned} \quad (5.2)$$

where $\bar{\mathbf{H}}_k$ is the new channel matrix with dimensions $N_r \times d_t$, and $d_t = \sum_{j=1}^K d_j$. In order to decode the original information in (5.2), we propose to use a joint minimum-distance (MD) detector. In the presence of interference, the authors in

[73] have shown that the solution of the joint MD detector becomes very close to the one obtained using the detector with ML criterion when the SNR increases (i.e. in the region of optimality) and requires less computational complexity. The MD detector is based on an exhaustive search over all possible transmitted vectors and selects the symbol vector with the minimum distance to the received signal. The detected signal is the solution of the following minimization problem

$$\hat{\mathbf{y}}_k = \arg \min_{\mathbf{x} \in \mathcal{Q}^{d_t}} \|\mathbf{y}_k - \bar{\mathbf{H}}_k \mathbf{x}\|^2. \quad (5.3)$$

Next, we show the receive diversity that can be achieved using the proposed strategy for joint interference and desired symbols decoding.

Our channel model in (5.3) can be seen as a single user $d_t \times N_r$ MIMO channel. For a single user MIMO channel, the generic receiver equation is equal to

$$\mathbf{y}_{D_R} = \mathbf{H}_{D_R \times d_t} \mathbf{x}_{d_t \times 1} + \mathbf{z}_{D_R}. \quad (5.4)$$

Assuming MD detector, the probability of error can be approximated at high SNR by [35]

$$P_e = \alpha \text{SNR}^{-D_T D_R}, \quad (5.5)$$

where α points out the horizontal shift of the P_e curve, D_T is the transmit diversity gain, and D_R is the receive diversity gain. Assuming $D_T = 1$, (5.5) indicates that the slope of the probability of error is proportional to the inverse of SNR to the power D_R . D_R is equal to the number of independent observations at the receiver, and remains independent of the number of transmit antennas. This result has been established in [74], where the authors have concluded that when using an MD detector, only an SNR penalty is introduced when the number of transmit antennas increases. Hence, for the channel model in (5.2) the expected receive diversity gain achieved with an MD detector is $D_R = N_r$. In the remaining of this chapter, the channel model in (5.2) will be adopted.

5.4 Sphere decoding

The MD detector exploits the receive channel diversity and performs near-optimally in the medium to high SNR region. However, it is based on an exhaustive search, for which the computational complexity grows exponentially. An alternative solution that performs similarly with reduced complexity is the sphere

decoding (SD). In the following, we revise briefly the concept of the sphere decoder with its computational efficiency.

The goal of the SD proposition is to reduce the computational cost of the joint MD detector while maintaining the same decoding performance [75]. It consists in searching over all possible transmitted symbols with the corresponding points in the received constellation lying within a hypersphere of radius r around the received vector \mathbf{y}_k . The SD problem can be represented by the following minimization problem

$$\arg \min_{\mathbf{x} \in \mathcal{Q}^{d_t}} \|\mathbf{y}_k - \bar{\mathbf{H}}_k \mathbf{x}\|^2 \quad \text{subject to} \quad \|\mathbf{y}_k - \bar{\mathbf{H}}_k \mathbf{x}\|^2 \leq r^2. \quad (5.6)$$

Assuming $\bar{\mathbf{H}}_k$ a square matrix, it can be QR decomposed as $\bar{\mathbf{H}}_k = \mathbf{Q}_k \mathbf{R}_k$, where \mathbf{Q}_k is a unitary matrix and \mathbf{R}_k is an upper triangular matrix at the receiver k . Using the decomposed $\bar{\mathbf{H}}_k$, and the fact that a Frobenius norm is unitarily invariant¹, the constraint of the problem in (5.6) can be formulated as

$$\|\hat{\mathbf{y}} - \mathbf{R}_k \mathbf{x}\|^2 \leq r^2, \quad (5.7)$$

where $\hat{\mathbf{y}} = \mathbf{Q}_k^H \mathbf{y}_k$. Equation (5.7) is equivalent to

$$r^2 \geq \sum_{j=1}^{d_t} \left(\hat{y}_j - \sum_{i=j}^{d_t} r_{ij,k} x_i \right)^2, \quad (5.8)$$

where $r_{ij,k}$ denotes the $(i, j)^{th}$ entry of the upper triangular matrix \mathbf{R}_k . The expansion of (5.8) yields

$$r^2 \geq (\hat{y}_{d_t} - r_{d_t d_t, k} x_{d_t})^2 + (\hat{y}_{d_t-1} - r_{(d_t-1)d_t, k} x_{d_t} - r_{(d_t-1)(d_t-1), k} x_{d_t-1}) + \dots, \quad (5.9)$$

where the first term depends only on x_{d_t} , the second term on (x_{d_t}, x_{d_t-1}) and so on. One can notice from (5.9) that a necessary condition for the decoded signal to be in the hypersphere of radius r is to have $(\hat{y}_{d_t} - r_{d_t d_t} x_{d_t})^2 \leq r^2$, which means

$$\lceil \frac{-r + \hat{y}_{d_t}}{r_{d_t d_t}} \rceil \leq x_{d_t} \leq \lfloor \frac{r + \hat{y}_{d_t}}{r_{d_t d_t}} \rfloor. \quad (5.10)$$

¹Unitarily invariant norm means $\|\mathbf{A}\| = \|\mathbf{U}\mathbf{A}\mathbf{V}\|$ where \mathbf{U} and \mathbf{V} are unitary matrices

Then, for every x_{d_t} satisfying this condition, we define $r^{[d_t-1]} = r - (\hat{y}_{d_t} - r_{d_t d_t} x_{d_t})^2$ and $\hat{y}_{d_t}^{[d_t-1]} = \hat{y}_{d_t-1} - r_{(d_t-1)d_t} x_{d_t}$, that yields a stronger necessary condition as

$$\left\lceil \frac{-r^{[d_t-1]} + \hat{y}_{d_t}^{[d_t-1]}}{r_{(d_t-1)(d_t-1)}} \right\rceil \leq x_{d_t-1} \leq \left\lfloor \frac{r^{[d_t-1]} + \hat{y}_{d_t}^{[d_t-1]}}{r_{(d_t-1)(d_t-1)}} \right\rfloor. \quad (5.11)$$

The condition in (5.11) is still necessary but not sufficient for a point to be in the hypersphere. One can continue in a similar way for x_{d_t-2} and so on until x_1 . At a position i with $1 \leq i < d_t$, if the condition is not satisfied, the decoder goes up to the level $i + 1$ and chooses another candidate value from the corresponding region for x_{i+1} . If the decoder reaches the symbol x_1 with a symbol vector \mathbf{x}' verifying the condition that the euclidean distance metric is less than r i.e. $\|\mathbf{y}_k - \bar{\mathbf{H}}_k \mathbf{x}'\|^2 \leq r^2$, then the radius r will be updated and the new search is limited by the new value of $\|\mathbf{y}_k - \bar{\mathbf{H}}_k \mathbf{x}'\|$. The above process continues until no further point is found inside the hypersphere, and the symbol vector achieving the smallest value of (5.7) is considered as the MD solution.

When the matrix $\bar{\mathbf{H}}_k$ is tall or fat, a preprocessing has to be applied before the process described above. When $\bar{\mathbf{H}}_k$ is tall, i.e. more observations than data symbols, $\bar{\mathbf{H}}_k$ is first decomposed as [67]

$$\bar{\mathbf{H}}_k = [\mathbf{Q}_{1,k} \ \mathbf{Q}_{2,k}] \begin{bmatrix} \left(\mathbf{R}_k \right) \\ \mathbf{0} \end{bmatrix}, \quad (5.12)$$

thereby the hypersphere equation in (5.6) can be written as

$$\|\mathbf{Q}_{1,k} \mathbf{y}_k - \mathbf{R}_k \mathbf{x}\|^2 \leq r^2 - \|\mathbf{Q}_{2,k} \mathbf{y}_k\|^2. \quad (5.13)$$

Using the new hypersphere equation in (5.13), the sphere decoding process can be applied as described above with the new radius $r' = \sqrt{r^2 - \|\mathbf{Q}_{2,k} \mathbf{y}_k\|^2}$. Now, when $\bar{\mathbf{H}}_k$ is fat and for constant modulus signals, i.e. more data symbols than observations, an equivalent minimization problem to (5.6) is given by [76]

$$\arg \min_{\mathbf{x} \in \mathcal{Q}^{d_t}} \|\mathbf{y}_k - \bar{\mathbf{H}}_k \mathbf{x}\|^2 + \alpha \mathbf{x}^H \mathbf{x}. \quad (5.14)$$

This is also equivalent to

$$\arg \min_{\mathbf{x} \in \mathcal{Q}^{d_t}} \|\tilde{\mathbf{y}}_k - \mathbf{D}_k \mathbf{x}\|^2, \quad (5.15)$$

where $\tilde{\mathbf{y}}_k = \mathbf{D}_k \mathbf{G}_k^{-1} \bar{\mathbf{H}}_k \mathbf{y}_k$, $\mathbf{G}_k = \bar{\mathbf{H}}_k^H \bar{\mathbf{H}}_k + \alpha \mathbf{I}_{d_t}$ and it is Cholesky factorized as $\mathbf{G}_k = \mathbf{D}_k^H \mathbf{D}_k$, where \mathbf{D}_k is an upper triangular matrix. The diagonal terms of \mathbf{D}_k are all non-zero and the sphere decoding process described above can be applied to (5.15).

5.5 Sparse decomposition

The goal of our work is to propose an efficient decoding scheme of the received data samples characterized by a polynomial complexity order over the whole SNR region. We assume a priori knowledge on the transmitted information. We exploit the fact that the original symbols belong to a finite alphabet, and we decompose each symbol on the basis of the vector space in which the finite alphabet vector $\mathbf{q} = [q_1, q_2, \dots, q_M]$ can be cast. That is, the data vector with N entries in the transmission model can be modeled as an equivalent sparse data vector with $d_t \times M$ entries. The j^{th} symbol x_j of \mathbf{x} is decomposed (c.f. Figure 5.1)

$$\begin{aligned} x_j &= \mathbf{q} \mathbf{s}_j^T, \\ \text{where } \mathbf{s}_j &= [\delta_{q_1}(x_j), \delta_{q_2}(x_j), \dots, \delta_{q_M}(x_j)], \\ \text{and } \delta_{q_i}(x_j) &= \begin{cases} 1 & \text{if } x_j = q_i \\ 0 & \text{otherwise} \end{cases}. \end{aligned} \quad (5.16)$$

Applying this decomposition over all symbols, the vector \mathbf{x} can be formulated in function of \mathbf{s} as

$$\begin{aligned} \mathbf{x} &= \mathbf{B}_q \mathbf{s}, \\ \text{where } \mathbf{s} &= [\mathbf{s}_1, \mathbf{s}_2, \dots, \mathbf{s}_{d_t}]^T, \text{ and } \mathbf{B}_q = \mathbf{I}_N \otimes \mathbf{q}. \end{aligned} \quad (5.17)$$

\mathbf{B}_q is a block diagonal matrix of size $d_t \times d_t M$. Substituting (5.17) into (5.1) yields the received signal

$$\mathbf{y}_k = \bar{\mathbf{H}}_k \mathbf{B}_q \mathbf{s} + \mathbf{z}_k. \quad (5.18)$$

Since \mathbf{s} is a sparse vector that contains lots of zero elements, the detection of the original information can be seen as a sparse source decoding. In the upcoming sections, we propose two minimization problems to detect \mathbf{s} . The first is inspired from problems of sparse source recovering [77]. The second is an approximation

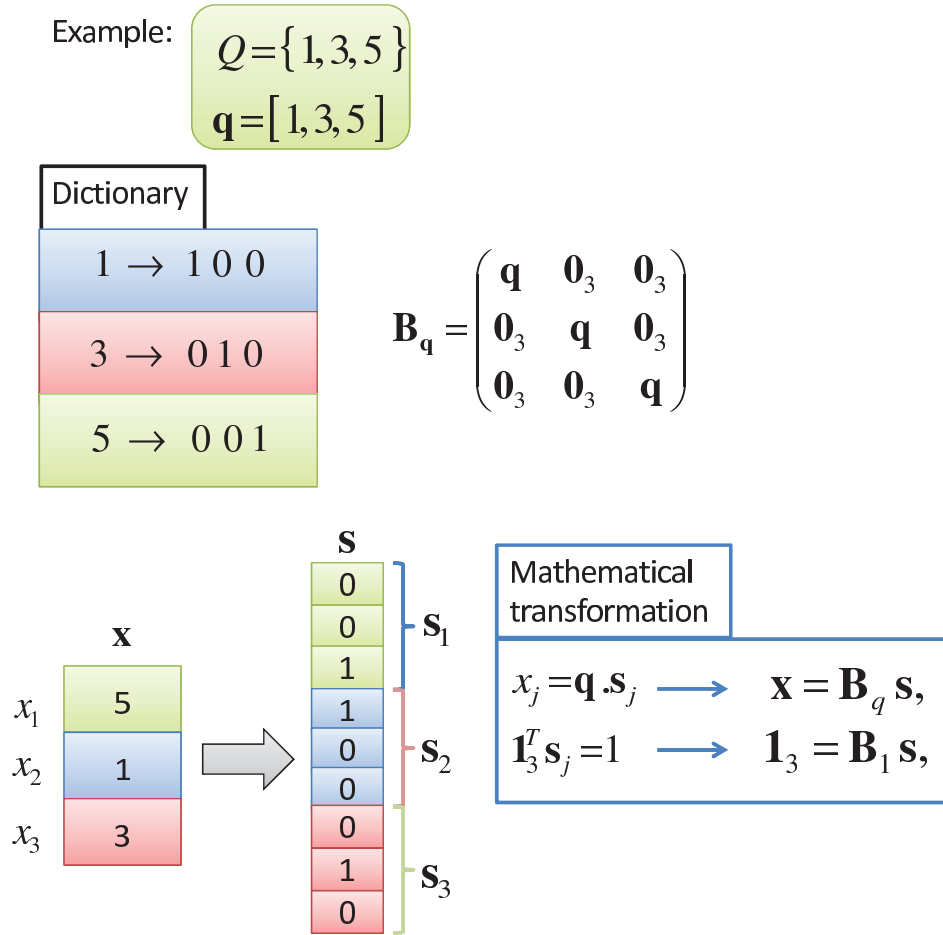


FIGURE 5.1: Sparse decomposition of a vector with components belonging to a finite alphabet set.

of the MD detector based on the euclidean distance minimization. Both problems detect the original signal iteratively using algorithms with polynomial complexity such as the primal-dual interior point method, the gradient descent method [41]. Related problems have proposed in [78, 79, 80, 81, 82, 83, 84] .

5.6 Iterative detection of sparse transformed MIMO via ℓ_1 -minimization

This section proposes to detect the desired signal using the ℓ_1 -norm minimization problem under linear and quadratic constraints. In order to solve the ℓ_1 -minimization problems, iterative methods are usually applied such as Primal Dual Interior Point (PDIP) method and Homothopy method [85]. In the following, we address two channel cases: noiseless and noisy MIMO interference channel, and

we formulate a minimization problem for signal detection in each case. We also show that in a noiseless case, and for binary alphabet constellation, the alternative detection problem is equivalent to the MD joint detection problem.

5.6.1 Noiseless MIMO channel

Using the sparse decomposition as in the previous section for a noiseless case, the transmission model becomes

$$\mathbf{y}_k = \bar{\mathbf{H}}_k \mathbf{B}_q \mathbf{s}. \quad (5.19)$$

This sparse source recovering problem has been addressed in [77]. It has been written as a minimization problem of an ℓ_0 -norm, i.e.

$$\arg \min_{\mathbf{s} \in \mathbb{R}^{d_t M}} \|\mathbf{s}\|_0 \quad \text{subject to } \mathbf{s} \in \{ \mathbf{y}_k = \bar{\mathbf{H}}_k \mathbf{B}_q \mathbf{s}, \text{ and } \mathbf{B}_1 \mathbf{s} = \mathbf{1}_{d_t} \}, \quad (5.20)$$

where the norm ℓ_0 is the total number of non-zero elements in a vector, and the $d_t \times d_t M$ block diagonal matrix \mathbf{B}_1 is defined as

$$\mathbf{B}_1 = \mathbf{I}_{d_t} \otimes \mathbf{1}_M^T. \quad (5.21)$$

The equality constraint $\mathbf{B}_1 \mathbf{s} = \mathbf{1}_{d_t}$ ensures that the solution $\mathbf{B}_q \mathbf{s}$ has d_t nonzero components. The authors in [77] have proved that such a problem has a unique sparse solution \mathbf{s} . Thus, the desired information \mathbf{x} is recovered by seeking the unique solution of (5.20). However, solving the ℓ_0 -minimization is NP-hard and requires an exhaustive search over all the coefficients of \mathbf{s} . Therefore, with the aim of reducing the complexity cost of the optimization, it has been proposed to relax the ℓ_0 -norm by the ℓ_1 -norm. In this respect, the optimization problem becomes

$$\arg \min_{\mathbf{s} \in \mathbb{R}^{d_t M}} \|\mathbf{s}\|_1 \quad \text{subject to } \mathbf{s} \in \{ \mathbf{y}_k = \bar{\mathbf{H}}_k \mathbf{B}_q \mathbf{s}, \text{ and } \mathbf{B}_1 \mathbf{s} = \mathbf{1}_{d_t} \}, \quad (5.22)$$

For a binary alphabet, the equivalence between the ℓ_1 -norm minimization problem in (5.22) and the ℓ_0 -norm minimization problem (5.20) has been proved with probability tending to 1 for large d_t and when the random mixing matrix $\bar{\mathbf{H}}_k$ satisfies $N_r \geq d_t/2$. Additionally, they have also conjectured that for a non-binary finite alphabet i.e. $M > 2$, the equivalence is still guaranteed for large N and when $\frac{(M-1)}{M} d_t \leq N_r$.

5.6.2 Noisy MIMO channel

In this subsection, we adapt the scheme described in [77] to the noisy MIMO channel case. In presence of noise, the received signal is given as in (5.1) and (5.18). The solution of \mathbf{x} that respects $\mathbf{y}_k = \bar{\mathbf{H}}_k \mathbf{x}$ is no longer in the finite constellation set due to the random noise added to the received signal. On the other hand, since the noise is assumed Gaussian distributed with zero mean and σ^2 variance, there exists a constant ϵ such that $\|\mathbf{y}_k - \bar{\mathbf{H}}_k \mathbf{B}_q \mathbf{s}\|_2^2 < \epsilon$. In this respect, using the decomposition of \mathbf{x} in its dictionary i.e. $\mathbf{x} = \mathbf{B}_q \mathbf{s}$, we propose the following minimization problem for the detection of \mathbf{s}

$$[\ell_0 - \min] : \arg \min_{\mathbf{s} \in \{0,1\}^{d_t M}} \|\mathbf{s}\|_0, \text{ subject to } \mathbf{s} \in \{ \|\mathbf{y}_k - \bar{\mathbf{H}}_k \mathbf{B}_q \mathbf{s}\|_2^2 < \epsilon, \text{ and } \mathbf{B}_1 \mathbf{s} = \mathbf{1}_{d_t} \}, \quad (5.23)$$

As previously, the equality constraint $\mathbf{B}_1 \mathbf{s} = \mathbf{1}_{d_t}$ ensures that a solution with symbols belonging to the finite constellation inputs exists. The other inequality constraint $\|\mathbf{y}_k - \bar{\mathbf{H}}_k \mathbf{B}_q \mathbf{s}\|_2^2 < \epsilon$, restricts the codewords searching area to be within an euclidean distance less than a constant ϵ to the received signal. The minimization problem is similar to the sphere decoding problem, but is written in a different manner. That is, the non-zero elements of the detected sparse vector are imposed to be equal to d_t with recovered symbols belonging to the transmit constellation set and to the hypersphere of radius $\sqrt{\epsilon}$.

In our problem, the detected symbols depend heavily on the choice of ϵ , which in turn depends on the current SNR value. We try to select ϵ such that the probability to only obtain the correct solution within the codewords searching area is maximized. Hence, we define ϵ as follows [86]

$$\epsilon = F_{\chi_d^2(\rho^2)}^{-1}(1 - \gamma), \quad (5.24)$$

where $F_{\chi_d^2(\rho^2)}$ is the cumulative distribution function of the non-central χ^2 distribution $\chi_d^2(\rho^2)$ with d degrees of freedom and non-central parameter ρ^2 . The threshold parameters in our problem are defined as follows: $d = 2N_r$ due to the complex noise, $\rho^2 = 2\sigma^2 \log(N_r)$ is the universal threshold, and $\gamma \in (0, 1]$. Discussion on the optimality of the chosen ϵ is given in the Appendix D.

The problem presented in (5.23) is NP-hard and is not convex. This means that an exhaustive search is required and a non-unique solution may be obtained. Therefore, as evoked in (5.23), we propose to relax the ℓ_0 -norm by the ℓ_1 -norm.

Subsequently, the decoding problem can be formulated as

$$[\ell_1 - \min] : \arg \min_{\mathbf{s} \in \mathbb{R}^{d_t M \times 1}} \|\mathbf{s}\|_1 \quad \text{subject to } \mathbf{s} \in \{ \|\mathbf{y}_k - \bar{\mathbf{H}}_k \mathbf{B}_q \mathbf{s}\|_2^2 < \epsilon, \text{ and } \mathbf{B}_1 \mathbf{s} = \mathbf{1}_{d_t} \}, \quad (5.25)$$

The ℓ_1 -norm minimization problems are based on an iterative processing that employs optimization algorithms solvable in polynomial time. One of the most performant and efficient methods is the primal-dual interior point (PDIP) [87]. The PDIP algorithm shows a significant computational gain compared to the NP-hard solver, since each iteration requires $\mathcal{O}(N^3 M^3)$ arithmetic operations where N is the vector length, whereas the NP-hard requires a number of operations that increases exponentially with N .

5.7 Iterative detection of sparse transformed MIMO via minimum distance minimization

The detection problem given in (5.23) looks for the sparse source that minimizes the norm ℓ_0 within a well-defined sphere-plane intersection. In this section, we reverse the problem, and we seek a solution with the smallest euclidean distance to the received signal on a well-defined plane, while a constant ℓ_0 -norm is maintained. The reason behind this criterion modification is that the previous minimization problem depends on both the sphere radius ϵ and the relaxation of the ℓ_0 -norm. Furthermore, the uniqueness of the solution is related to how accurate the sphere radius is. The proposed quadratic problem herein only depends on the ℓ_0 -norm relaxation, and can be seen as a relaxed MD detector.

Starting with the MD detector, it requires an exhaustive search over all possible transmitted symbol vectors, and selects the solution that corresponds to the closest point to the received signal in the received constellation. In other words, it selects the symbol vector that minimizes the euclidean distance between \mathbf{y}_k and $\bar{\mathbf{H}}_k \mathbf{x}$. Hence, the MD detection problem is defined as

$$[MD] : \arg \min_{\mathbf{x}} \|\mathbf{y}_k - \bar{\mathbf{H}}_k \mathbf{x}\|_2^2 \quad \text{subject to } \mathbf{x} \in \mathcal{Q}^{d_t}. \quad (5.26)$$

The main drawback of the MD problem is that it suffers from a high computational complexity because of the constraint $\mathbf{x} \in \mathcal{Q}^{d_t}$ that entails an exhaustive search. Herein, we propose an equivalence to this constraint using the following proposition

Proposition 1. The components of \mathbf{x} belong to the finite alphabet constellation \mathcal{Q} if and only if the following equalities hold: $\mathbf{B}_1 \mathbf{s} = \mathbf{1}_{d_t}$ and $\|\mathbf{s}\|_0 = d_t$.

Proof. Assuming first that the components of a d_t -dimensional vector \mathbf{x} belong to a finite alphabet set, thus \mathbf{x} can be sparsely decomposed as $\mathbf{x} = \mathbf{B}_q \mathbf{s}$ (see section 5.5), where \mathbf{s} consists of d_t sub-vectors with only one non-zero element equal to one for each. This means that the sum over each sub-vector is equal to one i.e. $\mathbf{B}_1 \mathbf{s} = \mathbf{1}_{d_t}$, and the total number of non-zero elements in \mathbf{s} is equal to d_t i.e. $\|\mathbf{s}\|_0 = d_t$.

Let us now assume both equalities $\mathbf{B}_1 \mathbf{s} = \mathbf{1}_{d_t}$ and $\|\mathbf{s}\|_0 = d_t$. The first equality $\mathbf{B}_1 \mathbf{s} = \mathbf{1}_{d_t}$, i.e. $\sum_{p=1}^M s_{(j-1)M+p} = 1$ for all $j \in \{1, \dots, d_t\}$, implies that at least one non-zero element exists in any sub-vector $j \in \{1, \dots, d_t\}$, with a minimum total non-zero elements number d_t . The second equality $\|\mathbf{s}\|_0 = d_t$ imposes the total non-zero elements number to be equal to d_t , thus along with the first equality each sub-vector can contain only one element different from zero and equal to one. Thereby, the projection of the whole vector \mathbf{s} onto the decomposition matrix \mathbf{B}_q yields a vector $\mathbf{x} = \mathbf{B}_q \mathbf{s}$ in the finite alphabet constellation \mathcal{Q}^{d_t} . \square

Using proposition 1, the [MD] minimization problem in (5.26) becomes

$$\arg \min_{\mathbf{s} \in \mathbb{R}^{d_t M}} \|\mathbf{y}_k - \bar{\mathbf{H}}_k \mathbf{B}_q \mathbf{s}\|_2^2 \quad \text{subject to } \mathbf{B}_1 \mathbf{s} = \mathbf{1}_{d_t}, \|\mathbf{s}\|_0 = d_t. \quad (5.27)$$

The $d_t \times d_t M$ matrix \mathbf{B}_1 is defined as in (5.21). The first constraint given by $\mathbf{B}_1 \mathbf{s} = \mathbf{1}_{d_t}$ is linear and does not require a high computational cost. The second constraint given by $\|\mathbf{s}\|_0 = d_t$ is discrete i.e. belongs to a finite discrete set, thereby making the problem NP-hard. Such problems necessitate exhaustive search to be solved yielding an exponential increase of the computational complexity with the signal dimension. To overcome this drawback, we propose to relax the ℓ_0 -norm by the ℓ_1 -norm. The relaxed constraint yields $\|\mathbf{s}\|_1 = d_t$. Such a constraint is not convex, thus, a global optimum is not necessarily achieved. In order to transform the problem into a quadratic minimization problem subject to convex constraints, we introduce the following lemma:

Lemma 1. Let \mathbf{B}_1 be a matrix defined as $\mathbf{B}_1 = \mathbf{I}_{N_r} \otimes \mathbf{1}_M^T$ and \mathbf{s} a $(d_t M)$ -length real vector satisfying $\mathbf{B}_1 \mathbf{s} = \mathbf{1}_{d_t}$. Then all components of \mathbf{s} are positive if and only if its ℓ_1 -norm equals d_t i.e. $\|\mathbf{s}\|_1 = d_t$.

Proof. Let $\mathbf{B}_1 = \mathbf{I}_{N_r} \otimes \mathbf{1}_M^T$. The k -th row of \mathbf{B}_1 has null components except components of indices ranging from $(k-1)N+1$ to kN which equal to one. Thus

$\mathbf{B}_1 \mathbf{s} = \mathbf{1}_{d_t}$ implies

$$\sum_{p=1}^M s_{(k-1)d_t+p} = 1 \quad \forall k. \quad (5.28)$$

By successive additions with respect to k , we obtain

$$\sum_{i=1}^{d_t} s_i = d_t. \quad (5.29)$$

Let us first assume that all components of \mathbf{s} be positive. Then $\mathbf{s}_i = |s_i|$ and using (5.29), we deduce that $\sum_{i=1}^{d_t M} |s_i| = d_t$, i.e. $\|\mathbf{s}\|_1 = d_t$.

Let us now assume that $\|\mathbf{s}\|_1 = d_t$. Considering (5.29), we can thus write

$$\sum_{i=1}^{d_t M} (|s_i| - s_i) = 0. \quad (5.30)$$

Let $\mathcal{N}(s)$ stand for the set of non-zero negative components of s . Then $\sum_{i=1}^{d_t M} (|s_i| - s_i)$ equals $2 \sum_{i \in \mathcal{N}(s)} |s_i|$ and is non-zero positive which is in contradiction with (5.30). We thus deduce that $\mathcal{N}(s)$ is empty and all components of s are positive. \square

Using the lemma above, the decoding problem becomes

$$[\mathbf{Quad-min}] : \arg \min_{\mathbf{s} \in \mathbb{R}^{N_M \times 1}} \|\mathbf{y}_k - \bar{\mathbf{H}}_k \mathbf{B}_q \mathbf{s}\|_2^2 \quad \text{subject to } \mathbf{B}_1 \mathbf{s} = \mathbf{1}_{d_t}, \mathbf{s} \geq 0. \quad (5.31)$$

This new optimization model is a quadratic programming model with linear equality constraints and nonnegative variables. It can be solved using iterative methods proposed for quadratic programming. One efficient method is the primal dual interior point (PDIP), especially when high accuracy is required. This method is largely discussed in the literature, and for more details the reader can refer to [41] (see Chap 11). The PDIP method is characterized by a significant computational gain compared to the NP-hard solver, since each iteration requires $\mathcal{O}(M^3 N^3)$ arithmetic operations, where N is the variable vector length, whereas the NP-hard requires a number of operations that increases exponentially with N i.e. $\mathcal{O}(M^N)$.

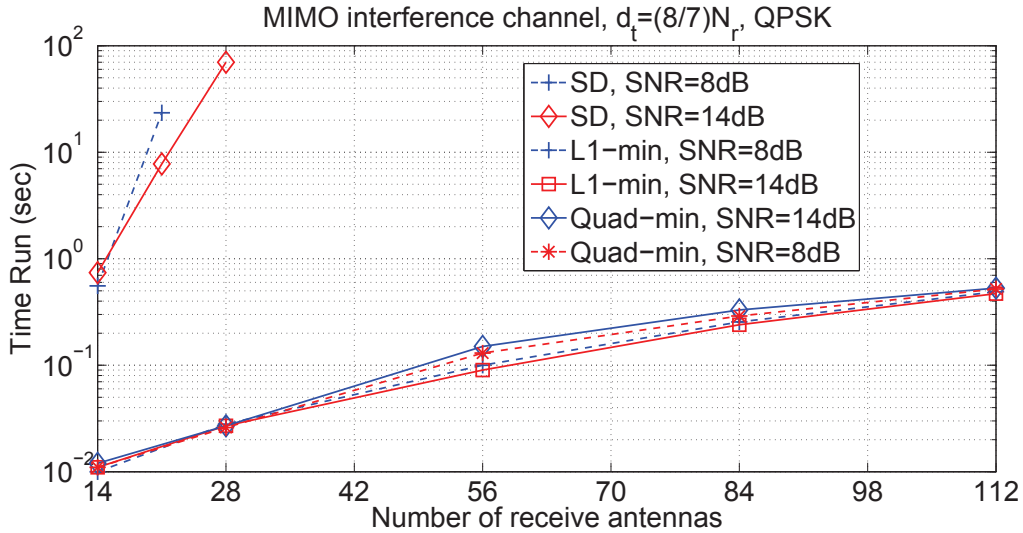


FIGURE 5.2: Time-run comparison of the proposed decoding schemes versus the sphere decoder for different SNR values under QPSK constellation inputs.

5.8 Complexity and bit error rate performance

In this section we evaluate the Bit Error Rate (BER) and the computational complexity of the proposed detectors based on quadratic minimization and ℓ_1 -minimization. We consider a multi-user MIMO interference channel as discussed in section 5.2, and assume a joint detection of the interference and the desired signal at each receiver, which means that for each receiver the interference channel can be modeled as an $d_t \times N_r$ MIMO single user channel, where d_t is the total number of the symbols from all transmitters and N_r is the number of receive antennas at the receivers. The channel coefficients are i.i.d. circularly symmetric complex Gaussian distributed with zero mean and unit variance, and the data symbols belong to a finite constellation. For our proposed detectors, we use the cvx toolbox which is a Matlab-based modeling system for convex optimization [88, 89]. Cvx is compatible with several solvers such as SeDuMi and SDPT3 [72, 90]. For our problems, we pick the Gurobi optimizer [91] to solve the [ℓ_1 -min] and the [Quad-min] problem proposed in section 5.6 and 5.7. We simulate this system using Matlab 7.10 on a processor Intel(R) Core(TM) i5-3317U CPU at 1.70GHz with memory 6GB RAM.

Fig. 5.2 compares the time run of the sphere decoder (SD), described in [76], to the time run of the proposed detectors [ℓ_1 -min] and [Quad-min]. The time-run represents the average processing time to decode the received signal. We assume a QPSK constellation mapping known at both the transmitter and the receiver. It

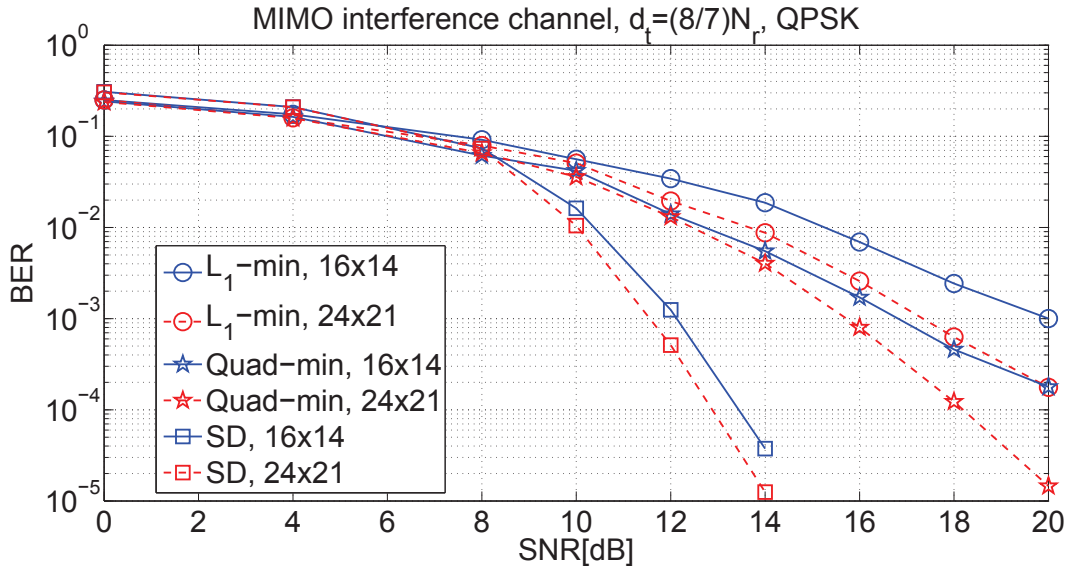


FIGURE 5.3: BER performance comparison of the proposed decoding schemes versus the sphere decoder under QPSK constellation inputs.

can be observed that with the iterative processing, the time-run increases slightly with the system dimensions, however, it remains independent of SNR. For example, the time run of the [Quad-min] problem is equal to 0.011 sec for both SNR values 8dB and 14dB using a 16×14 system dimensions. Moreover, increasing the dimensions from 16×14 to 32×28 entails an increase of only 0.019 sec. On the other hand, the SD time-run blows up when the dimensions or/and the SNR level increase. For instance, when going from 16×14 to 32×28 antennas dimension, the time run undergoes an increase of more than 20 sec. For the SD, we could not go beyond the 24×21 system dimensions due to a very high computational complexity, which is upper-bounded by $\mathcal{O}(M^{\gamma N})$, where $\gamma \in (0, 1]$ [68]. However, using any of our proposed detectors, any MIMO system with very high dimensions can be decoded, e.g. a signal with 128 transmitted symbol can be detected in less than half a second. Furthermore, the increase of the time run can be predicted from its slope in Fig. 5.2 which is much lighter than the SD slope.

Regarding the BER performance, Fig. 5.3 illustrates a slight performance gain of our schemes in the low SNR region. Otherwise, i.e. beyond 8dB, the SD outperforms the proposed schemes. For example, compared to the [Quad-min] decoding scheme, a gain between 2dB and 2.5dB is obtained respectively with the dimensions 16×14 and 24×21 . Comparing to the $[\ell_1$ -min] decoding scheme, we observe at BER 10^{-2} a gain of about 5dB with a 16×14 antennas and of 4dB with a 24×21 antennas. To compare the iterative detectors to each other, Fig. 5.4

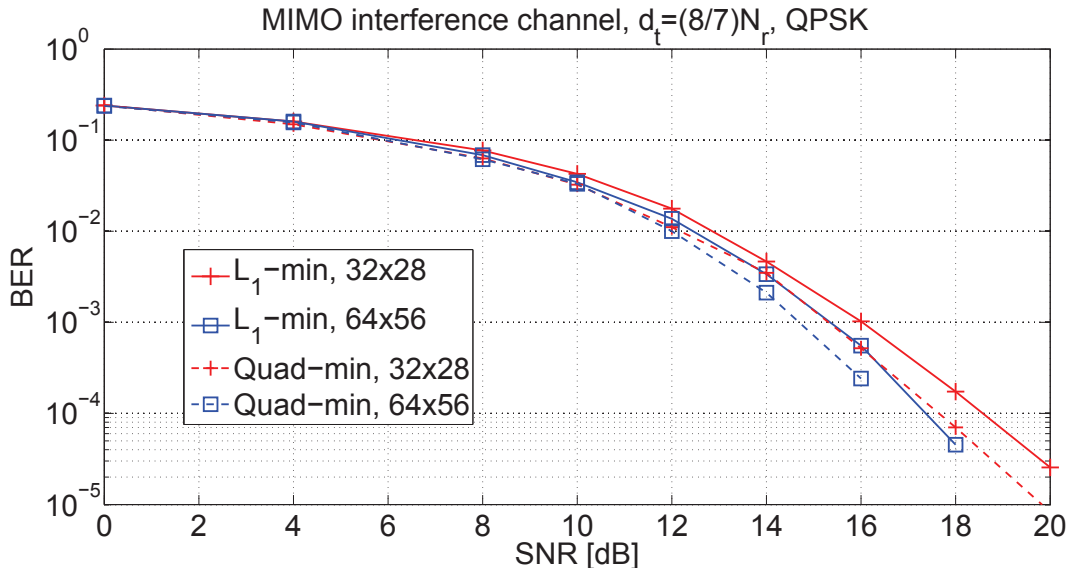


FIGURE 5.4: BER performance of the proposed decoding schemes for large antennas dimensions under QPSK constellation inputs.

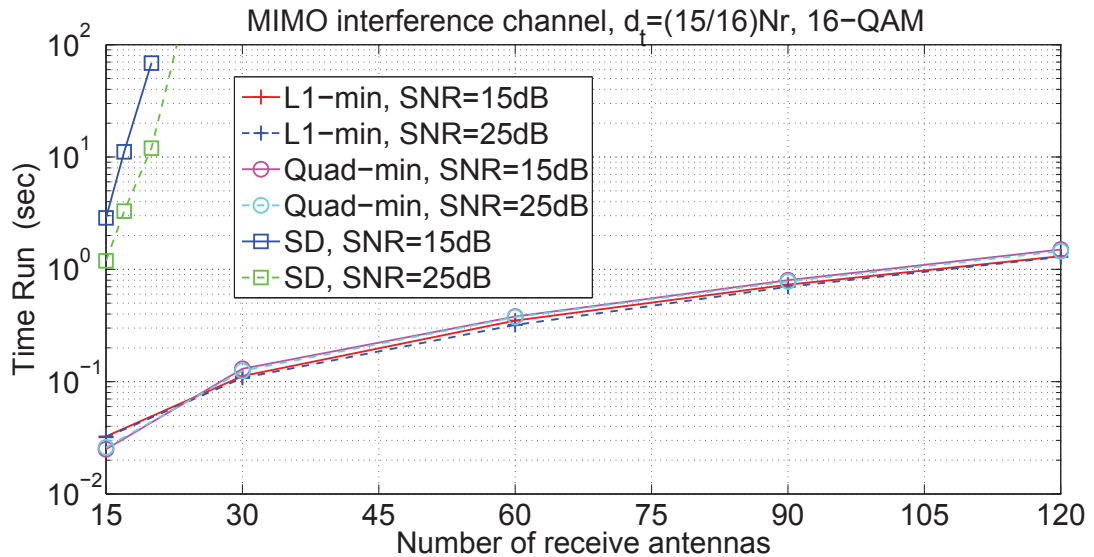


FIGURE 5.5: Time-run comparison of the proposed decoding schemes versus the sphere decoder for different SNR values under 16-QAM constellation inputs.

exhibits the BER performance in the underdetermined 32×28 and 64×56 MIMO systems. It can be first observed that both detectors exploit the receive diversity, i.e. when the antennas dimension increases the BER is improved. Second, we notice that the [Quad-min] outperforms the [ℓ_1 -min] in terms of BER, specially for high SNR values.

Fig. 5.5 and 5.6 represent the time run and the BER of the proposed detection

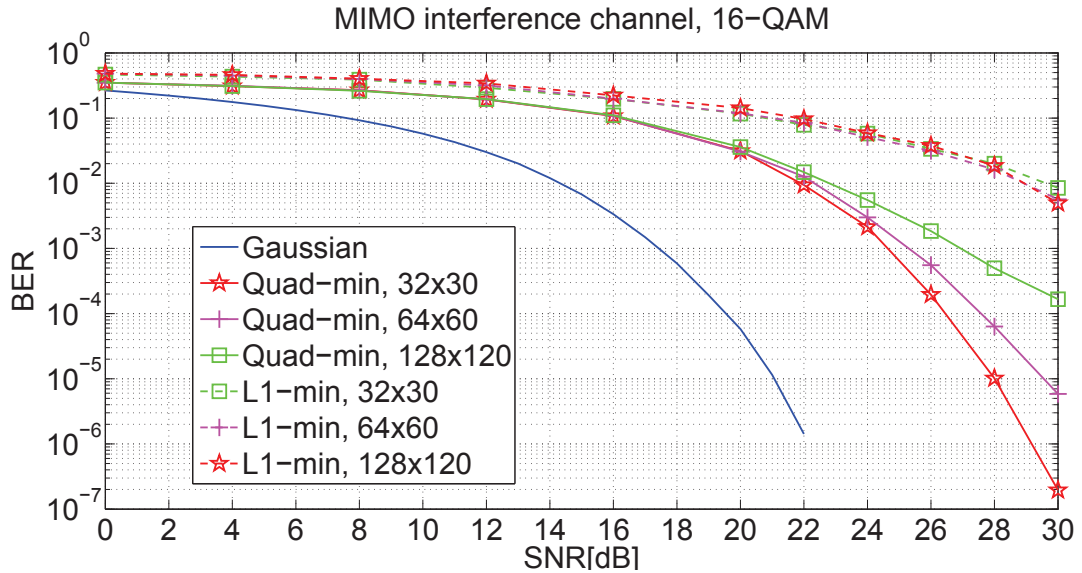


FIGURE 5.6: BER performance of the proposed decoding schemes for large antennas dimensions under 16-QAM constellation inputs.

schemes and the SD for a 16-QAM constellation. The analysis of the computational efficiency is similar to the one presented in Fig. 5.2, except that a higher time run is required for all detectors since the constellation dimension increases. In terms of BER performance, we do not compare to the SD that requires a prohibitive running time. The detectors performance are compared to each other and to the Gaussian channel reference curve. An important result is the gain obtained by the [Quad-min] over the [ℓ_1 -min], which exceeds 7dB at 10^{-2} . The [Quad-min] interest becomes more significant for large dimensions. It uses the same minimization criterion as the MD, and the only difference is that the ℓ_0 -norm constraint is relaxed by the ℓ_1 -norm. For some other problems, the relaxation of the ℓ_0 -norm by the ℓ_1 -norm does not affect the problem and an equivalence of both problems (original and relaxed) holds [77, 92]. We do not claim this equivalence herein, however, additional constraint might be found to yield similar performance as the original MD detector.

5.9 Turbo detection of a sparse detected signal

The previous sections have proposed alternative detectors that detect the signal using polynomial time solvable algorithms. Two detectors have been proposed. The first detector called [ℓ_1 - min], is based on the ℓ_1 -norm minimization under linear and quadratic constraints. The second detector called [**Quad-min**], involves

minimizing the distance between the received constellation and the received signal under linear constraints and a constant ℓ_1 -norm constraint. It has been shown from simulations in section 5.8, that the second detector results in better BER performance than the ℓ_1 -norm based detector. Therefore in the remaining of this chapter we will consider the [**Quad-min**] detector since it seems a better candidate for offering a trade-off between complexity and performance. Our goal is to associate the proposed detector with a channel decoding scheme that helps in minimizing the BER and yields a more reliable transmission [93]. We thus consider from now, that binary streams are forward error correcting (FEC) encoded then randomly interleaved before being converted into symbols.

5.9.1 Turbo detection concept

Turbo detection is based on the turbo principle used first for parallel concatenated convolutional codes (i.e. turbocodes) [94]. The originality of turbocodes is their capability for approaching the channel capacity in a computational feasible way [95]. The key idea is, at the receiver one soft-in soft-out decoder passes on the extrinsic part of the soft output to the other soft-in soft-out decoder and vice versa. To make an analogy, we give as an example the mechanism of the turbo engine, where the compressor (one decoder) feeds back the compressed air (extrinsic information) to the main engine (the other decoder).

The turbo concept can be successfully applied not only for the channel decoding, but also in a wide area of communication receivers yielding turbo detection, turbo equalization, multi-user detection [96, 97, 98] ... This part is dedicated to the association of a FEC decoder with the detector [**Quad-min**] at the receiver side. As shown in Fig. 5.7, the detector delivers extrinsic information from the soft output to the channel decoder and vice versa, which permits a detector-decoder iterative process [99]. Both the detector and the channel decoder must be soft-input/soft-output (SISO) devices, i.e., both must be able to accept and produce soft-decision information. The purpose behind is to let the receiver benefit from an improved error rate performance while maintaining acceptable computational cost. The turbo detection scheme consists of a main detector, a channel decoder, an interleaver, a deinterleaver, a symbol to binary converter, and a binary to symbol converter.

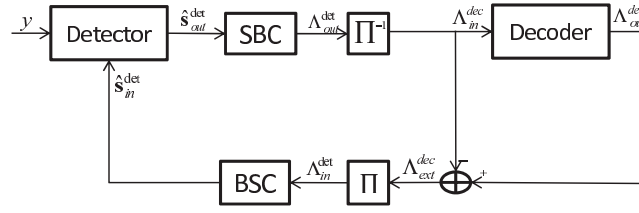


FIGURE 5.7: Turbo detection scheme

5.9.2 Turbo detection scheme

Back to our model, each symbol is seen as a projection of a sparse sub-vector onto the finite alphabet vector \mathbf{q} . Each sub-vector has only one non-zero component equals to one at the symbol position in the \mathbf{q} vector. In other words, the components of each sub-vector represent the probabilities of presence of the symbols. For example, when the transmitted symbol is the first element in \mathbf{q} , the probability of transmission of this element is equal to one, and the probability of transmission of any other element in \mathbf{q} is equal to zero. The probabilities are all in the binary set $\{0, 1\}$ since the elements in the sparse vector can only take the values zero or one. This interpretation will be useful for building the detector soft output to be delivered to the soft FEC decoder.

Regarding the detection based on the [Quad-min] problem, we introduce the following proposition

Proposition 2. Let us denote \mathbf{s}_{out}^{det} the detector output used as a soft estimate of \mathbf{s} . All the recovered elements of the sparse vector $\hat{\mathbf{s}}$ are in the interval $[0, 1]$. Moreover, the sum of the components in each sub-vector is equal to one, i.e. $\sum_{p=1}^M \hat{s}_{(j-1)M+p}^{det} = 1, \forall j \in \{1, \dots, d_t\}$.

Proof. The detection problem in (5.31) is subjected to a positive variable constraint. Also, the constraint $\mathbf{B}_1 \mathbf{s} = \mathbf{1}_{d_t}$ imposes that the sum of all components in each sub-vector is equal to one, i.e. $\sum_{p=1}^M \hat{s}_{(j-1)M+p}^{det} = 1, \forall j \in \{1, \dots, d_t\}$. Both constraints taken together imply that all elements of the sparse vector are positive and less than or equal to one, which means in the interval $[0, 1]$. \square

Using the proposition above, we will consider in the following the recovered elements in the interval $[0, 1]$ as the probabilities of a symbol to occur conditionally to \mathbf{y} .

Let $m = \log_2(M)$ and b be the length- md_t coded and interleaved binary information sequence at one channel use. Let also η be the binary to symbol conversion

defined as:

$$\eta : \left[b_{(k-1)m} \quad b_{(k-1)m+1} \quad \dots \quad b_{km-1} \right] \in \{0, 1\}^m \rightarrow x_k \in \mathcal{Q} \quad (5.32)$$

and $b_p = \eta^{-1}(q_p)$.

At first iteration, the sparse detector provides \hat{s}_{out}^{det} interpreted as a posteriori probabilities of x that is:

$$\hat{s}_{out}^{det}((k-1)m+p) = \Pr(x_k = q_p | y). \quad (5.33)$$

Using \hat{s}_{out}^{det} , the symbol to binary converter can compute log likelihood ratio on the i -th bit associated to the k -th symbol, denoted by Λ_{out}^{det} and defined as:

$$\Lambda_{out}^{det}((k-1)m+i) = \log_e \left(\frac{\Pr(b((k-1)m+i) = 1 | \hat{s}_{out}^{det})}{\Pr(b((k-1)m+i) = 0 | \hat{s}_{out}^{det})} \right) \quad (5.34)$$

$$= \log_e \left(\frac{\sum_{q_p \in \mathcal{Q} | \eta^{-1}(q_p)(i)=1} \Pr(x_k = q_p | \hat{s}_{out}^{det})}{\sum_{q_p \in \mathcal{Q} | \eta^{-1}(q_p)(i)=0} \Pr(x_k = q_p | \hat{s}_{out}^{det})} \right) \quad (5.35)$$

$$= \log_e \left(\frac{\sum_{q_p \in \mathcal{Q} | \eta^{-1}(q_p)(i)=1} \hat{s}_{out}^{det}((k-1)m+p)}{\sum_{q_p \in \mathcal{Q} | \eta^{-1}(q_p)(i)=0} \hat{s}_{out}^{det}((k-1)m+p)} \right) \quad (5.36)$$

Let Λ_{in}^{dec} be the sequence obtained after deinterleaving of Λ_{out}^{det} . We consider that the FEC code is a convolutional code and assume that the soft-in soft-out optimal BCJR decoder is used at the receiver. The FEC decoder produces Λ_{out}^{dec} from Λ_{in}^{dec} . It can be decomposed as the sum of Λ_{in}^{dec} and Λ_{ext}^{dec} , defined as an extrinsic information. The extrinsic information corresponds to the information on the current bit brought by a priori information on its neighbours in the codeword, which is independent of the input LLR. It translates the FEC coding constraint and will be used as input of the binary to symbol converter to provide a priori information to the detector in the following iteration. Let Λ_{in}^{det} be the result of interleaving of Λ_{ext}^{dec} . Let \hat{s}_{in}^{in} stand for the aforementioned a priori information. It is computed as follows:

$$\hat{s}_{in}^{det}((k-1)m+p) = \Pr(x_k = q_p | \Lambda_{in}^{det}) \quad (5.37)$$

$$= \prod_{\substack{0 \leq i \leq m-1 \\ b_p = \eta^{-1}(q_p)}} \Pr(b((k-1)m+i) = b_p(i) | \Lambda_{in}^{det}) \quad (5.38)$$

$$\text{with } \Pr(b((k-1)m+i) = b_p(i) | \Lambda_{in}^{det}) = \frac{\exp\left(\frac{(2b_p(i)-1)\Lambda_{in}^{det}((k-1)m+i)}{2}\right)}{\exp\left(\frac{\Lambda_{in}^{det}((k-1)m+i)}{2}\right) + \exp\left(\frac{-\Lambda_{in}^{det}((k-1)m+i)}{2}\right)}.$$

5.9.3 New detection criterion

s belongs to a size- M^{d_t} alphabet \mathcal{S} . Let denote $s^{(\ell)}$ an element of \mathcal{S} and $s_k^{(\ell)}$ the k -th subvector of length M . Then $s_k = s_k^{(\ell)}$ and $x_k = q_p$ impose that all components of $s_k^{(\ell)}$ be null except the p -th which is equal to 1.

We can write:

$$\Pr(s = s^{(\ell)} | \hat{s}_{in}^{det}) = \prod_{\substack{1 \leq k \leq d_t \\ s_k^{(\ell)}(i) = \delta_{i,p}}} \Pr(x_k = q_p | \Lambda_{in}^{det}) \quad (5.39)$$

$$= \prod_{\substack{1 \leq k \leq d_t \\ s_k^{(\ell)}(i) = \delta_{i,p}}} \hat{s}_{in}^{det}((k-1)m + p) \quad (5.40)$$

The MAP detector searches for s in the alphabet \mathcal{S} which maximizes the a posteriori probability, that is:

$$\max_{s^{(\ell)} \in \mathcal{S}} \Pr(s = s^{(\ell)} | y, \hat{s}_{in}^{det}) \quad (5.41)$$

which is equivalent to:

$$\min_{s^{(\ell)} \in \mathcal{S}} \|y - HB_q s^{(\ell)}\|_2^2 - \sigma_b^2 \sum_{\substack{1 \leq k \leq d_t \\ s_k^{(\ell)}(i) = \delta_{i,p}}} \log_e(\hat{s}_{in}^{det}((k-1)m + p)) \quad (5.42)$$

As seen before, the MAP detector computation cost is too high to be used in practice.

How can we take into account the a priori information delivered by the decoder in the proposed detector? As the distribution of \hat{s}_{out}^{det} is not trivial, we approximate it. We assume that \hat{s}_{out}^{det} is gaussian with mean equal to \hat{s}_{in}^{dec} . The proposed detector criterion becomes:

$$\min_{s \in \mathcal{C}} \|y - HB_q s\|_2^2 + \alpha \|s - \hat{s}_{in}^{dec}\|_2^2, \quad (5.43)$$

where α is a positive weight less than 1. It enables to take into account the imprecision of the distribution approximation. Using (5.42), another justification for the criterion is possible. The second term can be seen as a penalty, imposed to ensure that the detector output remains in the neighborhood of the decoder output all the closer as the iterative process progresses.

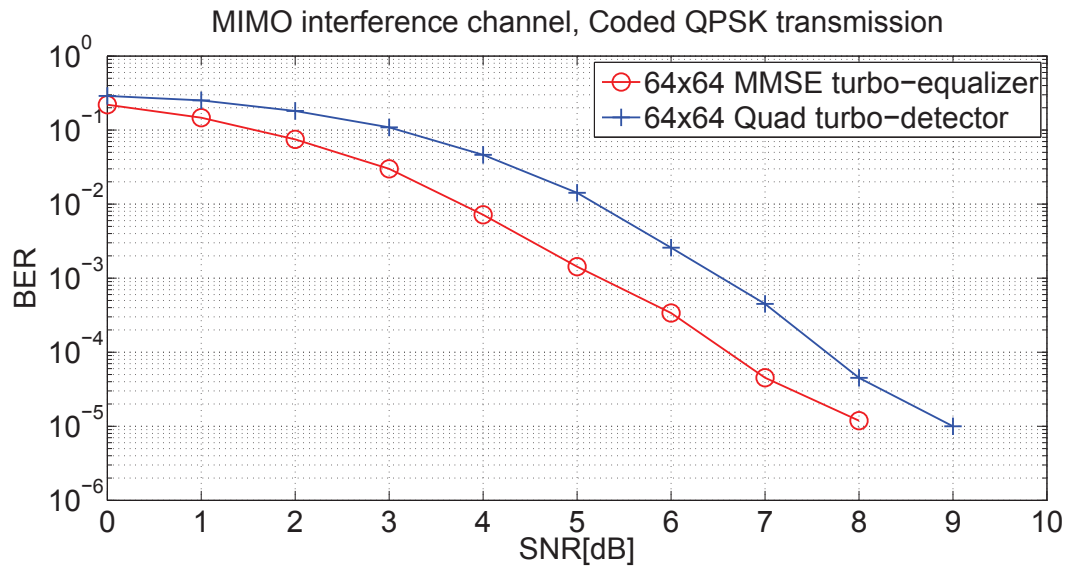


FIGURE 5.8: BER performance of the proposed turbo detector for large antennas dimensions under QPSK constellation inputs and code rate 1/2.

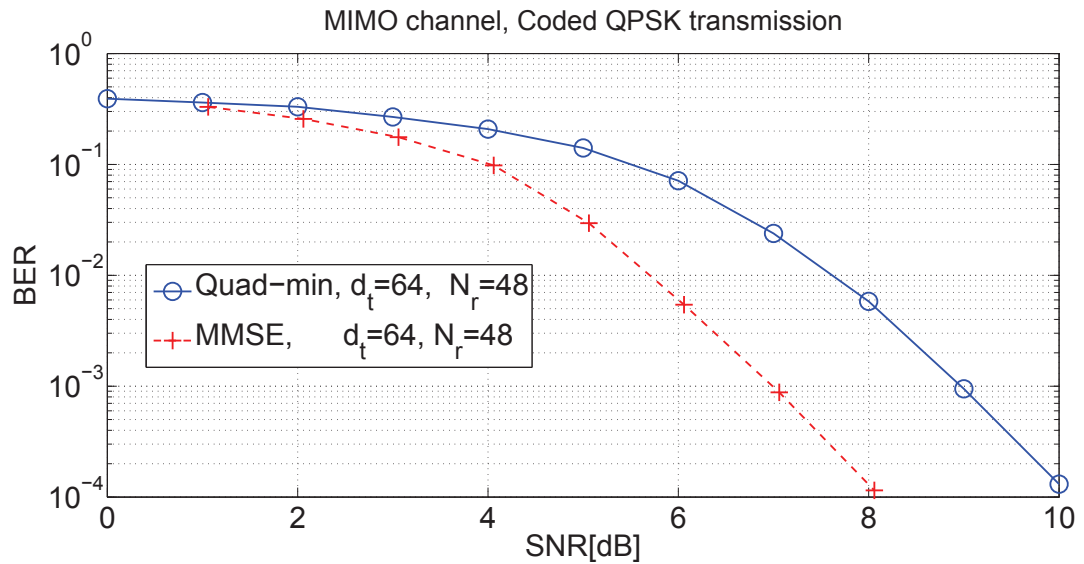


FIGURE 5.9: BER performance of the proposed turbo detector for underdetermined large MIMO under QPSK constellation inputs and code rate 1/2.

5.9.4 Bit error rate performance

Fig. 5.8 and Fig. 5.9 illustrate the BER performance of the proposed turbo detection scheme under 5 iterations and QPSK transmit constellation in $d_t \times N_r$ multiple antennas systems. For the determined systems, i.e. the total number of transmitted symbols is equal to number of observations, we compare our scheme to the MMSE turbo-equalizer in a 64×64 system assuming a 256 bits coded frame with a code rate equals to $1/2$. We notice an advantage for the MMSE turbo-equalizer [100] of 1 to 1.2dB over all SNR values. When the system is underdetermined, the BER of both schemes are plotted in Fig. 5.9 for the configuration 64×48 for a frame 512 coded bits with a code rate equals to $1/2$. It can be seen that with the increase of the SNR, the MMSE outperforms our scheme with a gain between 1.5 and 2dB. For instance, our scheme achieves a BER of 10^{-4} at 10dB of SNR whereas the MMSE achieves the same BER value at 8dB. This loss is mainly due to the inaccuracy of the LLR at the input of the channel decoder.

Remark 5.1: It is important to note the imprecision of the LLR at the detector output. Another sparse recovering approach that delivers the a posteriori probabilities known as Bayesian approach [101]. This means a reliable LLR at the detector output. However, most of the methods in the aforementioned approach assume the signal statistics to be Gaussian, e.g. [102, 103]. This is inadequate in practice since the source can pursue any distribution which is sometimes unknown. This approach also requires in general a higher computational cost than the non Bayesian approach. That is why we have proposed in our work to use methods that result in a unique solution, nevertheless the other approach as well as the optimization of the criterion (5.42) are perspectives for a future work.

5.10 Conclusion

In this chapter, we have first showed that decoding interference jointly with the desired signal can achieve higher receive diversity than canceling interference in a traditional manner using a zero-forcing (assuming the best case when interference are aligned). We have also addressed the problem of decoding in high dimension MIMO systems with finite constellation. We have modeled the transmission as a higher-dimension MIMO channel with sparse input vector. We have then defined two detectors to reconstruct the sparse data vector, the first based on the ℓ_1 -minimization problem and the second is a relaxed minimum distance detector named [**Quad-min**]. The "relaxed" term is used since we have relaxed the ℓ_0 -norm

constraint by the ℓ_1 -norm constraint. Iterative algorithms of polynomial moderate complexity are used to solve the problem. The performance are evaluated using Monte-Carlo simulations for different systems configurations. At the end, we have considered a FEC encoded MIMO system and proposed an iterative turbo-like receiver consisting of the cascade of our detector with a FEC decoder. The sparse detection criterion incorporating a priori information from the FEC decoder has still to be improved in the future.

Chapter 6

Conclusion and perspectives

6.1 Conclusion

This PhD thesis is incorporated within the framework of interference channel where each node is equipped with single or multiple antennas. The goal is to resolve the challenges that the communications face in an interference network taking into account the computational efficiency and the complexity cost.

In the first part, we have briefly presented the commonly used multiplexing techniques for interference avoidance (e.g. TDM, FDM, CDM) with a focus on their achievable rate limitations. By introducing the precoding concept at the transmitter, higher achievable rates can be obtained. A brief description of precoding techniques in different multi-user channel categories has been presented assuming Gaussian-distributed inputs. Then, we have showed the sub-optimality of the IA technique for multi-user interference channel under discrete constellation assumption.

In the second part, we have come back to the interference alignment scheme and have considered the case of a K -user SISO IC. We have introduced three optimized designs for the IA scheme proposed in [38]. The first and the second look for optimizing the precoding subspaces at the IA transmitters through a common diagonal matrix assuming an MMSE and a ZF linear detectors, respectively. The third assumes an MMSE linear detector, and seeks the optimal precoding vectors within a predefined subspace at each transmitter. The first and the third designs require iterative processing to converge to their optimum, whereas the second design is obtained in a closed-form solution. Then we have showed that the orthogonalization of the precoding vectors of the closed-form design enables to achieve a trade-off between complexity and data rate.

The third part has addressed the detection problem for the downlink of a multi-user MIMO system using IA scheme at the transmitters and without CSI at the receivers. The problem has been formulated as a blind source separation problem, and the ability of the joint diagonalization technique (JADE) has been shown to extract the desired streams. Training sequences have been introduced to solve the permutation and scaling ambiguities. From simulations, we have showed that the proposed scheme performs close to full-CSI MIMO IC-IA scheme with a small training sequence number.

In the last part, we have considered the multi-user MIMO IC assuming that the transmitters cannot cooperate and do not necessarily have knowledge of the CSI. We have addressed the problem of detection assuming a spatial multiplexing and no precoding due to a lack of CSI at the transmitters. We have first showed that decoding interference jointly with the desired signal can achieve higher receive diversity than canceling interference in a traditional manner using a zero-forcing (assuming the best case when interference are aligned). We have also tackled the problem of decoding in high dimension MIMO systems with finite constellation. We have modeled the transmission as a higher-dimension MIMO channel with sparse input vector. We have then defined two detectors to reconstruct the sparse data vector, the first based on the ℓ_1 -minimization problem and the second is a relaxed minimum distance detector named [**Quad-min**]. The "relaxed" term is used since we have relaxed the ℓ_0 -norm constraint by the ℓ_1 -norm constraint. Iterative algorithms of polynomial moderate complexity have been used to solve the problem. The performance have been assessed from simulations that carried out in the cases for different systems configurations. At the end, we have considered a FEC encoded MIMO system and have proposed an iterative turbo-like receiver consisting of the cascade of our detector with a FEC decoder. Compared to a usual MMSE-based turbo equalizer, the proposed scheme suffers from a maximum loss of 2dB due to the imperfect exploitation of a priori information provided by the FEC decoder.

6.2 Future works

One part of our works has addressed the IA design at the transmitters in an IC and has showed the complexity cost and performance in the finite SNR region. On the other hand, it is important to know how our IA based proposal could work in practice.

At the receiver side, the use of the BSS based detector as proposed in Chapter 4 does not take the noise variance into consideration. In many standards and networks, the noise variance is considered as a priori information at the receivers, and this can improve the channel estimation accuracy resulting in higher detection reliability. Also, how to integrate the BSS detectors with a turbo-detection scheme and how to obtain the LLR values?

With spatial multiplexing and without precoding design, the receiver can decide to decode the interference as in Chapter 5. Our perspective herein is to apply a Bayesian approach for solving the [ℓ_1 -min] and the [Quad-min] detection problems. The importance of this approach appears when the detector is followed by a soft channel decoder that requires the LLR as inputs. The sparse Bayesian approach for sparse signal recovering should produce the probability of each symbol to occur which yields a reliable LLR and thereby improved decoding scheme.

Appendix A

Mutual information in the MIMO interference channels

The mutual information between a transmitter- receiver pair is defined as [104]

$$I(\mathbf{y}_k; \mathbf{x}_k) = H(\mathbf{x}_k) - H(\mathbf{x}_k|\mathbf{y}_k), \quad (\text{A.1})$$

where $H(\mathbf{x}_k|\mathbf{y}_k)$ is the conditional entropy of the transmitted information \mathbf{x}_k given that \mathbf{y}_k is received. Each element of the vector \mathbf{x}_k is uniformly distributed over the M -cardinal transmit constellation \mathcal{Q} . Hence, the entropy is given as

$$H(\mathbf{x}_k) = \log_2(M). \quad (\text{A.2})$$

The conditional entropy in (A.1) is defined as

$$\begin{aligned} H(\mathbf{x}_k|\mathbf{y}_k) &= - \sum_{a_k} \int_{\mathbf{y}_k} p(\mathbf{x}_k^{a_k}, \mathbf{y}_k) \log_2 [p(\mathbf{x}_k^{a_k}|\mathbf{y}_k)] \\ &= - \sum_{a_1, \dots, a_K} \int_{\mathbf{y}_k} p(\mathbf{y}_k, \mathbf{x}_1^{a_1}, \dots, \mathbf{x}_K^{a_K}) \log_2 \left[\frac{p(\mathbf{y}_k|\mathbf{x}_k^{a_k}) p(\mathbf{x}_k^{a_k})}{p(\mathbf{y}_k)} \right] \\ &= - \frac{1}{M^K} \sum_{a_1, \dots, a_K} \int_{\mathbf{y}_k} p(\mathbf{y}_k|\mathbf{x}_1^{a_1}, \dots, \mathbf{x}_K^{a_K}) \log_2 \left[\frac{p(\mathbf{y}_k|\mathbf{x}_k^{a_k}) p(\mathbf{x}_k^{a_k})}{p(\mathbf{y}_k)} \right] \end{aligned} \quad (\text{A.3})$$

Assuming the indexes $a_j, a'_j, a''_j \in \{1, \dots, M^{d_j}\}$, and substituting the expansion of the following probabilities density in the main expression of the conditional entropy in (A.3)

$$\begin{aligned}
p(\mathbf{y}_k) &= \sum_{a'_1, \dots, a'_K} p(\mathbf{y}_k | \mathbf{x}_1^{a'_1}, \dots, \mathbf{x}_K^{a'_K}) \prod_{k=1}^K p(\mathbf{x}_j^{a'_j}) \\
&= \frac{1}{M^K} \sum_{a'_1, \dots, a'_K} p(\mathbf{y}_k | \mathbf{x}_1^{a'_1}, \dots, \mathbf{x}_K^{a'_K}) \tag{A.4}
\end{aligned}$$

$$\begin{aligned}
p(\mathbf{y}_k | \mathbf{x}_k^{a_k}) &= \sum_{a''_1, \dots, a''_{k-1}, a_k, \dots, a''_K} p(\mathbf{y}_k | \mathbf{x}_1^{a''_1}, \dots, \mathbf{x}_{k-1}^{a''_{k-1}}, \mathbf{x}_k^{a_k}, \dots, \mathbf{x}_K^{a''_K}) \prod_{j=1, j \neq k}^K p(\mathbf{x}_j^{a''_j}), \\
&= \frac{1}{M^{(K-1)}} \sum_{a''_1, \dots, a''_{k-1}, a_k, \dots, a''_K} p(\mathbf{y}_k | \mathbf{x}_1^{a''_1}, \dots, \mathbf{x}_{k-1}^{a''_{k-1}}, \mathbf{x}_k^{a_k}, \dots, \mathbf{x}_K^{a''_K}), \tag{A.5}
\end{aligned}$$

and

$$\begin{aligned}
p(\mathbf{y}_k | \mathbf{x}_1^{a_1}, \dots, \mathbf{x}_K^{a_K}) &= \frac{1}{(\pi\sigma^2)^{N_r}} \exp\left(-\frac{\|\mathbf{y}_k - \sum_{j=1}^K \hat{\mathbf{H}}_{kj} \mathbf{x}_j^{a_j}\|^2}{\sigma^2}\right) \\
&= \frac{1}{(\pi\sigma^2)^{N_r}} \exp\left(-\frac{\|\mathbf{n}_k\|^2}{\sigma^2}\right) \tag{A.6}
\end{aligned}$$

$$\begin{aligned}
p(\mathbf{y}_k | \mathbf{x}_1^{a'_1}, \dots, \mathbf{x}_K^{a'_K}) &= \frac{1}{(\pi\sigma^2)^{N_r}} \exp\left(-\frac{\|\mathbf{y}_k - \sum_{j=1}^K \hat{\mathbf{H}}_{kj} \mathbf{x}_j^{a'_j}\|^2}{\sigma^2}\right) \\
&= \frac{1}{(\pi\sigma^2)^{N_r}} \exp\left(-\frac{\|\mathbf{n}_k + \sum_{j=1}^K \hat{\mathbf{H}}_{kj} (\mathbf{x}_j^{a_j} - \mathbf{x}_j^{a'_j})\|^2}{\sigma^2}\right) \tag{A.7}
\end{aligned}$$

$$\begin{aligned}
p(\mathbf{y}_k | \mathbf{x}_1^{a''_1}, \dots, \mathbf{x}_{k-1}^{a''_{k-1}}, \mathbf{x}_k^{a_k}, \dots, \mathbf{x}_K^{a''_K}) &= \\
&= \frac{1}{(\pi\sigma^2)^{N_r}} \exp\left(-\frac{\|\mathbf{n}_k + \sum_{j \neq k}^K \hat{\mathbf{H}}_{kj} (\mathbf{x}_j^{a_j} - \mathbf{x}_j^{a''_j})\|^2}{\sigma^2}\right)
\end{aligned}$$

where $\hat{\mathbf{H}}_{kj} = \mathbf{H}_{kj} \mathbf{P}_j$ and \mathbf{n}_k the Gaussian distributed noise vector with zero mean and $\sigma^2 \mathbf{I}$ noise variance, the mutual information is obtained as

$$\begin{aligned}
I(\mathbf{x}_k; \mathbf{y}_k) &= \log_2(M) + \frac{1}{M^K} \sum_{a_1, \dots, a_K} \int_{\mathbf{n}_k} p(\mathbf{n}_k) \log_2 \left[J_k(\mathbf{y}_k, a'_1, \dots, a'_K) \right] \\
&\quad - \frac{1}{M^K} \sum_{a_1, \dots, a_K} \int_{\mathbf{n}_k} p(\mathbf{n}_k) \log_2 \left[J_k(\mathbf{y}_k, a''_1, \dots, a''_{k-1}, a_{k+1}, \dots, a''_K) \right] \tag{A.9}
\end{aligned}$$

where

$$J_k(\mathbf{y}_k, a'_1, \dots, a'_K) = \frac{1}{(\pi\sigma^2)^{N_r}} \sum_{a'_1, \dots, a'_K} \exp\left(-\frac{\|\mathbf{n}_k + \sum_{j=1}^K \hat{\mathbf{H}}_{kj}(\mathbf{x}_j^{a'_j} - \mathbf{x}_j^{a'_j})\|^2}{\sigma^2}\right),$$

$$J_k(\mathbf{y}_k, a''_1, \dots, a''_{k-1}, a_{k+1}, \dots, a''_K) = \frac{1}{(\pi\sigma^2)^{N_r}} \sum_{a''_1, \dots, a''_{k-1}, a''_{k+1}, \dots, a''_K} \exp\left(-\frac{\|\mathbf{n}_k + \sum_{j \neq k}^K \hat{\mathbf{H}}_{kj}(\mathbf{x}_j^{a''_j} - \mathbf{x}_j^{a''_j})\|^2}{\sigma^2}\right)$$

Appendix B

Projected gradient method

The projected gradient algorithm requires firstly the computation of the gradient with respect to $\tilde{\mathbf{w}}$

$$\frac{\partial R(\tilde{\mathbf{w}})}{\partial \tilde{w}_i} = \sum_{k=1}^K (\mathbf{X}_{ki} - \mathbf{Y}_{ki}), \quad (\text{B.1})$$

where \mathbf{X}_{ki} and \mathbf{Y}_{ki} are defined as

$$\mathbf{X}_{ki} = \frac{p}{N} \mathbf{l}_{Aki} \left(I + p \mathbf{L}_{Ak} \tilde{\mathbf{W}} \mathbf{L}_{Ak}^H \right)^{-1} \mathbf{l}_{Aki}^H \quad (\text{B.2})$$

$$\mathbf{Y}_{ki} = \frac{p}{N} \mathbf{l}_{Bki} \left(I + p \mathbf{L}_{Bk} \tilde{\mathbf{W}} \mathbf{L}_{Bk}^H \right)^{-1} \mathbf{l}_{Bki}^H$$

with \mathbf{l}_{Aki} and \mathbf{l}_{Bki} are the i^{th} rows of the matrices \mathbf{L}_{Ak} and \mathbf{L}_{Bk} , respectively. The constraint, defined in (3.5), can be formulated as

$$\sum_{k=1}^K \text{tr}[\mathbf{V}_k \tilde{\mathbf{W}} \mathbf{V}_k^H] = \sum_{i=1}^N \tilde{w}_i c_i, \quad (\text{B.3})$$

with c_i is the i^{th} component of the vector \mathbf{c} , $c_i = \sum_k \|\mathbf{v}_{ki}\|^2$, and \mathbf{v}_{ki} is the i^{th} row of the matrix \mathbf{V}_k .

Equation (B.3) defines the set of $\tilde{\mathbf{w}}$ that satisfies the constraint, thus, given the gradient, we project it on the constraint hyperplane and update $\tilde{\mathbf{w}}$ by

$$\tilde{\mathbf{w}}^{l+1} = \tilde{\mathbf{w}}^l + \mu \cdot \mathbf{p}_{\text{proj}}(\tilde{\mathbf{w}}^l), \quad (\text{B.4})$$

where μ is a variable step size and $\mathbf{p}(\tilde{\mathbf{w}})$ is the projected gradient defined as

$$\mathbf{p}_{\text{proj}}(\tilde{\mathbf{w}}^l) = \nabla_{\mathbf{w}} R(\tilde{\mathbf{w}}^l) - (\mathbf{c}^t \nabla_{\mathbf{w}} R(\tilde{\mathbf{w}}^l)) \cdot \frac{\mathbf{c}}{\|\mathbf{c}\|^2}. \quad (\text{B.5})$$

The convergence towards the steady state is achieved either when

$$\|\mathbf{p}(\tilde{\mathbf{w}}^l)\| < \epsilon, \quad (\text{B.6})$$

with ϵ is the tolerance factor for stopping the iterations, or a maximum number of iterations is attained. In this algorithm, the step size μ is a determining factor to ensure a faster convergence, thus, it must be judiciously selected. In [41], two line search methods are proposed: exact line search and inexact line search methods. In practice, most line searches are inexact, and many methods have been proposed. One is the backtracking method, which is employed for our design. It is very simple to implement and quite effective. Besides, the step size is updated at each iteration to satisfy $\tilde{w}_i > 0$ for all i .

Appendix C

Sum-rate gradient with respect to the combination matrix

Using the k^{th} information rate expression in (3.24), the sum rate can be written as

$$R \equiv \sum_{k=1}^K \log_2 |\mathbf{X}_k| - \log_2 |\mathbf{Y}_k| \quad (\text{C.1})$$

where

$$\mathbf{X}_k = \mathbf{I} + p \sum_{j=1}^K \bar{\mathbf{H}}_{kj} \mathbf{C}_j (\bar{\mathbf{H}}_{kj} \mathbf{C}_j)^H, \text{ and } \mathbf{Y}_k = \mathbf{I} + p \sum_{j \neq k}^K \bar{\mathbf{H}}_{kj} \mathbf{C}_j (\bar{\mathbf{H}}_{kj} \mathbf{C}_j)^H \quad (\text{C.2})$$

Since the sum-rate is real valued function and $\mathbf{C}_k \forall k$ are complex variables, the gradient of the sum-rate can be calculated using the differential with respect to \mathbf{C}_k . It is known to be $dR = 2\partial R/\mathbf{C}_k^*$. Details are given in [105]. Using the differential of $\log_2 |\mathbf{X}_k|$ computed as

$$d \log_2 |\mathbf{X}_k| = \text{trace} (\mathbf{X}_k^{-1} d\mathbf{X}_k), \text{ and } d\mathbf{X}_k = p \bar{\mathbf{H}}_{kj} \mathbf{C}_j d\mathbf{C}_j^H \bar{\mathbf{H}}_{kj}^H, \quad (\text{C.3})$$

Using the following properties: $\text{trace}(\mathbf{A}d\mathbf{B}^H) = \text{trace}(\mathbf{A}^T d\mathbf{B}^*)$, $d[\text{trace}(\mathbf{A})] = \text{trace}(d\mathbf{A})$, $\text{vec}(d\mathbf{A}) = d\text{vec}(\mathbf{A})$ and $\text{trace}(\mathbf{A}^T \mathbf{B}) = \text{vec}(\mathbf{A})^T \text{vec}(\mathbf{B})$, and referring to [105] that describes the first-order differential and the Jacobian matrix properties, we obtain

$$d \log_2 |\mathbf{X}_k| = \frac{2p}{\ln 2} \text{vec} (\bar{\mathbf{H}}_{kk}^H \mathbf{X}_k^{-1} \bar{\mathbf{H}}_{kk} \mathbf{C}_k)^T \cdot \text{vec}(d\mathbf{C}_k^*). \quad (\text{C.4})$$

Thus, the gradient of R w.r.t. \mathbf{C}_k^* is obtained as follows

$$\nabla_{\mathbf{C}_k^{(l)}} R = \frac{2p}{\ln 2} \sum_{i=1}^K \bar{\mathbf{H}}_{ik}^H \mathbf{X}_i^{-1} \bar{\mathbf{H}}_{ik} \mathbf{C}_k - \frac{2p}{\ln 2} \sum_{i \neq k}^K \bar{\mathbf{H}}_{ik}^H \mathbf{Y}_i^{-1} \bar{\mathbf{H}}_{ik} \mathbf{C}_k. \quad (\text{C.5})$$

Appendix D

Sphere Radius for the ℓ_1 -minimization problem constraint

From a general point of view, let Y, Θ, X be three d -dimensional real random vectors where $X \sim \mathcal{N}(0, \sigma^2 \mathbf{I}_d)$ when Θ and X are independent and $Y = \Theta + X$. Given tolerance $\tau \geq 0$, Random Distortion Testing (RDT) [106] is the problem of testing whether $\|\Theta(\omega) - \theta_0\| \leq \tau$ or not, when we are given Y and the probability distribution of Θ is unknown. By analogy with standard terminology in statistical inference, we say that this problem is the testing of the null event $[\|\Theta - \theta_0\| \leq \tau]$ against the alternative event $[\|\Theta - \theta_0\| > \tau]$ on the basis of observation Y . The RDT problem [106] is summarized as follows:

$$\text{RDT:} \begin{cases} \text{Observation: } Y = \Theta + X \begin{cases} \Theta \text{ and } X \text{ independent,} \\ X \sim \mathcal{N}(0, \sigma^2 \mathbf{I}_d), \end{cases} \\ \text{Null event: } [\|\Theta - \theta_0\| \leq \tau], \\ \text{Alternative event: } [\|\Theta - \theta_0\| > \tau]. \end{cases} \quad (\text{D.1})$$

Given any $\eta \geq 0$, let \mathcal{T}_η be any thresholding test with threshold height η defined for any $y \in \mathbb{R}^d$ by

$$\mathcal{T}_\eta(y) = \begin{cases} 1 & \text{if } \|y - \theta_0\| > \eta \\ 0 & \text{if } \|y - \theta_0\| \leq \eta. \end{cases} \quad (\text{D.2})$$

Given $\gamma \in (0, 1]$ and $\rho \geq 0$, there exists a unique solution $\lambda_\gamma(\rho) \geq 0$ in η to $1 - F_{\chi_d^2(\rho^2)}(\eta^2) = \gamma$, where $F_{\chi_d^2(\rho^2)}$ is the cumulative distribution function of the non-central χ^2 distribution $\chi_d^2(\rho^2)$ with d degrees of freedom and non-central parameter ρ^2 . In [86], it is then proved that the thresholding test $\mathcal{T}_{\lambda_\gamma(\tau)}$ with threshold height

$\lambda_\gamma(\tau)$ is such that the conditional probability values $P[\mathcal{T}_{\lambda_\gamma(\tau)}(\Theta + X) = 1 \mid \|\Theta - \theta_0\| \leq \tau]$ have supremum equal to γ , whatever Θ such that $P[\|\Theta - \theta_0\| \leq \tau] \neq 0$. We thus say that $\mathcal{T}_{\lambda_\gamma(\tau)}$ has size γ for RDT. Moreover, it turns out that $\mathcal{T}_{\lambda_\gamma(\tau)}$ is optimal for RDT among all tests with same size in the following sense: 1) Save for values of ρ in some subset $\mathcal{D} \subset (\tau, \infty)$ such that $P[\|\Theta - \theta_0\| \in \mathcal{D}] = 0$, the conditional probability $P[\mathcal{T}_{\lambda_\gamma(\tau)}(\Theta + X) = 1 \mid \|\Theta - \theta_0\| = \rho]$ does not depend on the distribution of Θ for every $\rho \in (\tau, \infty) \setminus \mathcal{D}$ and 2) $P[\mathcal{T}_{\lambda_\gamma(\tau)}(\Theta + X) = 1 \mid \|\Theta - \theta_0\| = \rho] \geq P[\mathcal{T}(\Theta + X) = 1 \mid \|\Theta - \theta_0\| = \rho]$ for all test \mathcal{T} with level γ and such that $P[\mathcal{T}(\Theta + X) = 1 \mid \|\Theta - \theta_0\| = \rho]$ does not depend on the distribution of Θ either. In other words, with respect to some criterion suitable for the natural invariance exhibited by RDT on the spheres centered at θ_0 in \mathbb{R}^d , thresholding tests $\mathcal{T}_{\lambda_\gamma(\tau)}$ are optimal.

List of Publications

1. Y. Fadlallah, A. Aissa-El-Bey, K. Abed-Meraim, K. Amis and R. Pyndiah, "Semi-blind source separation in a multi-user transmission system with interference alignment" *IEEE wireless communications letter*, to appear.
2. Y. Fadlallah, K. Amis, A. Aissa-El-Bey, and R. Pyndiah, "Interference alignment for a multi-user SISO interference channel" *Eurasip Journal on Wireless Communication and Networking*, under major revision.
3. Y. Fadlallah, A. Aissa-El-Bey, K. Amis, D. Pastor and R. Pyndiah, "Iterative decoding strategy for underdetermined MIMO transmission using sparse decomposition" *Submitted to IEEE Transactions on Vehicular Technology*.
4. A. Aissa-El-Bey, D. Pastor, S. Azizsbai and Y. Fadlallah, "Sparsity based Recovery of Finite Alphabet Solutions of Underdetermined Linear System" *Submitted to IEEE Transactions on Information Theory*.
5. Y. Fadlallah, A. Aissa-El-Bey, K. Amis and R. Pyndiah, "Interference Alignment : Improved Design via precoding Vectors," in *In Proc. of IEEE Vehicular Technology Conference (VTC)-Spring*, Japan, May 2012.
6. Y. Fadlallah, A. Aissa-El-Bey, K. Amis and R. Pyndiah, "Interference Alignment : Precoding Subspaces Design," in *In Proc. IEEE International Workshop on Signal Processing Advances in Wireless Communications (SPAWC)*, Turkey, June 2012.
7. Y. Fadlallah, K. Amis, A. Aissa-El-Bey and R. Pyndiah, "Formation de voie pour la maximisation du débit dans les schémas d'alignement d'interférence," in *24eme édition du colloque Gretsisi*, Brest, France, Sept. 2013.

8. Y. Fadlallah, A. Aissa-El-Bey, K. Amis and D. Pastor and R. Pyndiah, "New Decoding strategy for underdetermined MIMO transmission using sparse decomposition," in *European Signal Processing Conference (Eusipco)*, Maroc, Sept. 2013.
9. Y. Fadlallah, A. Khandani, K. Amis, A. Aissa-El-Bey and R. Pyndiah, "Pre-coding and Decoding in the MIMO Interference Channels for Discrete Constellation," in *IEEE International Symposium on Personal, Indoor and Mobile Radio Communications (PIMRC)*, UK, Sept. 2013.

Bibliography

- [1] S.W. Peters and R.W. Heath. Interference alignment via alternating minimization. In *Proc. of IEEE International Conference on Acoustics, Speech and Signal Processing, ICASSP*, pages 2445–2448, April 2009.
- [2] K. Gomadam, V.R. Cadambe, and S.A. Jafar. Approaching the capacity of wireless networks through distributed interference alignment. In *in Proc. of IEEE Globecom*, 2008.
- [3] Yasser Fadlallah, Abdeldjalil Aissa El Bey, Karine Amis Cavalec, and Ramesh Pyndiah. Interference alignment: improved design via precoding vectors. In *VTC 2012: 75th IEEE Vehicular Technology Conference*, 2012.
- [4] Yasser Fadlallah, Abdeldjalil Aissa El Bey, Karine Amis Cavalec, and Ramesh Pyndiah. Interference Alignment: Precoding Subspaces Design. In *SPAWC 2012: 13th IEEE International Workshop on Signal Processing Advances in Wireless Communications*, 2012.
- [5] Yasser Fadlallah, Karine Amis Cavalec, Abdeldjalil Aissa El Bey, and Ramesh Pyndiah. Formation de voie pour la maximisation du débit dans les schémas d’alignement d’interférence. In *GRETSI 2013 : 24ème colloque du Groupement de Recherche en Traitement du Signal et des Images*, 2013.
- [6] J-F. Cardoso and A. Souchoumiac. Blind beamforming for non-gaussian signals. *IEE-Proceedings F*, 140(6):362–370, 1993.
- [7] Yasser Fadlallah, Abdeldjalil Aissa El Bey, Karim Abed-Meraim, Ramesh Pyndiah, and Karine Amis Cavalec. Semi-Blind Source Separation in a Multi-User Transmission System with Interference Alignment. *IEEE wireless communications letters*, 2(5):551 – 554, october 2013.

- [8] Yasser Fadlallah, Abdeldjalil Aissa El Bey, Karine Amis Cavalec, Ramesh Pyndiah, and Dominique Pastor. New decoding strategy for underdetermined mimo transmission sparse decomposition. In *EUSIPCO 2013 : 21st European Signal Processing Conference*, 2013.
- [9] Yasser Fadlallah, Amir Khandani, Karine Amis, Abdeldjalil Aissa-El-Bey, and Ramesh Pyndiah. Precoding and decoding in the mimo interference channel for discrete constellation. In *Personal Indoor and Mobile Radio Communications (PIMRC), 2013 IEEE 24th International Symposium on*, pages 1152–1156, 2013.
- [10] Theodore S Rappaport et al. *Wireless communications: principles and practice*, volume second edition. Prentice Hall, 2002.
- [11] Donald C Cox, Roy R Murray, and AW Norris. 800-mhz attenuation measured in and around suburban houses. *AT&T Bell Laboratories technical journal*, 63(6):921–954, 1984.
- [12] Richard Bernhardt. Macroscopic diversity in frequency reuse radio systems. *Selected Areas in Communications, IEEE Journal on*, 5(5):862–870, 1987.
- [13] CE Shannon. A mathematical theory of communication. *ACM SIGMOBILE Mobile Computing and Communications Review*, 5(1):3–55, 2001.
- [14] John G Proakis. *Digital communications*, 1995.
- [15] H. Sampath and A. J. Paulraj. Joint transmit and receive optimization for high data rate wireless communication using multiple antennas. In *IEEE Conference Record of the Thirty-Third Asilomar Conference on Signals, Systems, and Computers*, volume 1, pages 215–219, 1999.
- [16] M. H M Costa. Writing on dirty paper (corresp.). *IEEE Transactions on Information Theory*, 29(3):439–441, 1983.
- [17] G. Caire and S. Shamai. On the achievable throughput of a multiantenna gaussian broadcast channel. *IEEE Transactions on Information Theory*, 49(7):1691–1706, 2003.
- [18] H. Weingarten, Y. Steinberg, and S. Shamai. The capacity region of the gaussian multiple-input multiple-output broadcast channel. *Information Theory, IEEE Transactions on*, 52(9):3936–3964, 2006.

- [19] Q.H. Spencer, A.L. Swindlehurst, and M. Haardt. Zero-forcing methods for downlink spatial multiplexing in multiuser mimo channels. *IEEE Transactions on Signal Processing*, 52(2):461–471, 2004.
- [20] Christian B Peel, Bertrand M Hochwald, and A Lee Swindlehurst. A vector-perturbation technique for near-capacity multiantenna multiuser communication-part i: channel inversion and regularization. *Communications, IEEE Transactions on*, 53(1):195–202, 2005.
- [21] Quentin H Spencer, Christian B Peel, A Lee Swindlehurst, and Martin Haardt. An introduction to the multi-user mimo downlink. *Communications Magazine, IEEE*, 42(10):60–67, 2004.
- [22] W. Yu, W. Rhee, S. Boyd, and J. M. Cioffi. Iterative water-filling for gaussian vector multiple-access channels. *IEEE Transactions on Information Theory*, 50(1):145–152, 2004.
- [23] Semih Serbetli and Aylin Yener. Transceiver optimization for multiuser mimo systems. *Signal Processing, IEEE Transactions on*, 52(1):214–226, 2004.
- [24] Xiaojun Yuan, Chongbin Xu, Li Ping, and Xiaokang Lin. Precoder design for multiuser mimo isi channels based on iterative lmmse detection. *Selected Topics in Signal Processing, IEEE Journal of*, 3(6):1118–1128, 2009.
- [25] Anders Host-Madsen and Aria Nosratinia. The multiplexing gain of wireless networks. In *Information Theory, 2005. ISIT 2005. Proceedings. International Symposium on*, pages 2065–2069, 2005.
- [26] V. R. Cadambe and S. A. Jafar. Interference alignment and degrees of freedom of the K-user interference channel. *IEEE Transactions on Information Theory*, 54(8), Aug. 2008.
- [27] M. Maddah-Ali, A. S. Motahari, and A. K. Khandani. Communication over MIMO X channels: interference alignment, decomposition, and performance analysis. *IEEE Transactions on Information Theory*, 54:3457–3470, Aug. 2008.
- [28] C. Yetis, T. Gou, S.A. Jafar, and A.H. Kayran. On feasibility of interference alignment in mimo interference networks. *IEEE Transactions on Signal Processing*, 8:4771–4782, 2010.

- [29] M. Maddah-Ali A. K. Khandani A. S. Motahari, S. O. Gharan. Real interference alignment: Exploiting the potential of single antenna systems. *arXiv:0908.2282*.
- [30] I. Santamaria, O. Gonzalez, R. Heath, and S. Peters. Maximum sum-rate interference alignment algorithms for mimo channels. In *in Proc. of IEEE Globecom*, 2010.
- [31] D. A. Schmidt, C. Shi, R. Berry, M. Honig, and W. Utschick. Minimum mean squared error interference alignment. In *Asilomar Conference on Signals, Systems and Computers, 2009 Conference Record of the Forty-Third*, pages 1106–1110, 2009.
- [32] S. Liu and Y. Du. A general closed-form solution to achieve interference alignment along spatial domain. In *in Proc. of IEEE Globecom*, 2010.
- [33] Chengshan Xiao, Yahong Rosa Zheng, and Zhi Ding. Globally optimal linear precoders for finite alphabet signals over complex vector gaussian channels. *Signal Processing, IEEE Transactions on*, 59(7):3301–3314, 2011.
- [34] Y. Wu, M. Wang, C. Xiao, Zhi Ding, and X. Gao. Linear Precoding for MIMO Broadcast Channels with Finite Alphabet Constraints. *IEEE Transactions on Wireless Communications*, 11(8), Aug. 2012.
- [35] Mingxi Wang, Weiliang Zeng, and Chengshan Xiao. Linear precoding for mimo multiple access channels with finite discrete inputs. *Wireless Communications, IEEE Transactions on*, 10(11):3934–3942, 2011.
- [36] H. Sato. On degraded gaussian two-user channels. *IEEE Transactions on Information Theory*, IT-24:637–640, Sept. 1978.
- [37] A. Carleial. Interference channels. *IEEE Transactions on Information Theory*, 24(1), Jan. 1978.
- [38] S. W. Choi, S. A. Jafar, and S.-Y. Chung. On the beamforming design for interference alignment. *IEEE Communication Letter*, 13(11):847–849, Nov. 2009.
- [39] Denis Serre. *Matrices: Theory and applications, second edition*. Springer, 2009.

- [40] N. J. Higham. Analysis of the cholesky decomposition of a semi definite matrix. *Oxford University Press*, pages 161–185, 1990.
- [41] S. Boyd and L. Vandenberghe. *Convex Optimization*. Cambridge University Press, New York, 2004.
- [42] D. Kim and M. Torlak. Optimization of interference alignment beamforming vectors. *IEEE Journal on Selected Areas In Communications*, 28(9):1425–1434, Dec. 2010.
- [43] H. Sung, S. Park, K. Lee, and I. Lee. Linear precoder designs for k-user interference channels. *IEEE Transactions on Wireless Communications*, 9(1):291–300, Jan. 2010.
- [44] Peter W Wolniansky, Gerard J Foschini, GD Golden, and Reinaldo A Valenzuela. V-blast: An architecture for realizing very high data rates over the rich-scattering wireless channel. In *Signals, Systems, and Electronics, 1998. ISSSE 98. 1998 URSI International Symposium on*, pages 295–300, 1998.
- [45] M. Shen, A. Host-Madsen, and J. Vidal. An improved interference alignment scheme for frequency selective channels. In *Proc. of IEEE International Symposium on Information Theory*, pages 6–11, July 2008.
- [46] Tiangao Gou and Syed A. Jafar. Degrees of freedom of the k user mxn mimo interference channel. *IEEE Transactions on Information Theory*, 56(12):6040–6057, dec 2010.
- [47] A. Ghasemi, S.A. Motahari, and A.K. Khandani. Interference alignment for the k user mimo interference channel. In *in Proc. IEEE International Symposium on Information Theory (ISIT)*, 2010.
- [48] G. Bresler, D. Cartwright, and D. Tse. Interference alignment for the mimo interference channel. *arXiv preprint arXiv:1303.5678*.
- [49] ETSI 3GPP. Lte; evolved universal terrestrial radio access (e-utra); and evolved universal terrestrial radio access network (e-utran); overall description.
- [50] J. J. Van de Beek, O. Edfors, M. Sandell, S.K. Wilson, and P.O. Borjesson. On channel estimation in ofdm systems. In *in Proc. IEEE International Vehicular Technology Conference (VTC)*, pages 815–819, July 1995.

- [51] D. Zhiguo, T. Ratnarajah, and C. Cowan. Hos-based semi-blind spatial equalization for mimo rayleigh fading channels. *IEEE Transactions on Signal Processing*, 56.
- [52] Y. Li, A. Cichoki, and L. Zhang. Blind separation and extraction of binary sources. *IEICE Transactions on Fundamentals*, E86-A(3):580–589, 2004.
- [53] Pierre Comon. Independent component analysis, a new concept? *Signal Processing*, pages 287–314, 1994.
- [54] M. Castella and P. Comon. Blind separation of instantaneous mixtures of dependent sources. In *in Proc. of Independent Component Analysis (ICA) Workshop*, 2007.
- [55] Cesar F. Caiafa. On the conditions for valid objective functions in blind separation of independent and dependent sources. *EURASIP Journal on Advances in Signal Processing*, 2012.
- [56] Alper T Erdogan. A family of bounded component analysis algorithms. In *IEEE International Conference on Acoustics, Speech and Signal Processing (ICASSP)*, pages 1881–1884. IEEE, 2012.
- [57] J.F. Cardoso. High-order contrasts for independent component analysis. *Neural Computation*, 11(1).
- [58] H. Bousbia-Salah. *Blind separation of source signals from their convolutive mixtures: Bloc Joint Diagonalization technique based on second order statistics*. PhD thesis, Ecole Nationale Polytechnique (ENP) Algeria, 2006.
- [59] I. Kacha, K. Abed-Meraim, and A. Belouchrani. Fast adaptive blind mmse equalizer for multichannel fir systems. *EURASIP Journal on Applied Signal Processing*, 2006.
- [60] E. Bingham and A. Hyvarinen. Ica of complex valued signals: a fast and robust deflationary algorithm. *International Journal Neural Systems*, 10(1), 2000.
- [61] Jean-François Cardoso and Antoine Souloumiac. Jacobi angles for simultaneous diagonalization. *SIAM J. Mat. Anal. Appl.*, 17(1):161–164, January 1996.

- [62] Jean-François Cardoso and Antoine Souchoumiac. A matlab function implementing the joint approximate diagonalization of real matrices. <http://perso.telecom-paristech.fr/~cardoso/jointdiag.html>.
- [63] H. Bolcskei and J. Thukral. Interference alignment with limited feedback. In *in Proc. of IEEE International Symposium on Information Theory (ISIT)*, 2009.
- [64] R. Krishnamachari and M. Varanasi. Interference alignment under limited feedback for mimo interference channels. In *in Proc. of IEEE International Symposium on Information Theory (ISIT)*, 2010.
- [65] R. Tresh and M. Guillaud. Cellular interference alignment with imperfect channel knowledge. In *in Proc. IEEE International Conference on Communications (ICC) Workshops*, 2009.
- [66] M. O. Damen, H. El Gamal, and G. Caire. On maximum-likelihood detection and the search for the closest lattice point. *IEEE Transactions on Information Theory*, 49(10):2389–2402, October 2003.
- [67] B. Hassibi and H. Vikalo. On the sphere decoding algorithm i. expected complexity. *IEEE Trans. on Signal Processing*, 53(8).
- [68] J. Jalden and B. Ottersten. On the Complexity of Sphere Decoding in Digital Communications. *IEEE Trans. on Signal Processing*, 2005.
- [69] Luis G Barbero and John S Thompson. A fixed-complexity mimo detector based on the complex sphere decoder. In *Signal Processing Advances in Wireless Communications, 2006. SPAWC'06. IEEE 7th Workshop on*, pages 1–5, 2006.
- [70] Zhan Guo and Peter Nilsson. Algorithm and implementation of the k-best sphere decoding for mimo detection. *Selected Areas in Communications, IEEE Journal on*, 24(3):491–503, 2006.
- [71] S. Foucart. A note on guaranteed sparse recovery via L1 minimization. *Applied and Computational Harmonic Analysis*, 29(1).
- [72] J.F. Sturm. Using SeDuMi 1.02, a MATLAB toolbox for optimization over symmetric cones. *Optimization Methods and Software*, 11-12:625-633, 1999. *Special issue on Interior Point Methods (CD supplement with software)*.

- [73] Jungwon Lee, D. Toumpakaris, and Wei Yu. Interference mitigation via joint detection. *Selected Areas in Communications, IEEE Journal on*, 29(6):1172–1184, 2011.
- [74] X. Zhu and R. D. Murch. Performance analysis of maximum likelihood detection in a mimo antenna system. *IEEE Transactions on Communications*, 50(2):187–191, February 2002.
- [75] M.O.Damen, H. El Gamal, and G. Caire. On maximum-likelihood detection and the search for the closest lattice point. *IEEE Transactions on Information Theory*, 49(10):2389–2402, 2003.
- [76] T. Cui and C. Tellambura. An Efficient Generalized Sphere Decoder for Rank-Deficient MIMO Systems. *IEEE Communications Letters*, 9(5), May 2005.
- [77] A. Aïssa-El-Bey, D. Pastor, S. M. Aziz-Sbai, and Y. Fadlallah. Recovery of Finite Alphabet Solutions of Underdetermined Linear System. *Submitted to IEEE Transactions on Information Theory*.
- [78] A Aïssa-El-Bey, M Grebici, K Abed-Meraim, and A Belouchrani. Blind system identification using cross-relation methods: further results and developments. In *Signal Processing and Its Applications, 2003. Proceedings. Seventh International Symposium on*, volume 1, pages 649–652. IEEE, 2003.
- [79] A Aïssa-El-Bey, K Abed-Meraim, and Y Grenier. Underdetermined blind source separation of audio sources in time-frequency domain. *Proc. Workshop on Signal Processing with Sparse/Structured Representations (SPARS), Rennes, France*, pages 67–70, 2005.
- [80] Nguyen Linh-Trung, Abdeldjalil Aïssa-El-Bey, K Abel-Meraim, and A Belouchrani. Underdetermined blind source separation of non-disjoint non-stationary sources in the time-frequency domain. In *Signal Processing and Its Applications, 2005. Proceedings of the Eighth International Symposium on*, volume 1, pages 46–49. IEEE, 2005.
- [81] Abdeldjalil Aïssa-El-Bey and Karim Abed-Meraim. Blind simo channel identification using a sparsity criterion. In *Signal Processing Advances in Wireless Communications, 2008. SPAWC 2008. IEEE 9th Workshop on*, pages 271–275. IEEE, 2008.

- [82] Abdeldjalil Aïssa-El-Bey, Karim Abed-Meraim, and Yves Grenier. Underdetermined blind audio source separation using modal decomposition. *EURASIP Journal on Audio, Speech, and Music Processing*, 2007(1):14–14, 2007.
- [83] Abdeldjalil Aïssa-El-Bey, Karim Abed-Meraim, and Yves Grenier. Blind separation of underdetermined convolutive mixtures using their time–frequency representation. *Audio, Speech, and Language Processing, IEEE Transactions on*, 15(5):1540–1550, 2007.
- [84] Abdeldjalil Aïssa-El-Bey, Nguyen Linh-Trung, Karim Abed-Meraim, Adel Belouchrani, and Yves Grenier. Underdetermined blind separation of nondisjoint sources in the time-frequency domain. *Signal Processing, IEEE Transactions on*, 55(3):897–907, 2007.
- [85] A. Yang, A. Ganesh, S. Sastry, and Y. Ma. Fast L1-Minimization Algorithms and An Application in Robust Face Recognition: A Review. *Technical Reports*, February 2010.
- [86] D. Pastor and Q.T. Nguyen. Testing the Mahalanobis distance between a random signal with unknown distribution and a known deterministic model in additive and independent standard Gaussian noise: the random distortion testing problem. *IEEE Transactions on Signal Processing*. to appear.
- [87] Lee J Lehmkuhl. A polynomial primal-dual interior point method for convex programming with quadratic constraints, 1993.
- [88] Michael Grant and Stephen Boyd. CVX: Matlab software for disciplined convex programming, version 2.0 beta. <http://cvxr.com/cvx>, September 2012.
- [89] Michael Grant and Stephen Boyd. Graph implementations for nonsmooth convex programs. In *Recent Advances in Learning and Control*, Lecture Notes in Control and Information Sciences, pages 95–110. Springer-Verlag Limited, 2008.
- [90] Reha H Tütüncü, Kim C Toh, and Michael J Todd. Solving semidefinite-quadratic-linear programs using sdpt3. *Mathematical programming*, 95(2):189–217, 2003.
- [91] Inc. Gurobi Optimizatoion. Gurobi optimizer reference manual, 2012.

- [92] Emmanuel J Candes, Michael B Wakin, and Stephen P Boyd. Enhancing sparsity by reweighted ℓ_1 minimization. *Journal of Fourier Analysis and Applications*, 14(5-6):877–905, 2008.
- [93] John Wozencraft and Irwin Jacobs. *Principles of Communication Engineering*. John Wiley and Sons, New York, 1966.
- [94] Claude Berrou, Alain Glavieux, and Punya Thitimajshima. Near shannon limit error-correcting coding and decoding: Turbo-codes. 1. In *Communications, 1993. ICC 93. Geneva. Technical Program, Conference Record, IEEE International Conference on*, volume 2, pages 1064–1070, 1993.
- [95] Claude Berrou and Alain Glavieux. Near optimum error correcting coding and decoding: Turbo-codes. *Communications, IEEE Transactions on*, 44(10):1261–1271, 1996.
- [96] Catherine Douillard, Michel Jézéquel, Claude Berrou, Annie Picart, Pierre Didier, Alain Glavieux, et al. Iterative correction of intersymbol interference: Turbo-equalization. *European Transactions on Telecommunications*, 6(5):507–511, 1995.
- [97] Annie Picart, Pierre Didier, and Alain Glavieux. Turbo-detection: a new approach to combat channel frequency selectivity. In *Communications, 1997. ICC 97 Montreal, 'Towards the Knowledge Millennium'*. 1997 *IEEE International Conference on*, volume 3, pages 1498–1502, 1997.
- [98] Simon Haykin, Mathini Sellathurai, Yvo de Jong, and Tricia Willink. Turbo-mimo for wireless communications. *Communications Magazine, IEEE*, 42(10):48–53, 2004.
- [99] Gerhard Bauch and Volker Franz. A comparison of soft-in/soft-out algorithms for turbo detection? In *Proc. Int. Conf. Telecomm*, pages 259–263, 1998.
- [100] Christophe Laot, Raphaël Le Bidan, and Dominique Leroux. Low-complexity mmse turbo equalization: a possible solution for edge. *Wireless Communications, IEEE Transactions on*, 4(3):965–974, 2005.
- [101] Shihao Ji, Ya Xue, and Lawrence Carin. Bayesian compressive sensing. *Signal Processing, IEEE Transactions on*, 56(6):2346–2356, 2008.

- [102] Erik G Larsson and Yngve Selén. Linear regression with a sparse parameter vector. *Signal Processing, IEEE Transactions on*, 55(2):451–460, 2007.
- [103] Philip Schniter, Lee C Potter, and Justin Ziniel. Fast bayesian matching pursuit. In *Information Theory and Applications Workshop, 2008*, pages 326–333, 2008.
- [104] Thomas M Cover and Joy A Thomas. *Elements of information theory*. John Wiley & Sons, 2012.
- [105] J. Magnus and H. Neudecker. *Matrix Differential Calculus with Applications in Statistics and Econometrics*. JHON WILEY SONS, revised version 2007.
- [106] D. Pastor and Q. T. Nguyen. Random distortion testing and applications. In *ICASSP 2013 : IEEE international conference on acoustics, speech and signal processing, Vancouver, Canada, Mai 26-31, 2013*.